

Elucidating Flow Matching ODE Dynamics with respect to Data Geometries

Gal Mishne^{*1}, Zhengchao Wan^{†2}, Qingsong Wang^{‡3}, and Yusu Wang^{§1}

²Department of Mathematics, University of Missouri

³Department of Mathematics, University of Utah

¹Halıcıoğlu Data Science Institute, University of California San Diego

December 30, 2024

Abstract

Diffusion-based generative models have become the standard for image generation. ODE-based samplers and flow matching models improve efficiency, in comparison to diffusion models, by reducing sampling steps through learned vector fields. However, the theoretical foundations of flow matching models remain limited, particularly regarding the convergence of individual sample trajectories at terminal time—a critical property that impacts sample quality and being critical assumption for models like the consistency model. In this paper, we advance the theory of flow matching models through a comprehensive analysis of sample trajectories, centered on the denoiser that drives ODE dynamics. We establish the existence, uniqueness and convergence of ODE trajectories at terminal time, ensuring stable sampling outcomes under minimal assumptions. Our analysis reveals how trajectories evolve from capturing global data features to local structures, providing the geometric characterization of per-sample behavior in flow matching models. We also explain the memorization phenomenon in diffusion-based training through our terminal time analysis. These findings bridge critical gaps in understanding flow matching models, with practical implications for sampling stability and model design.

Contents

1	Introduction	2
2	Background in Flow Matching Models	6
2.1	Preliminaries and notations	6
2.2	Conditional flow matching	7
2.3	Unifying scheduling functions through noise-to-signal ratio	8
3	Denoiser: the Guiding Component in Flow Matching Models	9
3.1	Basics of the denoiser	10
3.2	Denoiser and ODE dynamics: terminal time singularity	11
3.3	Denoiser and ODE dynamics: attracting and absorbing	13

*gmishne@ucsd.edu

†zwan@missouri.edu

‡qswang92@gmail.com

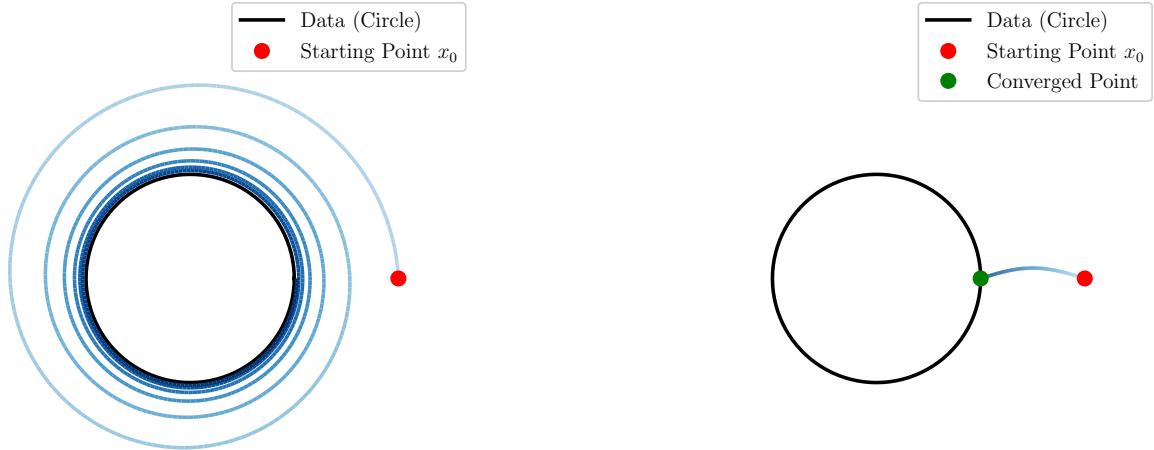
§yusuwang@ucsd.edu

4	Concentration and Convergence of the Posterior Distribution	14
4.1	Concentration and convergence of the posterior distribution	14
4.2	Distinct behaviors for posterior convergence rates under data geometry	15
5	Well-Posedness of Flow Matching ODEs	18
5.1	Well-posedness of flow matching ODEs at $t \in [0, 1)$	18
5.2	Well-posedness of flow matching ODEs at $t = 1$	18
5.3	Refined convergence rates for manifolds and discrete cases	20
5.4	Equivariance of the flow maps under data transformations	21
6	Attraction Dynamics of Flow Matching ODEs	21
6.1	Initial stage of the sampling process	22
6.2	Intermediate stage of the sampling process	23
6.3	Terminal stage of the sampling process and memorization behavior	23
7	Discussion	25
A	Geometric Notions and Results	29
A.1	Convex geometry notions and results	29
A.2	Metric geometry notions and results	30
B	Proofs	34
B.1	Proofs in Section 2	34
B.2	Proofs in Section 3	35
B.3	Proofs in Section 4	38
B.3.1	Proof of Theorem 4.8	43
B.4	Proofs in Section 5	47
B.4.1	Proof of Theorem 5.3	50
B.4.2	Proof of Theorem 5.4	54
B.5	Proofs in Section 6	55

1 Introduction

Diffusion-based generative models have become the de facto standard for the task of image generation [SDWGM15, HJA20, SE19]. Compared to previous generative models (e.g., GANs [GPAM⁺14]), diffusion models are easier to train but suffer from long sampling times due to the sequential nature of the sampling process. To address this limitation, (deterministic) ODE-based samplers were introduced, where the sampling process is done by integrating an ODE trajectory. This approach has been shown to be more efficient than traditional sampling with a significantly reduced number of sampling steps needed [SME21a, LZB⁺22, KAAL22]. Recently, a new class of models, known as **flow matching models** [LCBH⁺22, LGL23] has been developed to use an ODE flow map to interpolate between a prior and a target data distribution—generalizing diffusion models with ODE samplers. By learning a vector field u_t a new sample x_1 can be generated by integrating over the ODE below from some initial random sample x_0 :

$$\frac{dx_t}{dt} = u_t(x_t), t \in [0, 1].$$



(a) An ODE trajectory that winds towards the data distribution without convergence as $t \rightarrow 1$.

(b) An ODE trajectory smoothly converging to the data distribution as $t \rightarrow 1$.

Figure 1: **Comparing two ODE trajectory behaviors.** We show two types of ODE trajectories with the same data distribution supported on the unit circle: (a) winding instability, and (b) smooth convergence. Our convergence analysis at $t = 1$ (cf. Theorem 5.3) guarantees that flow matching ODE trajectories converge smoothly onto the data distribution, ensuring that the undesirable winding phenomenon does not occur.

Various versions of the flow matching model have gained popularity, such as the rectified flow model [LGL23], which is used in recent commercial image generation software [EKB⁺24]. Furthermore, the succinct and deterministic formulation of the flow matching model also makes theoretical analysis potentially easier.

However, despite their empirical success, the theoretical understanding of flow models remains incomplete, even for the well-posedness of the ODE trajectories, i.e., existence, uniqueness, as well as convergence as $t \rightarrow 1$ of the ODE trajectories. These are not thoroughly addressed in the pioneering papers [LCBH⁺22, LGL23], and only partially tackled in recent studies [GHJ24, LHH⁺24]. Specifically, in [LHH⁺24], well-posedness is established only on the open interval $[0, 1)$. [GHJ24] extended to $[0, 1]$ but under restrictive assumptions on the data distribution, which cannot include the popular case when the data distribution is supported on a low-dimensional manifold. In both works, the challenge arises from the singularity in the vector field u_t as the terminal time $t = 1$ is approached, influenced by both the ODE formulation and the data geometry. The convergence of the ODE trajectories lies in a broader context of sample trajectory analysis, which is less explored in the literature as most work focuses on distribution level analysis [BDD23, LC24].

We also highlight that pushing the well-posedness to $t = 1$ and performing sample trajectory analysis is not only theoretically interesting but also of practical importance. Suppose we know that the ODE trajectory exists in $[0, 1)$, and the intermediate distribution following the ODE flow is getting closer to the data distribution as t increases. However, if the ODE trajectory does not converge at $t = 1$, the final sampling following a single ODE trajectory can be very sensitive to the chosen ODE discretization scheme, i.e., a slight change in sampling schedule will result in a drastically different outcome. This could happen if the individual ODE trajectories are winding towards the data distribution but never converge at $t = 1$ as shown in Figure 1a. A more desirable behavior is as in Figure 1b, where the ODE trajectory converges to the data distribution as $t \rightarrow 1$. Empirical studies find the ODE trajectories tend to stabilize as $t \rightarrow 1$ and hence be more aligned

with that of Figure 1b, and this observation is utilized to guide the choice of the ODE discretization scheme [KAAL22, EKB⁺24]. Furthermore, the convergence of the ODE trajectories at $t = 1$ is a critical assumption for the consistency model [SDCS23], which utilizes the limit of the ODE trajectory to design a one-step diffusion model. These considerations motivate us to investigate the convergence of the ODE trajectories at $t = 1$ and per sample trajectory analysis.

In this paper, our approach focuses on the *denoiser*, a key component of flow matching models. The denoiser, defined as the mean of the posterior distribution of the data given a noisy observation, governs the evolution of ODE trajectories. Initially, the posterior distribution is broad, and the denoiser approximates the global mean of the data. As time progresses, the posterior measure becomes more concentrated around nearby data points, and the denoiser captures finer details of the data distribution.

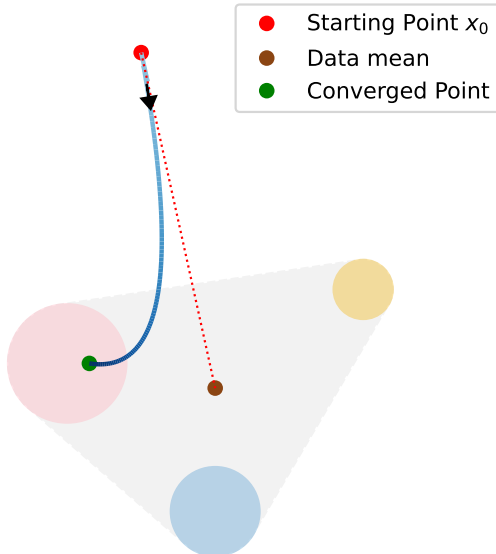


Figure 2: **Illustration of three stages of a flow matching ODE trajectory.** The three colored regions (yellow, blue, and pink) represent three local clusters in support of the data distribution. The trajectory first moves towards the mean (brown point) of the data distribution (cf. Proposition 6.1; note how the initial vector is pointing towards the data mean of the data distribution) and will be absorbed by the convex hull of the data distribution (cf. Proposition 6.2) in the shaded region. Later, it will be attracted by the local cluster of the data distribution (cf. Proposition 6.4) and will be guaranteed to converge onto the data support (green point) at terminal time (cf. Theorem 5.3).

We show that when approaching the terminal time, the posterior distribution concentrates on the nearest data, and the denoiser converges to the projection of the current sample onto the data support. This extends previous partial results [PY24, SBDS24] to a general setting beyond a small neighborhood of the data support. By carefully leveraging this denoiser convergence and integrating it with the analysis of the ODE dynamics, we find that near the terminal time, the ODE trajectories will stay in a region away from the singularity and converge to the data support. As a result, we establish the convergence of the entire sampling process with minimal assumptions and validate that the ODE trajectories in flow matching models are well-behaved (as in Figure 1b).

Notably, the terminal time analysis of the denoiser provides a new perspective on the *memorization phenomenon* observed in diffusion-based training where models only repeat the training samples

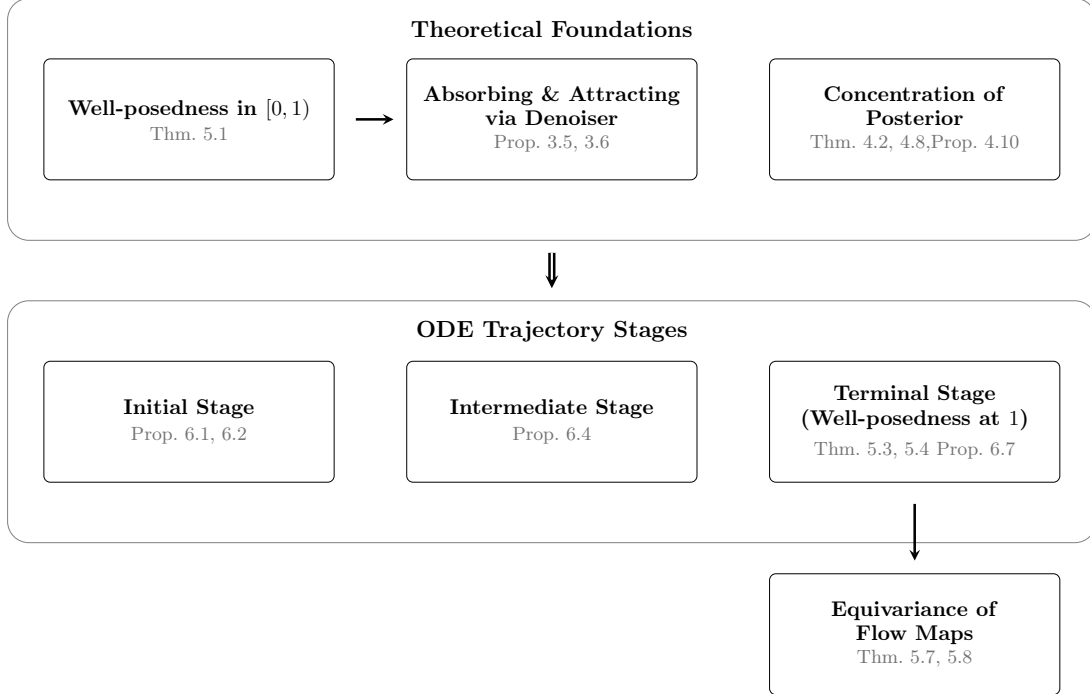


Figure 3: **Illustration of main theoretical results.** Our findings are divided into two main parts: the first focuses on the theoretical foundations of flow matching ODEs, emphasizing properties of denoisers and posterior distributions; the second builds on these insights to characterize the three stages of flow matching ODE trajectories. In the first part, we highlight that the well-posedness result serves as the cornerstone for understanding the absorbing and attracting properties of denoisers. Furthermore, leveraging the well-posedness at $t = 1$, we establish the existence of the flow map Ψ_t at $t = 1$, which enables us to derive key properties of flow maps.

[CHN⁺23, WLCL24], rather than generate new unseen data points. We identify that the denoiser’s terminal time convergence to the data support precisely leads to this memorization behavior. In particular, if a neural network trained denoiser is asymptotically trained optimally with empirical data, it can only sample memorized training data.

Finally, our analysis significantly strengthens the understanding of flow matching ODE dynamics, extending beyond the terminal time. By carefully examining the progressive concentration of the posterior distribution, we derive comprehensive insights into the behavior of ODE trajectories. Specifically, we establish a unified result demonstrating that trajectories are systematically attracted to, and ultimately absorbed by, the convex hulls associated with the data distribution. Initially, sample trajectories move towards the mean of the data distribution and will be absorbed into the convex hull of overall data distribution, capturing the global structure. As the process evolves, they are increasingly drawn towards local clusters within the data, reflecting a transition from global to local convergence. Ultimately, the trajectories converge to the data support at the terminal time, providing a geometric characterization of how samples naturally focus on local features. See Figure 2 for an illustration. In this way, we provide per sample trajectory analysis that complements the empirical, or distribution level discussion regarding the flow matching/diffusion model dynamics [BBDBM24, LC24].

Contributions and Organization. In summary, we provide a comprehensive theoretical analysis of flow matching models by examining the behavior of denoisers and posterior distributions. We establish the convergence of ODE trajectories and characterize their geometric evolution, bridging key gaps in the theoretical understanding of these models. Our results address critical challenges related to terminal time singularities and offer new insights into the memorization phenomenon in diffusion-based training. The geometric perspective we develop—showing how trajectories evolve from global to local features—provides a unified framework for understanding flow matching dynamics, laying a foundation for future theoretical developments. The paper is structured as follows, and Figure 3 provides an illustration of the main theoretical results and their inter-dependencies.

- In Section 2, we introduce the background on flow matching models, their training objectives, and the unification of different scheduling functions via the noise-to-signal ratio σ .
- In Section 3, we discuss key properties of the denoiser and highlight its role as the guiding component in the flow matching model ODE dynamics, illustrating terminal time singularity and general attracting and absorbing properties.
- In Section 4, we study the concentration and convergence of the posterior distribution, establishing its initial closeness to the data distribution and its convergence to the data support at the terminal time. We also derive specific convergence rates under different data geometries.
- In Section 5, we present the well-posedness of ODE trajectories first in $[0, 1)$ and then extend to $[0, 1]$ with minimal assumptions on the data distribution. We then obtain refined convergence results based on data geometry. Lastly, with the existence of flow maps, we analyze its equivariance property under data transformation.
- In Section 6, we analyze the ODE trajectories across different stages, demonstrating their initial attraction to the data mean and eventual absorption into the convex hull of the data distribution. Later, these trajectories are attracted to local clusters. We also provide quantitative results on the terminal time behavior for discrete data distributions and showcase the importance of terminal time behavior on the memorization phenomenon.

All technical proofs are deferred to the appendix.

2 Background in Flow Matching Models

In this section, we provide a brief overview of flow matching models and their training objectives and how the noise-to-signal ratio σ can be used to unify different scheduling functions.

2.1 Preliminaries and notations

We use \mathbb{R}^d to denote the d -dimensional Euclidean space, and $\|\cdot\|$ to denote the Euclidean norm. We use Ω to denote a general closed subset $\Omega \subset \mathbb{R}^d$ and usually use M to denote a manifold in \mathbb{R}^d . We let $d_\Omega : \mathbb{R}^d \rightarrow \mathbb{R}$ denote the distance function to Ω , i.e.,

$$d_\Omega(x) := \min_{y \in \Omega} d_\Omega(x, y)$$

The *medial axis* of Ω is defined as

$$\Sigma_\Omega := \left\{ x \in \mathbb{R}^d : \# \left\{ \operatorname{argmin}_{y \in \Omega} \|x - y\| \right\} > 1 \right\}$$

The *reach* of Ω is defined as $\tau_\Omega := \inf_{x \in \Omega} \text{dist}(x, \Sigma_\Omega)$. For any $x \in \mathbb{R}^d \setminus \Sigma_\Omega$, the nearest point on Ω is unique and we denote it by $\text{proj}_\Omega(x) := \arg \min_{y \in \Omega} \|x - y\|$. We let $\text{diam}(\Omega)$ denote the diameter of Ω , i.e., $\text{diam}(\Omega) := \sup_{x, y \in \Omega} \|x - y\|$. A set K is said to be convex if for any $x, y \in K$ and $t \in [0, 1]$, we have $tx + (1 - t)y \in K$. For any set Ω , we let $\text{conv}(\Omega)$ denote the convex hull of Ω which is the smallest convex set containing Ω .

We let p denote the target data distribution in \mathbb{R}^d , p_{prior} denote the prior, which is often chosen to be the standard Gaussian $\mathcal{N}(0, I)$. We say p has a finite 2-moment, denoted by $M_2(p)$, if $M_2(p) := \int_{\mathbb{R}^d} \|x\|^2 p(dx) < \infty$. For notation simplicity, we use $\mathbb{E}(p)$, $\text{Cov}(p)$ to denote the expectation and covariance of p , respectively. For any two probability measures μ and ν , the q -Wasserstein distance for $q \geq 1$ as

$$d_{W,q}(\mu, \nu) := \inf_{\gamma \in \mathcal{C}(\mu, \nu)} \left(\int_{\mathbb{R}^d \times \mathbb{R}^d} \|x - y\|^q \gamma(dx \times dy) \right)^{1/q},$$

where $\mathcal{C}(\mu, \nu)$ denotes the set of all couplings of μ and ν , i.e. the set of all probability measures on $\mathbb{R}^d \times \mathbb{R}^d$ with marginals μ and ν . The distance will be finite if μ and ν have finite q -moments, i.e. $\int_{\mathbb{R}^d} \|x\|^q \mu(dx) < \infty$ and $\int_{\mathbb{R}^d} \|x\|^q \nu(dx) < \infty$.

For any probability measures μ and ν on \mathbb{R}^d , we use $\mu * \nu$ to denote their convolution.

2.2 Conditional flow matching

Conditional flow matching models [LCBH⁺22, LGL23] are a class of generative models whose *training process* consists of learning a vector field u_t that generates a probability path $(p_t)_{t \in [0,1]}$ interpolating a prior p_{prior} and a target data distribution p and whose *sampling process* consists of integrating an ODE trajectory from an initial point $x_0 \sim p_{\text{prior}}$ to a terminal point $x_1 \sim p$. For simplicity, we will call these models flow models.

More specifically, the flow model assumes a probability path $(p_t)_{t \in [0,1]}$ interpolating $p_0 = p_{\text{prior}}$ and $p_1 = p$, and aims at finding a time-dependent vector field $(u_t : \mathbb{R}^d \rightarrow \mathbb{R}^d)_{t \in [0,1]}$ whose corresponding ODE

$$\frac{dx_t}{dt} = u_t(x_t) \tag{1}$$

has an integration flow map Ψ_t that sends any initial point x_0 to x_t along the ODE trajectory, satisfying $p_t = (\Psi_t)_\# p_0$. Within the framework, the probability path $(p_t)_{t \in [0,1]}$ is constructed conditionally as

$$p_t = \int p_t(\cdot | x_1 = x) p(dx),$$

where the conditional distribution $p_t(\cdot | x_1 = x)$ satisfies $p_0(\cdot | x_1 = x) = p_{\text{prior}}$ and $p_1(\cdot | x_1 = x) = \delta_x$, the Dirac delta measure at x . When the prior p_{prior} is the standard Gaussian $\mathcal{N}(0, I)$, the conditional distribution $p_t(\cdot | x_1 = x)$ are often specified as $p_t(\cdot | x_1 = x) := \mathcal{N}(\alpha_t x, \beta_t^2 I)$, where α_t and β_t are *scheduling functions* satisfying $\alpha_0 = \beta_1 = 0$ and $\alpha_1 = \beta_0 = 1$ and often being monotonic. Common choices include linear scheduling $\alpha_t = t$ and $\beta_t = 1 - t$ used in the rectified flow model [LGL23, EKB⁺24], as well as those arising from the original diffusion model, like DDPM [HJA20].

It turns out that the vector field u_t satisfying the above properties can be explicitly expressed as follows using the data distribution p . We first define the *conditional vector field* $u_t(x|x_1)$ which enjoys a closed-form

$$u_t(x|x_1) = \frac{\dot{\beta}_t}{\beta_t} x + \frac{\dot{\alpha}_t \beta_t - \alpha_t \dot{\beta}_t}{\beta_t} x_1,$$

where the dot represents the derivative with respect to t . Then the desired vector field u_t satisfies the following equation for any $t \in [0, 1]$

$$u_t(x) = \int u_t(x|x_1)p(dx_1|x_t = x) \quad (2)$$

where $p(\cdot|x_t = x)$ denotes the *posterior distribution* (which is different from the conditional distribution $p_t(\cdot|x_1 = x)$ defined earlier):

$$p(dx_1|x_t = x) = \frac{\exp\left(-\frac{\|x - \alpha_t x_1\|^2}{2\beta_t^2}\right)}{\int \exp\left(-\frac{\|x - \alpha_t x'_1\|^2}{2\beta_t^2}\right) p(dx'_1)} p(dx_1).$$

The guarantee that the vector field u_t generates the probability path p_t is stated in [LGL23, Theorem 3.3] and [LCBH⁺22, Theorem 1] under the explicit or implicit assumption that the ODE trajectory exists on $[0, 1]$. This result was further rigorously proved in [GHJ24] under some specific assumptions. We point out that the assumptions are very restrictive and cannot include the case when p is supported on a low-dimensional manifold. See our results in Section 5 for a more general statement.

Ultimately, specifying the conditional distribution $p_t(\cdot|x_1 = x)$ as Gaussian distributions allows one to train a neural network to learn the vector field u_t by minimizing the following loss function whose **unique** minimizer is $u_t(x)$ [LCBH⁺22]:

$$\begin{aligned} \mathcal{L}_v &= \mathbb{E}_{t \in [0,1], z \sim \pi, x_1 \sim p} \|u_t^\theta(\alpha_t x_1 + \beta_t z) - u_t(\alpha_t x_1 + \beta_t z|x_1)\|^2 \\ &= \mathbb{E}_{t \in [0,1], z \sim \pi, x_1 \sim p} \|u_t^\theta(\alpha_t x_1 + \beta_t z) - \dot{\alpha}_t x_1 - \dot{\beta}_t z\|^2 \end{aligned} \quad (3)$$

2.3 Unifying scheduling functions through noise-to-signal ratio

In this section, we describe a formulation that can unify different scheduling functions α_t and β_t . This is done by introducing the noise-to-signal ratio, which has been discussed in [SPC⁺24, CZW⁺24, KG24]. We find it useful in our analysis as it simplifies the ODE dynamics and allows us to present our results more cleanly.

When the scheduling functions α_t and β_t are assumed to be strictly monotonic, then the noise-to-signal ratio is defined as

$$\sigma_t := \frac{\beta_t}{\alpha_t}, \quad \text{for } t \in (0, 1].$$

By monotonicity, σ as a function of t is invertible and we let $t(\sigma)$ denote the inverse function of σ_t . As t goes from 0 to 1, the noise-to-signal ratio σ_t goes from ∞ to 0. For any $\sigma \in (0, \infty)$, we define q_σ as the convolution of p and a Gaussian kernel with variance $\sigma^2 I$:

$$q_\sigma := p * \mathcal{N}(0, \sigma^2 I) = \int \mathcal{N}(\cdot|y, \sigma^2 I) p(dy). \quad (4)$$

We also let $q_0 := p$. Then, we have the following result.

Proposition 2.1. *For any $t \in (0, 1]$, define $A_t : \mathbb{R}^d \rightarrow \mathbb{R}^d$ by sending x to x/α_t . Then, $q_{\sigma_t} = (A_t)_\# p_t$.*

Under the map A_t , the probability path q_{σ_t} satisfies an ODE with respect to σ .

Proposition 2.2. For any $[a, b] \subset (0, 1]$, let $(x_t)_{t \in [a, b]}$ denote an ODE trajectory of Equation (1). Then, $(x_\sigma := x_{t(\sigma)}/\alpha_{t(\sigma)})_{\sigma \in (\sigma_b, \sigma_b]}$ satisfies the following ODE:

$$\frac{dx_\sigma}{d\sigma} = -\sigma \nabla \log q_\sigma(x_\sigma), \quad (5)$$

where $q_\sigma(x)$ denotes the probability density of q_σ .

During sampling, the ODE with respect to σ integrates *backwards*, that is, for any $\sigma_T \in (0, \infty)$ and any $x \in \mathbb{R}^d$, the corresponding ODE trajectory x_σ is the solution of Equation (5) from x_σ with $\sigma \in [0, \sigma_T]$ that satisfies $x_{\sigma_T} = x$. So now, we have an ODE model depicted in Equation (5) generating a probability path q_σ for $\sigma \in (0, \infty)$. This way of parametrizing the ODE and its variants have been studied extensively in the literature of diffusion models [SME21b, KAAL22].

The above transition from the parameter t to the parameter σ works for any (monotonic) scheduling functions α_t and β_t . As a consequence, different choices of scheduling functions are equivalent up to a reparametrization. This is also discussed to some extent in [SPC⁺24] for creating a sampling schedule different from the ones used in the training process.

Remark 2.3 (Subtlety at the endpoints). When $t = 0$, $\alpha_0 = 0$ and there is an issue of division by zero which prevents the above transition from being valid. Furthermore, as σ goes to ∞ , the corresponding probability measure q_σ does not have a well-defined limit. Hence, one often uses a large σ_T instead of ∞ as the starting time of Equation (5), i.e., one samples $z \sim \mathcal{N}(0, \sigma_T^2 I)$ with σ_T as the initial point for the backward ODE. This may introduce an extra error term in the sampling process since at σ_T , one should have sampled from q_{σ_T} which may deviate from $\mathcal{N}(0, \sigma_T^2 I)$. Indeed, it is empirically observed in [ZYLX24b] that this error is related to the average brightness issue in the generated images. The validity of the above transition property suggests an easy correction though: first sample $z \sim \mathcal{N}(0, I)$ and then perform an ODE step in t to obtain z_{t_ϵ} , scale it by σ_{t_ϵ} and then continue the noise-to-signal ratio backward ODE using σ . This is termed as *SingDiffusion* in [ZYLX24b].

In this paper, it is much cleaner and easier to state / prove most theoretical results using the noise-to-signal ratio σ rather than t . Therefore, we will present these results in terms of σ (or alternatively $\lambda := -\log(\sigma)$). However, note the equivalence between the two models and hence the results stated in terms of σ can be translated to the flow matching model in a straightforward manner. For results regarding flow maps Ψ_t , we will use parameter t due to the inherent obstacles of defining a flow map as discussed in Remark 2.3 as well as the reverse process from ∞ to 0 in Equation (5).

3 Denoiser: the Guiding Component in Flow Matching Models

At the core of the flow matching model is the vector field u_t that generates the probability path p_t . It turns out that the vector field u_t is fully determined by the denoiser, i.e. the mean of the posterior distribution $p(\cdot | x_t = x)$ [KAAL22]. In this section, we will first talk about some basic properties of the denoiser, then mention certain difficulties in handling the denoiser and will eventually showcase how the ODE dynamics are guided by the denoiser and its implications in the flow model.

3.1 Basics of the denoiser

Recall that the vector field u_t is given by $u_t(x) = \int u_t(x|x_1)p(dx_1|x_t = x)$, and by plugging in the explicit formula of $u_t(x|x_1) = \frac{\dot{\beta}_t}{\beta_t}x + \frac{\dot{\alpha}_t\beta_t - \alpha_t\dot{\beta}_t}{\beta_t}x_1$, we have that

$$u_t(x) = \frac{\dot{\beta}_t}{\beta_t}x + \frac{\dot{\alpha}_t\beta_t - \alpha_t\dot{\beta}_t}{\beta_t} \mathbb{E}(p(\cdot|x_t = x)), \quad (6)$$

a formulation that is also given in [GHJ24, Equation (3.7)]. Here $\mathbb{E}(p(\cdot|x_t = x))$ can be explicitly written as follows:

$$\mathbb{E}(p(\cdot|x_t = x)) = \int \frac{\exp\left(-\frac{\|x - \alpha_t y\|^2}{2\beta_t^2}\right) y}{\int \exp\left(-\frac{\|x - \alpha_t y'\|^2}{2\beta_t^2}\right) p(dy')} p(dy). \quad (7)$$

Notice that the denoiser $\mathbb{E}(p(\cdot|x_t = x))$ is the only part of u_t dependent on the data distribution p and hence fully determines the vector field u_t . For simplicity, we use the notation $m_t(x) := \mathbb{E}(p(\cdot|x_t = x))$ to emphasize that it is the mean of the posterior distribution $p(\cdot|x_t = x)$.

Noise-to-signal ratio formulation. Likewise, the ODE in σ can also be expressed in terms of the denoiser $m_\sigma(x) := \mathbb{E}[p(\cdot|x_\sigma = x)]$ as follows from Tweedie's formula:

$$\frac{dx_\sigma}{d\sigma} = -\sigma \nabla \log q_\sigma(x_\sigma) = -\frac{1}{\sigma} (m_\sigma(x_\sigma) - x_\sigma). \quad (8)$$

Notably, the ODE in σ can be simply interpreted as moving towards the denoiser $m_\sigma(x)$ at a speed inversely proportional to σ . Similarly, one can explicitly write $m_\sigma(x)$ as follows.

$$m_\sigma(x) = \int \frac{\exp\left(-\frac{\|x - y\|^2}{2\sigma^2}\right) y}{\int \exp\left(-\frac{\|x - y'\|^2}{2\sigma^2}\right) p(dy')} p(dy). \quad (9)$$

An alternative parametrization for σ . This backward integration in σ might be cumbersome in analysis and we alternatively use the parameter $\lambda = -\log(\sigma)$. We similarly let $\sigma(\lambda)$ define the inverse function. Then, when σ changes from ∞ to 0, λ changes from $-\infty$ to ∞ . For an ODE trajectory $(x_\sigma)_{\sigma \in (0, \infty)}$, we define $(x_\lambda := x_{\sigma(\lambda)})_{\lambda \in (-\infty, \infty)}$. For any $x \in \mathbb{R}^d$, we define $m_\lambda(x) := m_{\sigma(\lambda)}(x)$. Then, the ODE in λ has a concise form:

$$\frac{dx_\lambda}{d\lambda} = m_\lambda(x_\lambda) - x_\lambda. \quad (10)$$

Jacobians of the denoiser and data covariance. We point out that the denoiser, under some mild condition on the data distribution p , is differentiable and its Jacobian is inherently connected with the covariance matrix of the posterior distribution $p(\cdot|x_t)$ (or $p(\cdot|y_\sigma)$). Similar formulas for computing the Jacobian have been utilized before for various purposes; see, for example, [ZYLX24a, Lemma B.2.1] and [GHJ24, Lemma 4.1]. Moreover, the covariance formula in Proposition 3.1 is a direct consequence of higher order generalization of Tweedie's formula, which has been studied in previous works (see, e.g., [Efr11], [MSLE21]).

Proposition 3.1. *Assume that p has a finite 2-moment. For any $t \in [0, 1)$, we have that m_t is differentiable. In particular, the Jacobian $\nabla_x m_t$ can be explicitly expressed as follows for any $x \in \mathbb{R}^d$:*

$$\begin{aligned}\nabla_x m_t(x) &= \frac{\alpha_t}{2\beta_t^2} \iint (z - z')(z - z')^T p(dz|x_t = x) p(dz'|x_t = x) \\ &= \frac{\alpha_t}{\beta_t^2} \text{Cov}[p(\cdot|x_t = x)].\end{aligned}$$

Furthermore, if we let $\sigma = \sigma_t$, then

$$\begin{aligned}\nabla_x m_\sigma(x) &= \frac{1}{2\sigma^2} \iint (z - z')(z - z')^T p(dz|x_\sigma = x) p(dz'|x_\sigma = x) \\ &= \frac{1}{\sigma^2} \text{Cov}[p(\cdot|x_\sigma = x)].\end{aligned}$$

Here $\text{Cov}[q]$ denotes the covariance matrix of a probability distribution q .

A note on the training process. As m_t is the only part in u_t dependent on p , instead of training the vector field u_t directly, one can train a neural network m_t^θ to learn the denoiser m_t directly. By plugging Equation (6) into Equation (3), we obtain the following training loss for m_t which turns out to be equivalent to the training loss for the vector field Equation (3):

$$\mathcal{L}_m = \mathbb{E}_{t \in [0,1], z \sim p_0, x \sim p} \|m_t^\theta(\alpha_t x + \beta_t z) - x\|^2. \quad (11)$$

The mean m_t will always be bounded, which is opposite to the fact that the vector field u_t can blow up when $t \rightarrow 1$ as discussed in Proposition 3.3. This makes the denoiser $m_t(x)$ much easier to train than the vector field $u_t(x)$. Meanwhile, training of the denoiser, an alternative to the vector field, is also utilized in the diffusion model literature [KAAL22] (with σ) and shows promising results.

Remark 3.2. *In the literature on diffusion models, the main object is the score function, which is the gradient of the log density of the probability distribution p_t . The score function view or the denoiser view are equivalent to each other by applying Tweedie’s formula [Efr11], see e.g., [GHJ24][Remark 3.5]. As the mean of the posterior distribution, the denoiser $m_t(x)$ is more interpretable and we will show its importance in the remainder of the paper.*

3.2 Denoiser and ODE dynamics: terminal time singularity

The terminal time is referred to as the time $t = 1$ (or $\sigma = 0$, $\lambda \rightarrow \infty$) in the flow model. The convergence of the ODE trajectory at the terminal time relies on the terminal time regularity of the vector field. We now elucidate two types of singularities of the vector field that arise at the terminal time in the flow model, one due to the ODE formulation and the other due to the data geometry.

Singularity due to the ODE formulation. Recall that the vector field u_t is given by $u_t(x) = \frac{\dot{\beta}_t}{\beta_t} x + \frac{\dot{\alpha}_t \beta_t - \alpha_t \dot{\beta}_t}{\beta_t} \mathbb{E}(p(\cdot|x_t = x))$. Since the denominator β_t approaches 0 as $t \rightarrow 1$, the vector field u_t faces an issue of division by zero when approaching the terminal time. This singularity is intrinsic to the flow matching ODE formulation. In the following proposition, we show that when the data distribution is not fully supported, the limit $\lim_{t \rightarrow 1} \|u_t(x)\|$ goes to infinity for almost all x while it is bounded when the data distribution is fully supported.

Proposition 3.3. *Assume that $\alpha, \beta : [0, 1] \rightarrow \mathbb{R}$ are smooth, and $\dot{\alpha}_1, \dot{\beta}_1$ exist and are non zero. Let $\Omega := \text{supp}(p)$ and let Σ_Ω denote its medial axis. Then, we have the following properties:*

- If p is fully supported, i.e., $\Omega = \mathbb{R}^d$, and has a Lipschitz density, then for any $x \in \mathbb{R}^d$, the vector field $u_t(x)$ is uniformly bounded for all $t \in [0, 1)$.
- If p is not fully supported, i.e., $\Omega \neq \mathbb{R}^d$, then for any $x \notin \Omega \cup \Sigma_\Omega$, $\lim_{t \rightarrow 1} \|u_t(x)\| = \infty$.

The deciding factor on whether the vector field u_t blows up for a given x is if $\lim_{t \rightarrow 1} m_t(x) = x$ or not. We will show in Corollary 4.3 that $\lim_{t \rightarrow 1} m_t(x) = \text{proj}_\Omega(x)$ for any $x \notin \Sigma_\Omega$, and thus when $x \notin \Omega \cup \Sigma_\Omega$, $\lim_{t \rightarrow 1} m_t(x) \neq x$ and hence the vector field u_t blows up. Another way to interpret the singularity of the ODE formulation is by considering the transformation of the ODE in σ in Equation (10) where the singularity corresponds to the $1/\sigma$ term. This singularity can be addressed by using the parameter λ as in Equation (10) which results in the ODE:

$$\frac{dx_\lambda}{d\lambda} = m_\lambda(x_\lambda) - x_\lambda, \quad \lambda \in (-\infty, \infty),$$

with the trade-off of turning a finite-time ODE into an infinite-time ODE.

Singularity due to the data geometry. When the data is not fully supported, the medial axis Σ_Ω of the data support plays a crucial role in the singularity of the denoiser m_σ which may result in discontinuity of the limit $\lim_{\sigma \rightarrow 0} m_\sigma(x)$. In this case, when the ODE is transformed into the λ , the vector field u_λ does not have a uniform Lipschitz bound for all $\lambda \in (a, \infty)$ and hence the typical ODE theory such as Picard-Lindelöf theorem can not be directly applied to analyze the flow matching ODEs.

The discontinuity behavior can be illustrated by the following simple example of a two-point data distribution which can be easily extended to higher dimensions. We specifically use the $\sigma = e^{-\lambda}$ and consider $\lim_{\sigma \rightarrow 0} m_\sigma(x)$ for illustration as the sampling process is often done in σ , e.g., as in [SME21a, KAAL22] and the σ values are more interpretable.

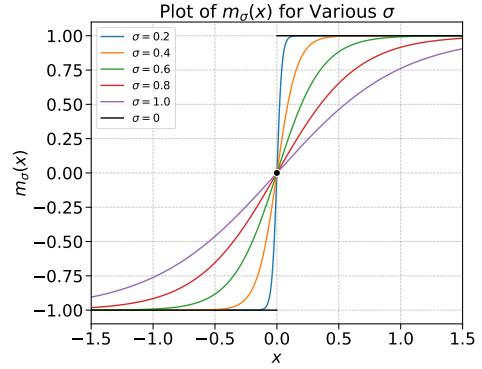


Figure 4: The denoiser $m_\sigma(x)$ for the two point example with various σ .

Example 3.4. Let $p = \frac{1}{2}\delta_{-1} + \frac{1}{2}\delta_1$ be a probability measure on \mathbb{R}^1 . Then, the support $\Omega := \text{supp}(p) = \{-1, 1\}$ is just a two-point set. The medial axis is the singleton $\Sigma_\Omega = \{0\}$ whose distance to either point is 1. Now, we can explicitly write down the denoiser m_σ as follows:

$$m_\sigma(x) = \frac{-\exp\left(-\frac{(x+1)^2}{2\sigma^2}\right) + \exp\left(-\frac{(x-1)^2}{2\sigma^2}\right)}{\exp\left(-\frac{(x+1)^2}{2\sigma^2}\right) + \exp\left(-\frac{(x-1)^2}{2\sigma^2}\right)}. \quad (12)$$

Notice that when σ approaches 0,

- The denoiser m_σ is converging to a function $f : \mathbb{R}^1 \rightarrow \{-1, 0, 1\}$ with $f(x) = 1$ for $x > 0$, $f(x) = -1$ for $x < 0$ and $f(0) = 0$.
- Certain singularity of m_σ is emerging at $\Sigma_\Omega = \{0\}$: the derivative (Jacobian if in high dimensions) $\frac{dm_\sigma(0)}{dx}$ is blowing up when $\sigma \rightarrow 0$.

A full characterization of the limit $\lim_{\sigma \rightarrow 0} m_\sigma(x)$ for discrete data distribution will be given in Corollary 4.11 where the discontinuity often arises at the medial axis of the data support. All these singularities pose challenges in theoretical analysis of the flow matching ODEs and particularly in the convergence of the ODE trajectory when approaching the terminal time. The data geometry singularity is more challenging to handle, especially the discontinuity behavior of the limit of the denoiser near the medial axis.

We will address these challenges in the convergence analysis of the flow matching ODEs in Section 5 by showing that even if the geometric singularities exist, the ODE trajectory will avoid the singularities and converge to the data support. This is done by identifying an absorbing and attracting property of the ODE dynamics, which will be discussed in the next section.

3.3 Denoiser and ODE dynamics: attracting and absorbing

Assume that the ODE trajectory exists and remains unique up to the terminal time—on $[0, 1)$ for the t and on $(0, \infty)$ (resp. $(-\infty, \infty)$) for σ (resp. λ). In Section 5.1, we will rigorously establish this well-posedness for any data distribution p with finite 2-moment. The Equation (8) ($\frac{dx_\lambda}{d\lambda} = m_\lambda(x_\lambda) - x_\lambda$) suggests that the sample simply moves towards the denoiser m_λ from x_λ ; however, the key lies in the Denoiser’s time dependence since m_λ changes as λ evolves. Nevertheless, when m_λ remains confined within certain convex sets, the ODE exhibits two notable properties: an *attracting property*—drawing trajectories towards specific convex sets, and an *absorbing property*—keeping trajectories within these sets. These properties are stated precisely in the next two meta-theorems. We describe them with respect to σ , but they can be translated to t or λ in a straightforward manner.

Theorem 3.5 (Attracting towards convex sets). *Let $(x_\sigma)_{\sigma \in (\sigma_2, \sigma_1]}$ be an ODE trajectory of Equation (8) starting from some x_{σ_1} . Assume that there exists a closed convex set K such that $m_\sigma(x_\sigma) \in K$ for any $\sigma \in (\sigma_2, \sigma_1]$. Then, we have that if $x_{\sigma_1} \notin K$, then x_σ moves towards K with a linear rate:*

$$d_K(x_\sigma) \leq \frac{\sigma}{\sigma_1} d_K(x_{\sigma_1}).$$

With a similar setup, we can also show that the ODE trajectory will stay within a convex set under certain conditions.

Theorem 3.6 (Absorbing of convex sets). *Let $(x_\sigma)_{\sigma \in (\sigma_2, \sigma_1]}$ be an ODE trajectory of Equation (8) starting from some x_{σ_1} . Then, we have the following results.*

1. *For any closed convex set K , if $m_\sigma(x_\sigma) \in K$ for any $\sigma \in (\sigma_2, \sigma_1]$ and $x_{\sigma_1} \in K$, then $x_\sigma \in K$ for any $\sigma \in (\sigma_2, \sigma_1]$;*
2. *For any open convex set K , assume that $m_\sigma(x) \in K$ for any $x \in \partial K$, the boundary of K , and any $\sigma \in (\sigma_2, \sigma_1]$. Then, if $x_{\sigma_1} \in K$, we have that $x_\sigma \in K$ for any $\sigma \in (\sigma_2, \sigma_1]$.*

Observe a subtle distinction between 1 and 2: in 1, we assume properties of the denoiser along the ODE trajectory, whereas in 2, we assume properties of the denoiser itself, independent of the flow matching ODE.

In view of Theorem 3.5 and Theorem 3.6, one can analyze the flow matching ODE dynamics by identifying where the denoiser will reside. Indeed, we leverage these theorems in Section 6.1 and Section 6.2 to analyze the initial and intermediate stages of flow matching ODEs.

For the terminal stage, we note the denoiser m_σ will concentrate towards a single point in the data distribution. More precisely, as σ decreases to 0, the posterior distribution $p(\cdot|x_\sigma)$ will be more and more concentrated around the data points near x_σ and eventually converge to the

delta distribution located at the nearest data almost surely. We will systematically analyze this concentration phenomenon of the posterior distribution in the next section. We will then be able to show in Section 5.2 and Section 6.3 that near the terminal time, an ODE trajectory that starts from a point x near the data support Ω will never leave a neighborhood of the Ω , which avoids the geometric singularities (cf. Section 3.2), and will eventually be attracted to the Ω .

4 Concentration and Convergence of the Posterior Distribution

The key construction in the overall flow matching model is the posterior distribution. We first establish the concentration and convergence of the posterior distribution for general data distribution p and then discuss the case when p is supported on a low-dimensional manifold. We also establish the convergence of the denoisers as a consequence of the convergence of the posterior distribution.

4.1 Concentration and convergence of the posterior distribution

Intuitively, for the posterior distribution $p(\cdot|x_t = x)$, as t goes to 1, the noise level β_t goes to 0 and hence the posterior distribution should concentrate around data points near x . We will establish this rigorously utilizing the parameter σ .

Initially, the posterior distribution $p(\cdot|x_\sigma = x)$ for large σ is close to the data distribution p and hence the ODE trajectory x_σ will move towards the mean of the data distribution. The following proposition quantifies the initial stability of the posterior distribution.

Proposition 4.1 (Initial stability of posterior measure). *Let p be a probability measure on \mathbb{R}^d with bounded support which is denoted as $\Omega := \text{supp}(p)$. Let x be a point and consider the posterior measure $p(\cdot|x_\sigma = x)$. We then have the following Wasserstein distance bound:*

$$d_{W,1}(p(\cdot|x_\sigma = x), p) < \left(\exp\left(\frac{2\|x - \mathbb{E}(p)\|\text{diam}(\Omega)}{\sigma^2}\right) - 1 \right) \text{diam}(\Omega).$$

Note that the bound above will only be meaningful when σ is large and will blow up to infinity as σ decreases to 0. This makes sense as the posterior distribution $p(\cdot|x_\sigma = x)$ will gradually depart from p and concentrate around the data points near x and eventually converge to the delta distribution located at the nearest data point. The following theorem quantifies the concentration and convergence of the posterior distribution.

Theorem 4.2. *Let $\Omega := \text{supp}(p)$. Assume that p has finite 2-moment, i.e., $M_2(p) := \int_{\mathbb{R}^d} \|x\|^2 p(dx) < \infty$. For all $x \in \mathbb{R}^d \setminus \Sigma_\Omega$, we let $x_\Omega := \text{proj}_\Omega(x)$. Then, we have that*

$$\lim_{\sigma \rightarrow 0} d_{W,2}(p(\cdot|x_\sigma = x), \delta_{x_\Omega}) = 0.$$

As a direct consequence of the convergence of the posterior distribution, we have the following convergence of the denoiser.

Corollary 4.3. *Under the same assumptions as in Theorem 4.2, we have that for any $x \in \mathbb{R}^d \setminus \Sigma_\Omega$, we have that*

$$\lim_{\sigma \rightarrow 0} m_\sigma(x) = \text{proj}_\Omega(x).$$

When we turn back to the parameter t , we have the following corollary. The proof turns out to be rather technical instead of being a direct consequence of the above theorem. The main difficulty lies in the scaling α_t within the exponential term. This is another example that the parameter σ is more convenient for theoretical analysis.

Corollary 4.4. *Let $\Omega := \text{supp}(p)$. Assume that p has finite 2-moment. For all $x \in \mathbb{R}^d \setminus \Sigma_\Omega$, we let $x_\Omega := \text{proj}_\Omega(x)$. Then, we have that*

$$\lim_{t \rightarrow 1} m_t(x) = \text{proj}_\Omega(x).$$

Finally, we establish the following convergence rate for the posterior distribution when more assumptions are made on the data distribution p .

Theorem 4.5. *Assume that the reach $\tau = \tau_\Omega > 0$ is positive. Consider any $x \in \mathbb{R}^d$. We assume that $d_\Omega(x) < \frac{1}{2}\tau$ and that there exists $g \geq 0$ such that there exist constants $C, c > 0$ so that for any small radius $0 < r < c$, one has $p(B_r(x_\Omega)) \geq Cr^k$. Then, for any $0 < \zeta < 1$ we have the following convergence rate for any $0 < \sigma < c^{1/\zeta}$:*

$$d_{W,2}(p(\cdot|x_\sigma = x), \delta_{x_\Omega}) \leq \sqrt{\sigma^{2\zeta} + \frac{10^k(2M_2(p) + \|x_\Omega\|^2) \max\{\tau^k, \sigma^{k\zeta}\}}{C\sigma^{2k\zeta}} \exp\left(-\frac{1}{8}\sigma^{2(\zeta-1)}\right)} \leq C_{\zeta,\tau}\sigma^\zeta,$$

where $C_{\zeta,\tau}$ is a constant depending only on ζ and τ_Ω .

This convergence rate result plays a central role in the subsequent analysis of the convergence of flow matching ODE trajectories (cf. Theorem 5.3). The assumptions underlying this theorem serve as a primary basis for the assumptions outlined in Assumption 1, which are critical for our analysis of ODEs. Consequently, any refinement or improvement of this theorem could potentially enhance the subsequent analysis of ODEs.

4.2 Distinct behaviors for posterior convergence rates under data geometry

In this subsection, we will revisit Theorem 4.2 under different data geometries. In particular, we focus on two cases: (1) p is supported on a low-dimensional manifold $M \subset \mathbb{R}^d$ with smooth density with respect to the Hausdorff measure (note that we do not exclude the case when $M = \mathbb{R}^d$); (2) p is a discrete distribution supported on a finite set.

The first case is motivated by the fact that many real-world data distributions are supported on low-dimensional manifolds. However, in practice, one usually has no access to the manifold M but only to some samples drawn from p . Let $M_N = \{x^{(1)}, \dots, x^{(N)}\}$ denote N independent samples drawn from p , and let p^N denote the corresponding empirical probability measure. When training the objective function in Equation (3) with the empirical p_1^N , one unfortunately will obtain the unique *empirical optimal solution* $u_t^N(x)$ with closed form:

$$u_t^N(x) = (\log \beta_t)'x + \beta_t \cdot (\alpha_t/\beta_t)' \underbrace{\sum_{i=1}^N \frac{\exp\left(-\frac{\|x - \alpha_t x^{(i)}\|^2}{2\beta_t^2}\right) x_i}{\sum_{j=1}^N \exp\left(-\frac{\|x - \alpha_t x^{(j)}\|^2}{2\beta_t^2}\right)}}_{m_t^N(x)}. \quad (13)$$

Solving the ODE $\frac{dx_t}{dt} = u_t^N(x_t)$ with $x_0 \sim p_0$ will almost surely result in $x_1 \in M_N$. This is an extremely undesired effect as no new samples can be generated from the model. To avoid this issue, we believe certain modification of the training objective must be made. In order to achieve this goal, we first need to theoretically contrast the solution $u_t(x)$ with the empirical solution $u_t^N(x)$ under the manifold hypothesis mentioned above. This is why we focus on the convergence rates of the posterior distribution in these two geometries in this section. We also point out that the comparison of posterior distributions is necessary as one can hardly tell the difference between the empirical solution and the ground truth solution at the level of the over all distributions.

Proposition 4.6. *Assume that M_N is a good sample of M such that $d_{W,2}(p^N, p) = \epsilon$. Then, for any $t \in [0, 1]$, one has that $d_{W,2}(p_t, p_t^N) \leq \epsilon$.*

This result follows trivially from the fact that convolution will decrease the Wasserstein distance. We point out that, however, there is no simple way of bounding the difference between the posterior distributions $d_{W,2}(p(\cdot|x_t = x), p^N(\cdot|x_t = x))$ using $d_{W,2}(p^N, p)$. See Theorem 4.3 and Remark 4.4 in [MSW19] for some relevant results along this line.

In this section, we first tackle the convergence rates for the posterior distributions and will complete the convergence analysis for ODEs in Section 5.3.

An intuitive observation regarding the convergence rates. We start with an observation regarding the Jacobian of the denoisers $m_\sigma(x)$ and $m_\sigma^N(x)$. By Corollary 4.3 we have that $\lim_{\sigma \rightarrow 0} m_\sigma(x) = \text{proj}_M(x)$ and $\lim_{\sigma \rightarrow 0} m_\sigma^N(x) = \text{proj}_{M^N}(x)$. Now, we consider the Jacobians of the two projection maps.

Proposition 4.7. *For almost everywhere $x \in \mathbb{R}^d$, we have that*

1. $\nabla \text{proj}_M(x) = \Pi_{T_{x_M} M}$ where $x_M := \text{proj}_M(x)$ and $\Pi_{T_{x_M} M}$ is the orthogonal projection onto the tangent space $T_{x_M} M$;
2. $\nabla \text{proj}_{M^N}(x) = 0$.

Then, Proposition 3.1 and Proposition 4.7 imply the following results: if we assume that the convergence of m_σ to proj_M (resp. m_σ^N to proj_{M^N}) holds up to the 1st order derivatives as $t \rightarrow 1$ (this assumption is made for illustrative purposes only and is not rigorously justified here, serving instead to motivate the later results), then one has the following convergence as $\sigma \rightarrow 0$:

- $\frac{1}{2\sigma^2} \iint (z - z')(z - z')^T p(dz|x_\sigma = x) p(dz'|x_\sigma = x) \rightarrow \Pi_{T_{x_M} M}$
- $\frac{1}{2\sigma^2} \iint (z - z')(z - z')^T p^N(dz|x_\sigma = x) p^N(dz'|x_\sigma = x) \rightarrow 0$.

Note the $1/\sigma^2$ term in front of the integrals above. That the limits above exist immediately implies the following rate estimates (otherwise, the $1/\sigma^2$ term will result in a blowup behaviour instead of the convergence above)

- $\iint (z - z')(z - z')^T p(dz|x_\sigma = x) p(dz'|x_\sigma = x) = O(\sigma^2)$
- $\iint (z - z')(z - z')^T p^N(dz|x_\sigma = x) p^N(dz'|x_\sigma = x) = o(\sigma^2)$.

From this, we see that the convergence rate of the posterior must be significantly different when p is supported on a manifold or on discrete points. The illustrative calculation above suggests that (1) the convergence rate for the manifold case should be $O(\sigma)$, (2) whereas the discrete case should be $o(\sigma)$. These can be seen by roughly taking a square root for the integrals above as one can vaguely think of the above integrals as certain squares of the posteriors. Now, we establish our final rigorous results below.

Convergence rates for the manifold case. We first consider the case when p is supported on a submanifold $M \subset \mathbb{R}^d$. Note that this does not exclude the case when $M = \mathbb{R}^d$. Under some mild conditions, we have the following convergence rate for the posterior distribution.

Theorem 4.8. *Let $M \subset \mathbb{R}^d$ be a m dimensional closed submanifold (without self-intersection) with a positive reach τ_M . Assume that $dp(x) = \rho(x)d\text{vol}_M(x)$ has a smooth non-vanishing density $\rho : M \rightarrow \mathbb{R}$. For any $x \in \mathbb{R}^d$ and $\sigma \in (0, \infty)$, we let $x_M := \text{proj}_M(x)$. If $x \in \mathbb{R}^d$ satisfies that $d_M(x) < \frac{1}{2}\tau_M$, then we have that*

$$d_{W,2}(p(\cdot|x_\sigma = x), \delta_{x_M}) = \sqrt{m}\sigma + O(\sigma^2).$$

Note that the first-order convergence rate depends solely on the dimension of the submanifold, while higher-order information, such as the second fundamental form, is encapsulated within the big O notation. Specifying these higher-order contributions in detail would be an interesting direction for future work.

As a direct consequence of the convergence of the posterior distribution, we have the following convergence of the denoiser.

Corollary 4.9. *Under the same assumptions as in Theorem 4.8, for any $x \in \mathbb{R}^d$ satisfying $d_M(x) < \frac{1}{2}\tau_M$, we have that*

$$\|m_\sigma(x) - x_M\| = O(\sigma).$$

Convergence rates for the discrete case. Let the data distribution $p = \sum_{i=1}^N a_i \delta_{x_i}$ be a general discrete distribution with $x_1, \dots, x_N \in \mathbb{R}^d$ and $a_1, \dots, a_N > 0$. We use $\Omega = \{x_1, \dots, x_N\}$ to denote the support of p . We study the concentration and convergence of the posterior measure $p(\cdot|x_\sigma = x)$ for each $x \in \mathbb{R}^d$, including those x on Σ_Ω , the medial axis of Ω . To this end, we introduce the following notations.

For each point $x \in \mathbb{R}^d$, we denote the set of distance values from x to each point in Ω as follows:

$$\text{DV}_\Omega(x) := \{\|x - x_i\| : x_i \in \Omega\}. \quad (14)$$

We use $d_\Omega(x; i)$ to denote the i -th smallest distance value in $\text{DV}_\Omega(x)$. A useful geometric notion will be the gap between the squares of the two smallest distances which we denote by

$$\Delta_\Omega(x) := d_\Omega^2(x; 2) - d_\Omega^2(x; 1). \quad (15)$$

We further let

$$\text{NN}_\Omega(x) := \text{argmin}_{x_i \in \Omega} d_\Omega(x, x_i) = \left\{ x_i \in \Omega : \|x - x_i\| = d_\Omega(x; 1) = \min_{x_j \in \Omega} \|x - x_j\| \right\}.$$

We use the notation $\hat{p}_{\text{NN}(x)}$ to denote the normalized measure restricted to the points in Ω that are closest to x :

$$\hat{p}_{\text{NN}(x)} := \frac{1}{\sum_{x_i \in \text{NN}_\Omega(x)} a_i} \sum_{x_i \in \text{NN}_\Omega(x)} a_i \delta_{x_i}. \quad (16)$$

Whenever x is not on Σ_Ω , we have $\text{NN}_\Omega(x) = \{\text{proj}_\Omega(x)\}$ and $\hat{p}_{\text{NN}(x)} = \delta_{\text{proj}_\Omega(x)}$. With the above notation, we have the following convergence result for the posterior measure $p(\cdot|x_\sigma = x)$ as $\sigma \rightarrow 0$.

Theorem 4.10. *Let $p = \sum_{i=1}^N a_i \delta_{x_i}$ be a discrete distribution. For any $x \in \mathbb{R}^d$, we have the following convergence of the posterior measure $p(\cdot|x_\sigma = x)$ towards $\hat{p}_{\text{NN}(x)}$:*

$$d_{W,2}(p(\cdot|x_\sigma = x), \hat{p}_{\text{NN}(x)}) \leq \text{diam}(\Omega) \sqrt{\frac{1 - p(\text{NN}_\Omega(x))}{p(\text{NN}_\Omega(x))}} \exp\left(-\frac{\Delta_\Omega(x)}{4\sigma^2}\right).$$

As a corollary, we have the following convergence of the denoiser.

Corollary 4.11. *Let $p = \sum_{i=1}^N a_i \delta_{x_i}$ be a discrete distribution. For any $x \in \mathbb{R}^d$, we have the following convergence of the denoiser $m_\sigma(x)$ towards the mean of $\hat{p}_{\text{NN}(x)}$:*

$$\|m_\sigma(x) - \mathbb{E}(\hat{p}_{\text{NN}(x)})\| \leq \text{diam}(\Omega) \sqrt{\frac{1 - p(\text{NN}_\Omega(x))}{p(\text{NN}_\Omega(x))}} \exp\left(-\frac{\Delta_\Omega(x)}{4\sigma^2}\right).$$

In particular, when $x \notin \Sigma_\Omega$, assume that $x_i = \text{proj}_\Omega(x)$ we have that

$$\|m_\sigma(x) - x_i\| \leq \text{diam}(\Omega) \sqrt{\frac{1 - a_i}{a_i}} \exp\left(-\frac{\Delta_\Omega(x)}{4\sigma^2}\right).$$

Compared to the linear convergence rate in Corollary 4.9, the discrete setting exhibits an exponential convergence rate. Interestingly, this significant difference does not lead to any notable variation in the flow map convergence rate described in Theorem 5.4. Nevertheless, this discrepancy remains intriguing and could provide valuable insights into understanding the interplay between memorization and generalization in the future. Later in Section 6.3, we will utilize the above results to analyze the memorization behavior.

5 Well-Posedness of Flow Matching ODEs

With the concentration and convergence of the posterior distribution established, we now establish the well-posedness of the flow matching ODEs within the interval $t \in [0, 1)$ as well as the convergence property when $t \rightarrow 1$, in a general setting, including when the target data distribution p is not fully supported such as those concentrated on a submanifold. This is the first theoretical guarantee for such cases, addressing gaps in prior works [LHH⁺24, GHJ24] that impose restrictive assumptions excluding manifold-supported data.

5.1 Well-posedness of flow matching ODEs at $t \in [0, 1)$

First of all, we establish the existence of the flow map Ψ_t for $t \in [0, 1)$, i.e., the uniqueness and existence of the solution of Equation (1) for $t \in [0, 1)$. The following result was stated in the original flow matching paper [LCBH⁺22] under unspecified conditions and later on was proved in [GHJ24] in the case when p satisfies many regularity assumptions such as absolute continuity w.r.t. the Lebesgue measure. In our case, we only require that p has finite 2-moment, which significantly expands the applicability of the flow model.

Theorem 5.1. *As long as p has finite 2-moment, for any initial point $x_0 \sim p_{\text{prior}} = \mathcal{N}(0, I)$, there exists a unique solution $(x_t)_{t \in [0, 1)}$ for the ODE Equation (1). Furthermore, the corresponding flow map Ψ_t is continuous and satisfies that $(\Psi_t)_{\#} p_{\text{prior}} = p_t$ for all $t \in [0, 1)$.*

This proof involves carefully analyzing $\text{Cov}[p(\cdot|x_t)]$ to establish the locally Lipschitz property of the vector field $u_t(x)$ as well as establishing the integrability of the vector field so that we can apply the classic mass concentration result (see [Vil09]).

5.2 Well-posedness of flow matching ODEs at $t = 1$

Now, we establish the convergence of flow map Ψ_t as $t \rightarrow 1$ under mild assumptions and hence rule out the potential risk of divergence which can be a disaster for the flow model as shown in Figure 1a.

Assumption 1 (Regularity assumptions for the data distribution). Let p be a probability measure on \mathbb{R}^d . We assume that p satisfies the following properties:

1. p has a finite 2-moment, i.e., $\int_{\mathbb{R}^d} \|x\|^2 p(dx) < \infty$;
2. the support $\Omega := \text{supp}(p)$ has a positive reach $\tau_\Omega > 0^1$;
3. there exists $k \geq 0$ such that for any radius $R > 0$, there exist constants C_R, c_R so that for any small radius $0 \leq r < c_R$ and any $x \in B_R(0) \cap \Omega$, one has $p(B_r(x)) \geq C_R r^k$ for any $x \in \Omega$.

Many common data distributions satisfy the above assumptions and we list some of them below:

Example 5.2. 1. Any data distribution fully supported on \mathbb{R}^d with finite 2 moment and non-vanishing density, e.g., normal distribution, satisfies all the assumptions with $k = d$.

2. Any data distribution supported on a m -dimensional linear subspace with finite 1 moment and non-vanishing density, e.g., projected normal distribution, satisfies all the assumptions with $k = m$.

3. Any data distribution supported on a m -dimensional compact submanifold M with positive reach with a non-vanishing density with respect to the volume measure on M satisfies all the assumptions with $k = m$.

4. Any empirical data distribution with a finite number of samples satisfies all the assumptions with $k = 0$.

Now, we establish the main result of this section below. The major reason that we require the reach τ_Ω to be positive is to handle the geometric singularity mentioned in Section 3.2. In fact, due to the convergence of the posterior towards the projection, a small neighborhood of the support has a certain intricate attraction property as the one established in Theorem 3.5 for convex sets. In this way, we are able to ensure that an ODE trajectory will diverge from the medial axis and hence avoid the potential singularity issue. We need item 3 in Assumption 1 to ensure that at least locally, we can apply the posterior convergence rate result in Theorem 4.5 in a uniform way.

Theorem 5.3. Let p be a probability measure on \mathbb{R}^d satisfying the regularity assumptions in Assumption 1. Then,

1. The limit $\Psi_1(x) := \lim_{t \rightarrow 1} \Psi_t(x)$ exists almost everywhere with respect to the Lebesgue measure.
2. Ψ_1 is a measurable map and $(\Psi_1)_\# p_0 = p$.

Furthermore, we have the following estimate of the convergence rate of the flow map. Recall that $\sigma_t := \beta_t/\alpha_t$, then, we have that for any fixed $0 < \zeta < 1$,

$$\|\Psi_1(x) - \Psi_t(x)\| = O\left(\sigma_t^{\zeta/2}\right).$$

The ζ in the theorem above is inherited from Theorem 4.5. As such, we chose to retain the original formulation, avoiding the simplification of $\sigma_t^{\zeta/2}$ to σ_t^ζ , which would have required redefining $\zeta \in (0, 1/2)$.

Notice that the convergence rate is for very general data distribution p . In fact, if we further assume that p is supported on a compact manifold or a discrete set, then the convergence rate can be improved. See Section 5.3 below for more details.

¹The support Ω can be the whole space \mathbb{R}^d and in this case the reach $\tau = \infty$.

5.3 Refined convergence rates for manifolds and discrete cases

Now, we go back to the manifold hypothesis and give a detailed convergence analysis for the manifold case and the sampling case. Based on the convergence rates we established in Section 4.2, we develop the following ODE convergence result which is a refined version of Theorem 5.3. Unlike the vast difference in posterior convergence and in denoiser convergence, the ODE convergence rates of the manifold case and the discrete case are rather similar. This is a bit surprising but we will explain intuitively why this should be the case at the end.

Theorem 5.4. *When p is supported on a submanifold or a discrete set, we have the following convergence rates for the flow map Ψ_t as $t \rightarrow 1$.*

- *Let M be a m dimensional closed submanifold (without self-intersection). Assume that $dp(x) = \rho(x)d\text{vol}_M(x)$ has a smooth nonvanishing density $\rho : M \rightarrow \mathbb{R}$, a positive reach τ_M and a positive injective radius r_M . We further assume that the second fundamental form \mathbf{II} and its covariant derivative $\nabla\mathbf{II}$ are bounded on M . Then, for almost everywhere $x \in \mathbb{R}^d$, we have that*

$$\|\Psi_1(x) - \Psi_t(x)\| = O(\sqrt{\sigma_t});$$

- *If $p = \sum_{i=1}^N a_i x_i$ denotes a discrete probability measure, then for almost everywhere $x \in \mathbb{R}^d$, we have that*

$$\|\Psi_1(x) - \Psi_t(x)\| = O(\sigma_t).$$

Note that the geometric conditions for manifolds in the theorem are mild. These conditions only guarantee that the submanifold will not have “sharp turns” in the ambient space \mathbb{R}^d . For example, it includes the case when $M = \mathbb{R}^d$ and M is any low dimensional subspace or any compact submanifold, such as a sphere, torus, etc.

The rate for the discrete case is optimal as shown in the example below.

Example 5.5. *Consider the one point set $M_1 = \{x_1\}$ with $p := \delta_{x_1}$. Then, when choosing $\alpha_t = t$ and $\beta_t = 1 - t$, one has that starting with any $x_0 \in \mathbb{R}^d$, its ODE trajectory is given by $(x_t = (1 - t)x_0 + tx_1)_{t \in [0,1]}$. Therefore, $\|x_1 - x_t\| = (1 - t)\|x_0 - x_1\| = O(1 - t) = O(\sigma_t)$. Hence, the flow map Ψ_t has a linear convergence rate.*

However, we do not know whether the rate for the manifold case is optimal or not. In fact, we conjecture that the rate can be improved to the linear rate σ_t for the manifold case as well and hence the ODE convergence rate does not differ between the manifold case and the discrete case. This conjecture is motivated from the fact that the distribution $q_\sigma \rightarrow p$ with linear rate $O(\sigma)$ (see the proposition below) and hence its associated ODE should intuitively converge with the same rate.

Proposition 5.6. *For any probability measure p with finite 2-moment, we have that*

$$d_{W,2}(q_\sigma, p) = O(\sigma).$$

We note that the above proposition is relatively straightforward compared to the posterior convergence established in Theorem 4.2. This provides further evidence (in addition to Proposition 4.6 and the subsequent discussion) for the importance of focusing on analyzing the posterior rather than the entire data distribution.

5.4 Equivariance of the flow maps under data transformations

We have established in Theorem 5.3 the existence of the flow map $\Psi_1 : \mathbb{R}^d \rightarrow \mathbb{R}^d$ sending directly any sampled point $x_0 \sim p_0 = \pi$ to a point x_1 following the target data distribution $p_1 = p$. In this regard, it is of interest to establish theoretical properties of the flow map. In this subsection, we examine how the flow map Ψ_1 behaves under certain transformations $T : \mathbb{R}^d \rightarrow \mathbb{R}^d$ of the data distribution p . More precisely, after certain transformation, one obtains a new data distribution $\tilde{p} := T_{\#}p$. We then consider applying the flow model to the new data distribution \tilde{p} and examine the corresponding flow map. In this paper, we focus on rigid transformations and scaling, leaving the investigation of other transformations for future work.

Rigid transformations Consider the rigid transformation $y = \mathbf{O}x + b$ where $\mathbf{O} \in \mathbb{R}^{d \times d}$ is an orthogonal matrix and $b \in \mathbb{R}^d$ is any vector. It turns out that if we apply the flow model to such a transformed data distribution \tilde{p} with the same scheduling functions α_t and β_t , the flow map $\tilde{\Psi}_1$ is also a rigid transformation of the original flow map Ψ_1 , i.e.,

$$\tilde{\Psi}_1(y) = \mathbf{O}\Psi_1(x) + b$$

In fact, if we let $\tilde{m}_t, \tilde{u}_t, \tilde{\Psi}_t$ denote the corresponding denoiser, vector field, and flow map associated with \tilde{p} , we establish the following result.

Theorem 5.7 (Equivariance under rigid transformations). *For any $x \in \mathbb{R}^d$ and $t \in [0, 1]$, if we let $y = \mathbf{O}x + \alpha_t b$, then*

$$\tilde{m}_t(y) = \mathbf{O}m_t(x) + b, \quad \tilde{u}_t(y) = \mathbf{O}u_t(x) + \dot{\alpha}_t b, \quad \tilde{\Psi}_t(y) = \mathbf{O}\Psi_t(x) + \alpha_t b,$$

where $\dot{\alpha}_t$ represents the derivative of α_t with respect to t . In particular, $\tilde{\Psi}_1(y) = \mathbf{O}\Psi_1(x) + b$.

Scaling We now consider the effect on the flow map when the data is scaled by a factor $k > 0$, i.e., $y = kx$. This case is more intricate than the previous two cases, as one needs to change the scheduling functions to obtain the invariance property of the flow map.

Assume that an initial flow model is applied to p_1 with scheduling functions α_t and β_t . Let $s_t : [0, 1] \rightarrow \mathbb{R}$ denote any smooth function so that $s_0 = 1$ and $s_1 = k$. Then, consider $\bar{\alpha}_t = s_t \alpha_t / k$ and $\bar{\beta}_t = s_t \beta_t$. These are still legitimate scheduling functions. We let $\bar{m}_t, \bar{u}_t, \bar{\Psi}_t$ denote the corresponding denoiser, vector field, and flow map associated with the scaled data distribution $k \cdot p$ and the new scheduling functions $\bar{\alpha}_t$ and $\bar{\beta}_t$. We establish the following result.

Theorem 5.8 (Equivariance under scaling transformations). *For any $x \in \mathbb{R}^d$ and $t \in [0, 1]$, if we let $y = s_t x$, then*

$$\bar{m}_t(y) = s_t \cdot m_t(x), \quad \bar{\Psi}_t(y) = s_t \cdot \Psi_t(x).$$

In particular, $\bar{\Psi}_1(y) = k \cdot \Psi_1(x)$.

6 Attraction Dynamics of Flow Matching ODEs

In this section, we utilize the concentration and convergence results of the posterior distribution to analyze the attraction dynamics of the flow matching ODEs.

Following the flow matching ODE, when using σ , the ODE trajectory can be simply interpreted as moving towards the denoiser at each time step. Intuitively, the posterior measure $p(\cdot | x_\sigma)$ initially agrees with the true data distribution p , then progressively concentrates on nearby data points as

the ODE trajectory evolves. Eventually, as the noise level σ goes to zero, the ODE trajectory will be attracted to the nearest data point almost surely. We will instantiate this intuition and provide rigorous results. We will first analyze the initial stage of the sampling process and then discuss the attraction dynamics towards a local cluster of data points in the intermediate stage. Finally, we will discuss the terminal behavior of the ODE trajectory under the discrete measure along with its connection with memorization.

6.1 Initial stage of the sampling process

We work under the mild assumption that the data distribution p is either supported or concentrated on some bounded set. More precisely, we assume that p has the form $p = p_b * \mathcal{N}(0, \delta^2 I)$ where p_b has a bounded support for $\delta \in [0, \infty)$ with 2-moment and hence the ODE trajectories of the flow model are well-defined (cf. Section 5.1). We now apply the above proposition to analyze the initial stage of the sampling process in the flow model.

The initial stage of the sampling process corresponds with σ being with a large value T with which the initial sample $x_{\sigma=T}$ is transformed from $x_{t_{\sigma=T}}/\alpha_{t_{\sigma=T}}$. As T is large, $t_{\sigma=T}$ is close to 0, and hence $x_{t_{\sigma=T}}/\alpha_{t_{\sigma=T}}$ has an very large norm. In this case, $x_{\sigma=T}$ is likely outside the support of p_b . Therefore, the above corollary describes the initial stage of the sampling process.

By the initial stability of the posterior distribution, the denoiser will be close to the mean of the data distribution. We then have the following proposition which describes the initial stage as moving towards the mean of the data distribution.

Proposition 6.1 (Initial stage: Moving towards the data mean). *Let $p = p_b * \mathcal{N}(0, \delta^2 I)$ be a probability measure on \mathbb{R}^d with p_b having a bounded support which is denoted as $\Omega := \text{supp}(p_b)$. Let x_0 be a point and denote $\|x_0 - \mathbb{E}(p)\| = R_0$. Let ζ be a parameter such that $0 < \zeta < 1$. Then there exist a constant*

$$\sigma_{\text{init}}(\Omega, \zeta, R_0) := \sqrt{\frac{2R_0 \text{diam}(\Omega)}{\log\left(1 + \frac{\zeta R_0}{\text{diam}(\Omega)}\right)}}$$

such that for all $\sigma_1 > \sqrt{\sigma_{\text{init}}(\Omega, \zeta, R_0)^2 + \delta^2}$, a trajectory $(x_\sigma)_{\sigma \in (\sqrt{\sigma_{\text{init}}(\Omega, \zeta, R_0)^2 + \delta^2}, \sigma_1]}$ starting from $x_{\sigma_1} = x_0$ will move towards the mean of the data distribution p . Additionally, we have the following decay result:

$$\|x_\sigma - \mathbb{E}(p)\| < \frac{(\sigma^2 + \delta^2)^{\frac{1-\zeta}{2}}}{(\sigma_1^2 + \delta^2)^{\frac{1-\zeta}{2}}} R_0.$$

Note that an ζ close to 1 will make $\sigma_{\text{init}}(\Omega, \zeta, R_0)$ smaller and hence better convergence of the entire sampling process. However, the decay guarantee will be weaker as ζ approaches 1.

How close the trajectory will be to the mean of the data distribution depends on the initial distance and how fast the posterior distribution concentrates. However, the trajectory will necessarily reach the convex hull of the support of p_b as σ goes to zero.

Proposition 6.2. *Given the data distribution p defined above, for any $\sigma_1 > 0$, let x_σ be an ODE trajectory of Equation (8) from $\sigma = \sigma_1$ to $\sigma = 0$. Then, we have that*

1. If $x_{\sigma_1} \in \text{conv}(\text{supp}(p_b))$, then $x_\sigma \in \text{conv}(\text{supp}(p_b))$ for any $\sigma \in (0, \sigma_1]$;
2. If $x_{\sigma_1} \notin \text{conv}(\text{supp}(p_b))$, then x_σ moves towards $\text{conv}(\text{supp}(p_b))$ with the following decay guarantee:

$$d_{\text{conv}(\text{supp}(p_b))}(x_\sigma) \leq \frac{\sqrt{\sigma^2 + \delta^2}}{\sqrt{\sigma_1^2 + \delta^2}} d_{\text{conv}(\text{supp}(p_b))}(x_{\sigma_1}),$$

for any $\sigma \in (0, \sigma_1]$.

6.2 Intermediate stage of the sampling process

Now we have described the flow matching ODE dynamics at initial (cf. Section 3.3). In this subsection, we shed light on the intermediate stage by showing that the ODE trajectory will be attracted towards the convex hull of local clusters of data under some assumptions.

We start by assuming that the data distribution p contains a “local cluster” or “local mode”. More precisely, we consider the following assumptions.

Assumption 2. Let p be a probability measure on \mathbb{R}^d . We assume that p that has a well separated local cluster S , specifically, we assume that p satisfies the following properties:

1. $\text{supp}(p) = S \cup (\Omega \setminus S)$, where S is a closed bounded set with diameter $D := \text{diam}(S) < \infty$.
2. $\Omega \setminus S$ satisfies $d_{\text{conv}(S)}(x) > 2D$ for all $x \in \Omega \setminus S$.

Then, it turns out that for any point y that is close to the convex hull of S , the denoiser $m_\sigma(y)$ will be attracted to the convex hull of S as σ goes to zero.

Proposition 6.3. *Assume that p satisfies Assumption 2. Then, for any $x \in \mathbb{R}^d$ such that $d_{\text{conv}(S)}(x) \leq D/2 - \epsilon$, we have that*

$$d_{\text{conv}(S)}(m_\sigma(x)) \leq \text{diam}(\text{supp}(p)) \sqrt{\frac{1 - a_S}{a_S}} \exp\left(-\frac{3D\epsilon}{2\sigma^2}\right),$$

where $a_S := p(S)$ which is obviously positive.

From the above proposition, we can show that the ODE trajectory starting from y will be attracted to the convex hull of S as σ goes to zero.

Proposition 6.4. *Assume that p satisfies Assumption 2. There exists a parameter $\sigma_0(S, \epsilon)$ such that for all $\sigma_0 < \sigma_0(S, \epsilon)$, and for any x such that $d_{\text{conv}(S)}(x) \leq D/2 - \epsilon$, the trajectory $(x_\sigma)_{\sigma \in (0, \sigma_0]}$ starting from $x_{\sigma_0} = x$ will converge to the convex hull of S as $\sigma \rightarrow 0$.*

Remark 6.5. *A well separated local cluster can be regarded as a local mode of the data distribution. The above proposition give a quantitative measure when the ODE trajectory will be attracted to the local mode.*

6.3 Terminal stage of the sampling process and memorization behavior

The local cluster dynamics described in the previous subsection can be manifested in the terminal stage of a discrete data distribution where each data point can eventually be regarded as a local cluster. In this subsection, we will show that the ODE trajectory will be attracted to the nearest data point as σ goes to zero and discuss the memorization behavior of the flow model.

We will first introduce some necessary notations and definitions. *Throughout this subsection, p denotes a discrete distribution $p = \sum_{i=1}^n a_i \delta_{x_i}$.* We let $\Omega = \{x_1, \dots, x_n\}$ denote its support. The *Voronoi diagram* of Ω gives a partition of \mathbb{R}^d into regions V_i 's based on the closeness to the data points:

$$V_i := \{x : \|x - x_i\| \leq \|x - x_j\|, \forall x_j \in \Omega\}.$$

In particular, each V_i is a connected closed convex region and the union of all V_i 's covers the whole space \mathbb{R}^d . The boundary of the region V_i consists of exactly the points on Σ_Ω , the medial axis of Ω .

We will also consider a family of regions V_i^ϵ that lies inside V_i and covers all interior points of V_i as ϵ goes to zero. Specifically, let $0 < \epsilon < d_\Omega(x_i)$ be a small positive number, we use V_i^ϵ to denote the region

$$V_i^\epsilon := \{x : \|x - x_i\|^2 \leq \|x - x_j\|^2 - \epsilon^2, \forall x_j \in \Omega, j \neq i\}. \quad (17)$$

Similar to the condition for V_i , each V_i^ϵ is intersection of finitely many half-spaces and hence is a convex region.

For each $y \in V_i^\epsilon$, x_i is the unique nearest data point to y and the posterior measure $p(\cdot | x_\sigma = y)$ will be fully concentrated at x_i as σ goes to zero as shown in Theorem 4.10. As a consequence, we can identify a time $\sigma_0(V_i^\epsilon)$ as follows such that the ODE trajectory will never leave the region V_i^ϵ for $\sigma < \sigma_0(V_i^\epsilon)$. We use $\text{sep}(x_i)$ to denote the minimum distance from x_i to other data points in Ω and introduce a constant $C_{i,\epsilon}^\Omega = \frac{2\text{sep}(x_i)}{\text{sep}^2(x_i) - \epsilon^2} \cdot \sqrt{\frac{1-a_i}{a_i}} \cdot \text{diam}(\Omega)$ that depends on the data support Ω , specific point x_i , and the parameter $\epsilon \in (0, \text{sep}(x_i)/2)$. Then the time $\sigma_0(V_i^\epsilon)$ is defined as

$$\sigma_0(V_i^\epsilon) = \begin{cases} \infty, & \text{if } C_{i,\epsilon} \leq 1, \\ \frac{\epsilon}{2} (\log(C_{i,\epsilon}))^{-1/2}, & \text{if } C_{i,\epsilon} > 1, \end{cases}$$

We have the following proposition.

Proposition 6.6 (Terminal absorbing behavior under discrete distribution). *Fix an arbitrary $0 < \sigma_1 < \sigma_0(V_i^\epsilon)$. Then, for any $y \in V_i^\epsilon$, the ODE trajectory $(x_\sigma)_{\sigma \in (0, \sigma_0]}$ starting from $x_{\sigma_0} = y$ will stay inside V_i^ϵ , i.e., $x_\sigma \in V_i^\epsilon$.*

With the above propositions, we can show that the ODE trajectory inside V_i^ϵ will be attracted to x_i as σ goes to zero.

Proposition 6.7. *Fix an arbitrary $0 < \sigma_0 < \sigma_0(V_i^\epsilon)$. Then, for any $y \in V_i^\epsilon$, the ODE trajectory $(x_\sigma)_{\sigma \in (0, \sigma_0]}$ starting from $x_{\sigma_0} = y$ will converge to x_i as σ goes to zero.*

Note that this result is complementary to the discrete part of Theorem 5.4 in the sense that we can identify a fairly explicit time $\sigma_0(V_i^\epsilon)$ such that the current nearest data point is what the ODE trajectory will converge to. This is in contrast to the general convergence rate of the flow map as $t \rightarrow 1$ in Theorem 5.4.

Discussion on Memorization The constant $\sigma_0(V_i^\epsilon)$ in Proposition 6.7 can be regarded as a time under which a trajectory near the data point x_i will eventually converge to x_i under the flow matching ODE for the empirical data distribution. In particular, the empirical optimal solution will only be able to repeat the training data points in the terminal stage of the sampling process—a phenomenon known as *memorization*. The constant $\sigma_0(V_i^\epsilon)$ can then be used as a measure of the memorization time for the empirical optimal solution. When considering the CIFAR-10 dataset and choose $\epsilon = 1.0$, the averaged value of $\sigma_0(V_i^\epsilon)$ over all data points is around 0.17 which covers the last one fourth of the sampling process in the popular sampling schedule used in [KAAL22].

Furthermore, we want to emphasize that the memorization for the flow model is particularly depends on the denoiser near terminal time. In particular, if the denoiser is asymptotically close to the empirical denoiser, the flow model will only memorize the empirical data. This is formalized in the following proposition.

For the following, we will consider a neural network trained denoiser m_σ^θ and its corresponding ODE trajectory $(x_\sigma^\theta)_{\sigma \in (0, \sigma_0]}$ following the flow matching ODE with m_σ replaced by m_σ^θ , that is,

$$\frac{dx_\sigma^\theta}{d\sigma} = -\frac{1}{\sigma} \left(m_\sigma^\theta(x_\sigma) - x_\sigma^\theta \right), \quad (18)$$

Proposition 6.8 (Memorization of trained denoiser). *Let p denote a discrete probability measure and let m_σ denote its denoiser. Let $m_\sigma^\theta : \mathbb{R}^d \rightarrow \mathbb{R}^d$ be any smooth map (which should be regarded as any neural network trained denoiser). Assume that there exists a function $\phi(\sigma)$ such that $\lim_{\sigma \rightarrow 0} \phi(\sigma) = 0$ and*

$$\|m_\sigma^\theta(x) - m_\sigma(x)\| \leq \phi(\sigma), \text{ for all } x \in \mathbb{R}^d.$$

Then, there exists a parameter $\sigma_0(V_i^\epsilon, \phi) > 0$ such that for all $\sigma_0 < \sigma_0(V_i^\epsilon, \phi)$, and for any $y \in V_i^\epsilon$, the ODE trajectory $(x_\sigma^\theta)_{\sigma \in (0, \sigma_0]}$ for Equation (8) (with m_σ replaced by m_σ^θ) starting from $x_{\sigma_0} = y$ will converge to x_i as $\sigma \rightarrow 0$.

Note that the above proposition do not necessarily specifying the convergence of x_σ^θ and can be applied in general. In the case where we do have convergence of x_σ^θ and the the limit of the denoiser $m_\sigma^\theta(x_\sigma^\theta)$, the two limits will coincide. This is formalized in the following proposition.

Proposition 6.9. *Let $m_\sigma^\theta : \mathbb{R}^d \rightarrow \mathbb{R}^d$ be any smooth map (which should be regarded as any neural network trained denoiser). Assume that the ODE trajectory $(x_\sigma^\theta)_{\sigma \in (0, \sigma_0]}$ for Equation (8) has a limit as $\sigma \rightarrow 0$ and the limit $\lim_{\sigma \rightarrow 0} m_\sigma^\theta(x_\sigma^\theta)$ also exist. Then, we must have that*

$$\lim_{\sigma \rightarrow 0} \|m_\sigma^\theta(x_\sigma^\theta) - x_\sigma^\theta\| = 0.$$

This proposition shows that the final output of the flow model is determined by the behavior of the denoiser near the terminal time. In particular, the output is confined by the pointwise limits of the denoiser unlike a generic ODE where the near terminal time behavior only partially influence the final output. Therefore, for a flow model to have good generalization ability, it is crucial to ensure that the trained denoiser is diverse near terminal time and covers the entire data distribution—where the empirical optimal solution fails.

7 Discussion

Our study lays a steady theoretical foundation for the flow-matching model, especially in the case when data distribution is supported on a low dimensional manifold. Our analysis of the ODE dynamics, as well as the contrast between the manifold and sampling scenarios, will help shed light on designing better variants of the flow matching model that are memorization-free and with better generalization ability.

In particular, we point out the following two possible future directions. Suppose the submanifold M has intrinsic dimension k . Then, $\text{tr} \nabla_x m_1 \equiv k$ whereas $\text{tr} \nabla_x m_1^N \equiv 0$ (cf. Proposition 4.7). From this perspective, one can already see a huge difference between the empirical solution and the ground truth solution. This motivates us to consider incorporating the Jacobian of the denoiser into the training of the flow matching model to minimize memorization. Our analysis of the attraction region of the flow matching ODE in the discrete case also suggests that one should be careful on training the denoiser near the terminal time to avoid memorization.

Our general convergence result contains a coefficient that depends on the reach of the data support which is not stable under perturbations. However, some of our results can potentially be refined by using local variants of the reach, such as the local feature size, which could yield more robust and stronger theoretical guarantees.

Acknowledgements. This work is partially supported by NSF grants CCF-2112665, CCF-2217058, CCF-2310411 and CCF-2403452.

References

- [AB98] Nina Amenta and Marshall Bern. Surface reconstruction by voronoi filtering. In *Proceedings of the fourteenth annual symposium on Computational geometry*, pages 39–48, 1998.
- [BBDBM24] Giulio Biroli, Tony Bonnaire, Valentin De Bortoli, and Marc Mézard. Dynamical regimes of diffusion models. *Nature Communications*, 15(1):9957, 2024.
- [BDD23] Joe Benton, George Deligiannidis, and Arnaud Doucet. Error bounds for flow matching methods. *arXiv preprint arXiv:2305.16860*, 2023.
- [BHHS22] Clément Berenfeld, John Harvey, Marc Hoffmann, and Krishnan Shankar. Estimating the reach of a manifold via its convexity defect function. *Discrete & Computational Geometry*, 67(2):403–438, 2022.
- [Bia23] Adam Białyzyt. The tangent cone, the dimension and the frontier of the medial axis. *Nonlinear Differential Equations and Applications NoDEA*, 30(2):27, 2023.
- [CHN⁺23] Nicolas Carlini, Jamie Hayes, Milad Nasr, Matthew Jagielski, Vikash Sehwal, Florian Tramèr, Borja Balle, Daphne Ippolito, and Eric Wallace. Extracting training data from diffusion models. In *32nd USENIX Security Symposium (USENIX Security 23)*, pages 5253–5270, 2023.
- [CZW⁺24] Defang Chen, Zhenyu Zhou, Can Wang, Chunhua Shen, and Siwei Lyu. On the trajectory regularity of ode-based diffusion sampling. In *Forty-first International Conference on Machine Learning*, 2024.
- [dM37] MR de Mises. La base géométrique du théoreme de m. mandelbrojt sur les points singuliers d’une fonction analytique. *CR Acad. Sci. Paris Sér. I Math*, 205:1353–1355, 1937.
- [Efr11] Bradley Efron. Tweedie’s formula and selection bias. *Journal of the American Statistical Association*, 106(496):1602–1614, 2011.
- [EKB⁺24] Patrick Esser, Sumith Kulal, Andreas Blattmann, Rahim Entezari, Jonas Müller, Harry Saini, Dominik Lorenz Yam Levi, Axel Sauer, Frederic Boesel, Dustin Podell, Tim Dockhorn, Zion English, and Robin Rombach. Scaling rectified flow transformers for high-resolution image synthesis. In *Forty-first International Conference on Machine Learning*, 2024.
- [Fed59] Herbert Federer. Curvature measures. *Transactions of the American Mathematical Society*, 93(3):418–491, 1959.
- [GHJ24] Yuan Gao, Jian Huang, and Yuling Jiao. Gaussian interpolation flows. *Journal of Machine Learning Research*, 25(253):1–52, 2024.
- [GPAM⁺14] Ian Goodfellow, Jean Pouget-Abadie, Mehdi Mirza, Bing Xu, David Warde-Farley, Sherjil Ozair, Aaron Courville, and Yoshua Bengio. Generative adversarial nets. *Advances in neural information processing systems*, 27, 2014.
- [HJA20] Jonathan Ho, Ajay Jain, and Pieter Abbeel. Denoising diffusion probabilistic models. *Advances in neural information processing systems*, 33:6840–6851, 2020.

- [HW20] Daniel Hug and Wolfgang Weil. *Lectures on convex geometry*, volume 286. Springer, 2020.
- [KAAL22] Tero Karras, Miika Aittala, Timo Aila, and Samuli Laine. Elucidating the design space of diffusion-based generative models. *Advances in neural information processing systems*, 35:26565–26577, 2022.
- [KG24] Diederik Kingma and Ruiqi Gao. Understanding diffusion objectives as the elbo with simple data augmentation. *Advances in Neural Information Processing Systems*, 36, 2024.
- [LC24] Marvin Li and Sitan Chen. Critical windows: non-asymptotic theory for feature emergence in diffusion models. *arXiv preprint arXiv:2403.01633*, 2024.
- [LCBH⁺22] Yaron Lipman, Ricky TQ Chen, Heli Ben-Hamu, Maximilian Nickel, and Matthew Le. Flow matching for generative modeling. In *The Eleventh International Conference on Learning Representations*, 2022.
- [LGL23] Xingchao Liu, Chengyue Gong, and Qiang Liu. Flow straight and fast: Learning to generate and transfer data with rectified flow. In *International conference on learning representations (ICLR)*, 2023.
- [LHH⁺24] Yaron Lipman, Marton Havasi, Peter Holderrieth, Neta Shaul, Matt Le, Brian Karrer, Ricky TQ Chen, David Lopez-Paz, Heli Ben-Hamu, and Itai Gat. Flow matching guide and code. *arXiv preprint arXiv:2412.06264*, 2024.
- [LZB⁺22] Cheng Lu, Yuhao Zhou, Fan Bao, Jianfei Chen, Chongxuan Li, and Jun Zhu. Dpm-solver: A fast ODE solver for diffusion probabilistic model sampling in around 10 steps. *Advances in Neural Information Processing Systems*, 35:5775–5787, 2022.
- [MMASC14] Maria G Monera, A Montesinos-Amilibia, and Esther Sanabria-Codesal. The taylor expansion of the exponential map and geometric applications. *Revista de la Real Academia de Ciencias Exactas, Físicas y Naturales. Serie A. Matemáticas*, 108:881–906, 2014.
- [MMWW23] Facundo Mémoli, Axel Munk, Zhengchao Wan, and Christoph Weitkamp. The ultrametric Gromov–Wasserstein distance. *Discrete & Computational Geometry*, 70(4):1378–1450, 2023.
- [MSLE21] Chenlin Meng, Yang Song, Wenzhe Li, and Stefano Ermon. Estimating high order gradients of the data distribution by denoising. *Advances in Neural Information Processing Systems*, 34:25359–25369, 2021.
- [MSW19] Facundo Memoli, Zane Smith, and Zhengchao Wan. The Wasserstein transform. In *International Conference on Machine Learning*, pages 4496–4504. PMLR, 2019.
- [PY24] Frank Permenter and Chenyang Yuan. Interpreting and improving diffusion models from an optimization perspective. In *Forty-first International Conference on Machine Learning*, 2024.
- [RTG98] Yossi Rubner, Carlo Tomasi, and Leonidas J Guibas. A metric for distributions with applications to image databases. In *Sixth international conference on computer vision (IEEE Cat. No. 98CH36271)*, pages 59–66. IEEE, 1998.

- [SBDS24] Jan Pawel Stanczuk, Georgios Batzolis, Teo Deveney, and Carola-Bibiane Schönlieb. Diffusion models encode the intrinsic dimension of data manifolds. In *Forty-first International Conference on Machine Learning*, 2024.
- [SDCS23] Yang Song, Prafulla Dhariwal, Mark Chen, and Ilya Sutskever. Consistency models. In *International Conference on Machine Learning*, pages 32211–32252. PMLR, 2023.
- [SDWGM15] Jascha Sohl-Dickstein, Eric Weiss, Niru Maheswaranathan, and Surya Ganguli. Deep unsupervised learning using nonequilibrium thermodynamics. In *International conference on machine learning*, pages 2256–2265. PMLR, 2015.
- [SE19] Yang Song and Stefano Ermon. Generative modeling by estimating gradients of the data distribution. *Advances in neural information processing systems*, 32, 2019.
- [SME21a] Jiaming Song, Chenlin Meng, and Stefano Ermon. Denoising diffusion implicit models. In *International Conference on Learning Representations*, 2021.
- [SME21b] Jiaming Song, Chenlin Meng, and Stefano Ermon. Denoising diffusion implicit models. In *9th International Conference on Learning Representations, ICLR 2021, Virtual Event, Austria, May 3-7, 2021*. OpenReview.net, 2021.
- [SPC⁺24] Neta Shaul, Juan Perez, Ricky TQ Chen, Ali Thabet, Albert Pumarola, and Yaron Lipman. Bespoke solvers for generative flow models. In *The Twelfth International Conference on Learning Representations*, 2024.
- [Vil03] Cédric Villani. *Topics in Optimal Transportation*. Number 58. American Mathematical Soc., 2003.
- [Vil09] Cédric Villani. *Optimal transport: old and new*, volume 338. Springer, 2009.
- [WLCL24] Yuxin Wen, Yuchen Liu, Chen Chen, and Lingjuan Lyu. Detecting, explaining, and mitigating memorization in diffusion models. In *The Twelfth International Conference on Learning Representations*, 2024.
- [ZYLX24a] Pengze Zhang, Hubery Yin, Chen Li, and Xiaohua Xie. Formulating discrete probability flow through optimal transport. *Advances in Neural Information Processing Systems*, 36, 2024.
- [ZYLX24b] Pengze Zhang, Hubery Yin, Chen Li, and Xiaohua Xie. Tackling the singularities at the endpoints of time intervals in diffusion models. In *Proceedings of the IEEE/CVF Conference on Computer Vision and Pattern Recognition*, pages 6945–6954, 2024.

A Geometric Notions and Results

In this section, we recall some basic geometric notions and establish some results that are used in the proofs. The geometric results are of independent interest and can be used in other contexts as well.

A.1 Convex geometry notions and results

In this subsection, we collect some basic notions and results in convex geometry that are used in the proofs. Our main reference is the book [HW20].

We first introduce the definition of a convex set and convex function.

Definition 1 (Convex set). A set $K \subset \mathbb{R}^d$ is called a *convex set* if for any $x_1, \dots, x_n \in K$ and $0 \leq \alpha_1, \dots, \alpha_n \leq 1$ such that $\sum_{i=1}^n \alpha_i = 1$, we have that $\sum_{i=1}^n \alpha_i x_i \in K$.

Definition 2 (Convex function). A function $f : \mathbb{R}^d \rightarrow \mathbb{R}$ is called a *convex function* if for any $x, y \in \mathbb{R}^d$ and $0 \leq \alpha \leq 1$, we have that $f(\alpha x + (1 - \alpha)y) \leq \alpha f(x) + (1 - \alpha)f(y)$.

An intermediate result that the sublevel sets $\{f < c\}$ or $\{f \leq c\}$ of a convex function f are convex sets, see [HW20, Remark 2.6].

We then introduce the definition of the convex hull of a set.

Definition 3 (Convex hull [HW20, Definition 1.3, Theorem 1.2]). The *convex hull* of a set $\Omega \subset \mathbb{R}^d$ is the smallest convex set that contains Ω and is denoted by $\text{conv}(\Omega)$. Additionally, we have that

$$\text{conv}(\Omega) = \left\{ \sum_{i=1}^n \alpha_i x_i : k \in \mathbb{N}, x_i \in \Omega, \alpha_i \in [0, 1], \sum_{i=1}^n \alpha_i = 1 \right\}.$$

Let Ω be a set, and $x \in \Omega$. We say a hyperplane give by a linear function H is a supporting hyperplane of Ω at x if the following holds:

1. $H(x) = 0$.
2. $H(y) \geq 0$ for all $y \in \Omega$.

For a closed convex set Ω , every boundary point of Ω has a supporting hyperplane.

Proposition A.1 (Supporting hyperplane [HW20, Theorem 1.16]). *Let K be a closed convex set in \mathbb{R}^d and $x \in \partial K$. Then, there exists a supporting hyperplane of K at x .*

The following lemma will be of useful in the later proofs.

Lemma A.2. *Let K be a closed convex set, and x_t be a trajectory in \mathbb{R}^d such that $x_{t_0} \in K$ for some t_0 and $x_t \notin K$ for all $t \in (t_0 - \epsilon, t_0)$ for some $\epsilon > 0$. Then, if we write the tangent vector of the trajectory at x_{t_0} as $\dot{x}_{t_0} = v - x_{t_0}$, then v cannot lie in the interior of K .*

Proof. Let H be a supporting hyperplane of K at x_{t_0} such that $H(x_{t_0}) = 0$ and $H(y) \geq 0$ for all $y \in K$. In particular, we can write $H(y) = \langle y - x_{t_0}, n \rangle$, where n is the unit normal vector of the hyperplane. Since $x_t \in K$ for all $t \in (t_0 - \epsilon, t_0)$, we must have that $\frac{dH(x_t)}{dt}|_{t=t_0} \leq 0$. Therefore, we have that

$$\frac{dH(x_t)}{dt}|_{t=t_0} = \langle \dot{x}_{t_0}, n \rangle = \langle v - x_{t_0}, n \rangle \leq 0.$$

Note that for any point z in the interior of K , we have that $H(z) = \langle z - x_{t_0}, n \rangle > 0$. Therefore, v cannot lie in the interior of K . \square

We collect some basic properties regarding the convex set the distance function.

Proposition A.3. *Let K be a convex set in \mathbb{R}^d and Ω be a set in \mathbb{R}^d . Then, we have that*

1. *For each $x \in \mathbb{R}^d$, there exists a unique point $\text{proj}_K(x) \in K$ such that $\|x - \text{proj}_K(x)\| = d_K(x)$.*
2. *The distance function $d_K(x)$ is a convex function.*
3. *The thickening of K by a distance r is a convex set, that is $B_r(K) := \{x \in \mathbb{R}^d : d_K(x) \leq r\}$ is a convex set.*
4. *The diameter of Ω is the same as the diameter of its convex hull, that is $\text{diam}(\Omega) = \text{diam}(\text{conv}(\Omega))$.*
5. *Let $a > 0$, then a set Ω is convex if and only if $a \cdot \Omega$ is convex.*

A.2 Metric geometry notions and results

Let $\Omega \subset \mathbb{R}^d$ be a closed subset and Σ_Ω be the medial axis of Ω .

The goal of this section is to establish (1) a quantitative inclusion result (Corollary A.8) that ensures points that are closest to $x \in (\Omega \cup \Sigma_\Omega)^c$ are inside the ball around the projection $\text{proj}_\Omega(x)$, (2) the local Lipschitzness of the projection function (Lemma A.9), and (3) the Differentiability of distance function (Lemma A.11).

We first recall the definition of the local feature size of a point x in [AB98].

Definition 4 ([AB98]). For any $x \in \mathbb{R}^d$, we define the *local feature size* $\text{lfs}(x)$ of x as the distance from x to the medial axis of Ω .

Let x be a point in \mathbb{R}^d such that it has a unique projection to Ω . For any point $b \in \Omega$, the following standard lemma from geometric measure theory [Fed59] gives a lower bound of the angle $\angle xab$ in terms of how far x can be extended in the direction of $x - \text{proj}_\Omega(x)$ while still maintaining projection to Ω as the point $\text{proj}_\Omega(x)$.

Lemma A.4. *For any $x \in (\Omega \cup \Sigma_\Omega)^c$ and any $t > 0$ such that $\text{proj}_\Omega(x) + t \frac{x - \text{proj}_\Omega(x)}{\|x - \text{proj}_\Omega(x)\|} \notin \Sigma_\Omega$, the following holds for any $b \in \Omega$:*

$$\langle x - \text{proj}_\Omega(x), \text{proj}_\Omega(x) - b \rangle \geq -\frac{\|\text{proj}_\Omega(x) - b\|^2 \|x - \text{proj}_\Omega(x)\|}{2t}$$

Proof. Since point $\text{proj}_\Omega(x) + t \frac{x - \text{proj}_\Omega(x)}{\|x - \text{proj}_\Omega(x)\|}$ has a unique projection to Ω and by triangle inequality, it must be $\text{proj}_\Omega(x)$. Therefore, we have that

$$\begin{aligned} \left\| \text{proj}_\Omega(x) + t \frac{x - \text{proj}_\Omega(x)}{\|x - \text{proj}_\Omega(x)\|} - b \right\|^2 &\geq t^2 \\ \|\text{proj}_\Omega(x) - b\|^2 + 2t \left\langle \text{proj}_\Omega(x) - b, \frac{x - \text{proj}_\Omega(x)}{\|x - \text{proj}_\Omega(x)\|} \right\rangle + t^2 &\geq t^2 \\ 2t \langle \text{proj}_\Omega(x) - b, x - \text{proj}_\Omega(x) \rangle &\geq -\|\text{proj}_\Omega(x) - b\|^2 \|x - \text{proj}_\Omega(x)\| \\ \langle x - \text{proj}_\Omega(x), \text{proj}_\Omega(x) - b \rangle &\geq -\frac{\|\text{proj}_\Omega(x) - b\|^2 \|x - \text{proj}_\Omega(x)\|}{2t} \end{aligned}$$

□

The above lemma gives a lower bound of the angle $\angle xab$ and a larger t implies a larger angle. Inspired by the above lemma, we define the local projection feature size of x which is the largest t such that $\text{proj}_\Omega(x) + t \frac{x - \text{proj}_\Omega(x)}{\|x - \text{proj}_\Omega(x)\|} \notin \Sigma_\Omega$.

Definition 5. For any $x \in (\Omega \cup \Sigma_\Omega)^c$, we define the *local projection feature size* of x as

$$\text{lpfs}(x) := \sup \left\{ t : \text{proj}_\Omega(x) + t \frac{x - \text{proj}_\Omega(x)}{\|x - \text{proj}_\Omega(x)\|} \notin \Sigma_\Omega \right\}$$

Remark A.5. We have that

1. $\text{lpfs}(x) \geq d_\Omega(x)$.
2. $\text{lpfs}(x) \geq \text{lfs}(\text{proj}_\Omega(x))$.

We then have the following corollary.

Corollary A.6. For any $b \in \Omega$, $x \in \Omega^c$ and $a = \text{proj}_\Omega(x)$, such that $\text{lpfs}(x) > 0$, we have that

- if $\text{lpfs}(x) < \infty$, then $(x - a) \cdot (a - b) \geq -\frac{\|a-b\|^2 \|x-a\|}{2\text{lpfs}(x)}$;
- if $\text{lpfs}(x) = \infty$, then $(x - a) \cdot (a - b) \geq 0$.

From the estimation of angle $\angle xab$ in Lemma A.4, we can derive the following result that bounds the distance between $b \in \Omega$ and the projection $\text{proj}_\Omega(x)$ in terms of the distance between b and x .

Lemma A.7. For any $x \in (\Omega \cup \Sigma_\Omega)^c$ and any $t \geq d_\Omega(x)$ such that $\text{proj}_\Omega(x) + t \frac{x - \text{proj}_\Omega(x)}{\|x - \text{proj}_\Omega(x)\|} \notin \Sigma_\Omega$, we have that for any $b \in \Omega$,

$$\|x - b\| \geq \sqrt{d_\Omega(x)^2 + \|b - \text{proj}_\Omega(x)\|^2 \left(1 - \frac{d_\Omega(x)}{t}\right)}.$$

Proof. By the law of cosines, we have that

$$\cos(\angle xab) = \frac{d_\Omega(x)^2 + \|b - \text{proj}_\Omega(x)\|^2 - \|x - b\|^2}{2d_\Omega(x)\|b - \text{proj}_\Omega(x)\|}$$

Suppose $\|x - b\|^2 < d_\Omega(x)^2 + \|b - \text{proj}_\Omega(x)\|^2(1 - \frac{d_\Omega(x)}{t})$, then we have that

$$\begin{aligned} \cos(\angle xab) &= \frac{d_\Omega(x)^2 + \|b - \text{proj}_\Omega(x)\|^2 - \|x - b\|^2}{2d_\Omega(x)\|b - \text{proj}_\Omega(x)\|} \\ &> \frac{\|d_\Omega(x)^2 + \|b - \text{proj}_\Omega(x)\|^2 - d_\Omega(x)^2 - \|b - \text{proj}_\Omega(x)\|^2 + \|b - \text{proj}_\Omega(x)\|^2 \frac{d_\Omega(x)}{t}}{2d_\Omega(x)\|b - \text{proj}_\Omega(x)\|} \\ &= \frac{\|b - \text{proj}_\Omega(x)\|^2}{2t}. \end{aligned}$$

By applying Lemma A.4 to b and x , we have that

$$\langle x - \text{proj}_\Omega(x), \text{proj}_\Omega(x) - b \rangle \geq -\frac{\|\text{proj}_\Omega(x) - b\|^2 \|x - \text{proj}_\Omega(x)\|}{2t}.$$

That is we have the following estimate for the cosine of the angle $\angle xab$:

$$\cos(\angle xab) = \frac{\langle x - \text{proj}_\Omega(x), b - \text{proj}_\Omega(x) \rangle}{\|x - \text{proj}_\Omega(x)\| \|b - \text{proj}_\Omega(x)\|} \leq \frac{\|\text{proj}_\Omega(x) - b\|^2}{2t}.$$

This contradicts the inequality above and hence we must have that

$$\|x - b\|^2 \geq d_\Omega(x)^2 + \|b - \text{proj}_\Omega(x)\|^2 \left(1 - \frac{d_\Omega(x)}{t}\right).$$

□

Corollary A.8. *For any $x \in \Sigma_\Omega^c$, we have that*

- *assume that $\text{lpfs}(x) < \infty$. Then, for any $\epsilon > 0$, we let $\delta := \epsilon^2 \left(1 - \frac{d_\Omega(x)}{\text{lpfs}(x)}\right)$, then*

$$B_{\sqrt{d_\Omega(x)^2 + \delta}}(x) \cap \Omega \subseteq B_\epsilon(\text{proj}_\Omega(x)) \cap \Omega$$

- *assume that $\text{lpfs}(x) = \infty$. Then, for any $\epsilon > 0$, we have that*

$$B_{\sqrt{d_\Omega(x)^2 + \epsilon^2}}(x) \cap \Omega \subseteq B_\epsilon(\text{proj}_\Omega(x)) \cap \Omega$$

Proof. For the first case, it suffices to show that

$$B_\epsilon(\text{proj}_\Omega(x))^c \cap \Omega \subseteq B_{\sqrt{d_\Omega(x)^2 + \delta}}(x)^c \cap \Omega$$

That is, if $b \in \Omega$ and $\|b - \text{proj}_\Omega(x)\| \geq \epsilon$, then we have that $\|x - b\| \geq \sqrt{d_\Omega(x)^2 + \delta}$ which is a direct consequence of Lemma A.7.

The second case is similar. □

Lemma A.9 (Local Lipschitz continuity of the projection). *For any $\epsilon > 0$ and for any $x, y \in \mathbb{R}^d$ such that $d_{\Sigma_\Omega}(x) > \epsilon$ and $d_{\Sigma_\Omega}(y) > \epsilon$, we have that*

$$\|\text{proj}_\Omega(x) - \text{proj}_\Omega(y)\| \leq \left(\frac{\max\{d_\Omega(x), d_\Omega(y)\}}{\epsilon} + 1 \right) \|x - y\|.$$

Proof. Since $d(x, \Sigma_\Omega) > \epsilon$ and $d(y, \Sigma_\Omega) > \epsilon$, then the projection of

$$\text{proj}_\Omega(x) + (\epsilon + d_\Omega(x)) \frac{x - \text{proj}_\Omega(x)}{\|x - \text{proj}_\Omega(x)\|}$$

is $\text{proj}_\Omega(x)$ and the projection of

$$\text{proj}_\Omega(y) + (\epsilon + d_\Omega(y)) \frac{y - \text{proj}_\Omega(y)}{\|y - \text{proj}_\Omega(y)\|}$$

is $\text{proj}_\Omega(y)$. For simplicity, we use p_x to denote the projection of a to Ω and use p_y to denote the projection of b to Ω .

Therefore, we have that

$$\begin{aligned} \|p_x + (\epsilon + d_\Omega(x)) \frac{x - p_x}{\|x - p_x\|} - p_y\|^2 &\geq (\epsilon + d_\Omega(x))^2 \\ \|p_x - p_y\|^2 + (\epsilon + d_\Omega(x))^2 + 2(\epsilon + d_\Omega(x)) \left\langle p_x - p_y, \frac{x - p_x}{\|x - p_x\|} \right\rangle &\geq (\epsilon + d_\Omega(x))^2 \\ \left\langle p_x - p_y, \frac{x - p_x}{\|x - p_x\|} \right\rangle &\geq -\frac{\|p_x - p_y\|^2}{2(\epsilon + d_\Omega(x))} \\ \langle p_x - p_y, x - p_x \rangle &\geq -\frac{\|p_x - p_y\|^2}{2(\epsilon + d_\Omega(x))} d_\Omega(x) \end{aligned}$$

With the same argument for y , we have that

$$\langle p_y - p_x, y - p_y \rangle \geq -\frac{\|p_x - p_y\|^2}{2(\epsilon + d_\Omega(y))} d_\Omega(y)$$

By adding the two inequalities about the inner products, we have that

$$\begin{aligned} \langle p_x - p_y, x - p_x - y + p_y \rangle &\geq -\frac{\|p_x - p_y\|^2}{2(\epsilon + d_\Omega(x))} d_\Omega(x) - \frac{\|p_x - p_y\|^2}{2(\epsilon + d_\Omega(y))} d_\Omega(y) \\ \langle p_x - p_y, x - y \rangle - \|p_x - p_y\|^2 &\geq -\frac{\|p_x - p_y\|^2}{2(\epsilon + d_\Omega(x))} d_\Omega(x) - \frac{\|p_x - p_y\|^2}{2(\epsilon + d_\Omega(y))} d_\Omega(y) \\ \langle p_x - p_y, x - y \rangle &\geq \|p_x - p_y\|^2 - \frac{\|p_x - p_y\|^2}{2(\epsilon + d_\Omega(x))} d_\Omega(x) - \frac{\|p_x - p_y\|^2}{2(\epsilon + d_\Omega(y))} d_\Omega(y) \end{aligned}$$

Therefore by using the Cauchy-Schwarz inequality, we have that

$$\begin{aligned} \|x - y\| &\geq \frac{\langle p_x - p_y, x - y \rangle}{\|p_x - p_y\|} \geq \|p_x - p_y\| \left(1 - \frac{d_\Omega(x)}{2(\epsilon + d_\Omega(x))} - \frac{d_\Omega(y)}{2(\epsilon + d_\Omega(y))} \right) \\ &\geq \|p_x - p_y\| \left(1 - \frac{m}{m + \epsilon} \right), \end{aligned}$$

where $m = \max\{d_\Omega(x), d_\Omega(y)\}$. By rearranging the terms, we have that

$$\|p_x - p_y\| \leq \left(\frac{m + \epsilon}{\epsilon} \right) \|x - y\|$$

□

Differentiability of the distance function Let $\Omega \subset \mathbb{R}^d$ be any closed subset. Consider the function $d_\Omega : \mathbb{R}^d \rightarrow \mathbb{R}$ defined by $d_\Omega(x) := \inf_{y \in \Omega} \|x - y\|$. We let $\Sigma(x) := \{y \in \Omega : \|x - y\| = d_\Omega(x)\}$ denote the set of points in Ω that achieve the infimum. When x is not in the medial axis of Ω , the set $\Sigma(x)$ is a singleton and we denote it by $\text{proj}_\Omega(x)$.

Interestingly, there is the following result showing the existence of one sided directional derivatives for d_Ω by [dM37] (see also [Bia23] for a more recent English treatment).

Lemma A.10 ([dM37]). *For any vector $v \in \mathbb{R}^d$, the one-sided directional derivative of d_Ω at $x \in \mathbb{R}^d \setminus \Omega$ in the direction v exists and is given by*

$$D_v d_\Omega(x) = \inf \left\{ -\frac{\langle v, y - x \rangle}{\|y - x\|} : y \in \Sigma(x) \right\}$$

Motivated by the this result, we mimick the proof and establish the following result for the squared distance function d_Ω^2 . Notice that, we can remove the constraint for $x \notin \Omega$.

Lemma A.11. *For any $x \in \mathbb{R}^d \setminus \Sigma_\Omega$, the directional derivative of d_Ω^2 at x exists and is given by*

$$D_v d_\Omega^2(x) = -2\langle v, \text{proj}_\Omega(x) - x \rangle$$

Proof. Without loss of generality, we assume that $x = 0$ is the origin and $v = (c, 0, \dots, 0)$ for some $c > 0$ (one can achieve these by applying rigid transformations).

We let $x_\Omega = \text{proj}_\Omega(x)$, $x_t = tv$ and $x_t^* = \text{proj}_\Omega(x_t)$. Since $\|x_t^* - x_t\| \leq \|x_\Omega - x_t\|$, we have that

$$\|x_t^*\|^2 - \|x_\Omega\|^2 \leq 2ct(x_t^{*,(1)} - x_0^{*,(1)}),$$

where $x_t^{*,(1)}$ denotes the first coordinate of x_t^* . Note that $\|x_t^*\| = \|x_t^* - x\| \geq \|x_\Omega - x\| = \|x_\Omega\|$. So we have that

$$0 \leq x_t^{*,(1)} - x_0^{*,(1)}.$$

Now we have that by the cosine rule of the triangle formed by $x_t = tv$, $x = 0$ and x_t^* , we have that

$$d_\Omega^2(x_t) = \|x_t^*\|^2 + t^2c^2 - 2t\langle v, x_t^* - x \rangle.$$

Therefore, we have that

$$\frac{d_\Omega^2(x_t) - d_\Omega^2(x)}{t} = \frac{\|x_t^*\|^2 - \|x_\Omega\|^2}{t} - 2\langle v, x_t^* - x \rangle$$

As discussed above, we have that

$$0 \leq \frac{\|x_t^*\|^2 - \|x_\Omega\|^2}{t} \leq 2c(x_t^{*,(1)} - x_0^{*,(1)})$$

By continuity of proj_Ω outside Σ_Ω , we have that $x_t^* \rightarrow x^*$ as $t \rightarrow 0$. Therefore, we have that

$$\lim_{t \rightarrow 0} \frac{d_\Omega^2(x_t) - d_\Omega^2(x)}{t} = -2\langle v, x^* - x \rangle = -2\langle v, \text{proj}_\Omega(x) - x \rangle$$

□

Corollary A.12. *Let $(x_t)_t$ be a differentiable curve in $x \in \mathbb{R}^d \setminus \Sigma_\Omega$, then we have that $d_\Omega^2(x_t)$ is differentiable with respect to t and we have that*

$$\frac{d}{dt} d_\Omega^2(x_t) = D_{\dot{x}_t} d_\Omega^2(x_t) = -2\langle \dot{x}_t, \text{proj}_\Omega(x_t) - x_t \rangle$$

B Proofs

B.1 Proofs in Section 2

Proof of Proposition 2.1. For any $x \in \mathbb{R}^d$ and $t \in (0, 1]$, $\alpha_t > 0$ and the map F_t is well-defined.

$$\begin{aligned} (F_t)_\# p_t &= (F_t)_\# \left(\int \mathcal{N}(\cdot | \alpha_t x_0, \beta_t^2 I) p(dx_0) \right) \\ &= \int \mathcal{N}(\cdot | x_0, (\beta_t / \alpha_t)^2 I) p(dx_0) \\ &= \int \mathcal{N}(\cdot | x_0, \sigma_t^2 I) p(dx_0) \end{aligned}$$

□

Proof of Proposition 2.2. We first write down the density of q_σ explicitly as follows:

$$q_\sigma(x) = \frac{1}{(2\pi\sigma^2)^{d/2}} \int \exp\left(-\frac{\|x - x_1\|^2}{2\sigma^2}\right) p(dx).$$

Then, we have that

$$\nabla \log q_\sigma(x) = -\frac{1}{\sigma^2} \left(x - \frac{\int y \exp\left(-\frac{\|x-y\|^2}{2\sigma^2}\right) p(dy)}{\int \exp\left(-\frac{\|x-y'\|^2}{2\sigma^2}\right) p(dy')} \right).$$

Note that $\frac{dt}{d\sigma} = \frac{\alpha_t^2}{\beta_t \alpha_t - \beta_t \dot{\alpha}_t}$. Therefore with the reparametrization $x_\sigma := x_t/\alpha_t$, we have that

$$\begin{aligned} \frac{dx_\sigma}{d\sigma} &= \frac{dx_\sigma}{dt} \frac{dt}{d\sigma} \\ &= \frac{1}{\alpha_t^2} \left(\alpha_t \frac{dx_t}{dt} - \dot{\alpha}_t x_t \right) \frac{dt}{d\sigma} \\ &= \frac{\alpha_t}{\beta_t} \left(\frac{x_t}{\alpha_t} - \int \frac{\exp\left(-\frac{\|x_t - \alpha_t y\|^2}{2\beta_t^2}\right) y}{\int \exp\left(-\frac{\|x_t - \alpha_t y'\|^2}{2\beta_t^2}\right) p(dy')} p(dy) \right) \\ &= -\sigma \nabla \log q_\sigma(x_\sigma). \end{aligned}$$

□

B.2 Proofs in Section 3

Proof of Equation (10). Since $\lambda = -\log \sigma$, we have that

$$\frac{d\lambda}{d\sigma} = -\frac{1}{\sigma}$$

and thus the ODE equation Equation (8) becomes

$$\begin{aligned} \frac{dx_\lambda}{d\lambda} &= \frac{dx_{\sigma(\lambda)}}{d\sigma} \frac{d\sigma}{d\lambda} \\ &= -\sigma \nabla \log q_\sigma(x_\sigma) \cdot (-\sigma) \\ &= -x_\sigma + \frac{\int y \exp\left(-\frac{\|x_\sigma - y\|^2}{2\sigma^2}\right) p(dy)}{\int \exp\left(-\frac{\|x_\sigma - y'\|^2}{2\sigma^2}\right) p(dy')} \\ &= m_\lambda(x_\lambda) - x_\lambda. \end{aligned}$$

□

Proof of Proposition 3.1. Recall that

$$m_t(x) = \frac{\int \exp\left(-\frac{\|x - \alpha_t z\|^2}{2\beta_t^2}\right) z p(dz)}{\int \exp\left(-\frac{\|x - \alpha_t z\|^2}{2\beta_t^2}\right) p(dz)} \text{ and } p(dz|x_t = x) = \frac{\exp\left(-\frac{\|x - \alpha_t z\|^2}{2\beta_t^2}\right) p(dz)}{\int \exp\left(-\frac{\|x - \alpha_t z\|^2}{2\beta_t^2}\right) p(dz)}.$$

We let $w_t(x, z) := \exp\left(-\frac{\|x - \alpha_t z\|^2}{2\beta_t^2}\right)$. Then,

$$\begin{aligned}
\nabla_x m_t(x) &= \int z \nabla_x \left(\frac{\exp\left(-\frac{\|x - \alpha_t z\|^2}{2\beta_t^2}\right)}{\int \exp\left(-\frac{\|x - \alpha_t z'\|^2}{2\beta_t^2}\right) p(dz')} \right) p(dz) \\
&= \left(\int w_t(x, z') p(dz') \right)^{-2} \int z \left(w_t(x, z) \left(-\frac{x - \alpha_t z}{\beta_t^2}\right)^T \int w_t(x, z') p(dz') \right) p(dz) \\
&\quad - \left(\int w_t(x, z') p(dz') \right)^{-2} \int z \left(w_t(x, z) \int w_t(x, z') \left(-\frac{x - \alpha_t z'}{\beta_t^2}\right)^T p(dz') \right) p(dz) \\
&= \left(\int w_t(x, z') p(dz') \right)^{-2} \iint w_t(x, z) w_t(x, z') z \left(-\frac{x - \alpha_t z}{\beta_t^2} + \frac{x - \alpha_t z'}{\beta_t^2}\right)^T p(dz) p(dz') \\
&= \frac{\alpha_t}{\beta_t^2} \left(\int w_t(x, z') p(dz') \right)^{-2} \iint w_t(x, z) w_t(x, z') z (z - z')^T p(dz) p(dz') \\
&= \frac{\alpha_t}{2\beta_t^2} \left(\int w_t(x, z') p(dz') \right)^{-2} \iint w_t(x, z) w_t(x, z') (z - z') (z - z')^T p(dz) p(dz') \\
&= \frac{\alpha_t}{2\beta_t^2} \iint (z - z') (z - z')^T p(dz|x_t = x) p(dz'|x_t = x).
\end{aligned}$$

The second equation follows from standard calculations. \square

Proof of Proposition 3.3. Let $\Omega := \text{supp}(p)$. Recall that

$$\begin{aligned}
u_t(x) &= (\log \beta_t)' x + \beta_t (\alpha_t / \beta_t)' m_t(x) \\
&= \dot{\beta}_t \frac{x - \alpha_t m_t(x)}{\beta_t} + \dot{\alpha}_t m_t(x).
\end{aligned}$$

Then, we have that

$$\|m_t(x) - \text{proj}_\Omega(x)\| \leq \|m_{\sigma_t}(x/\alpha_t) - \text{proj}_\Omega(x/\alpha_t)\| + \|\text{proj}_\Omega(x/\alpha_t) - \text{proj}_\Omega(x)\|.$$

By Lemma A.9, there exists a positive constant C_x such that $\|\text{proj}_\Omega(x) - \text{proj}_\Omega(y)\| \leq C_x \|x - y\|$ for any y close to x . Therefore,

$$\|\text{proj}_\Omega(x/\alpha_t) - \text{proj}_\Omega(x)\| \leq C_x \left\| \frac{x}{\alpha_t} - x \right\| = O(1 - \alpha_t).$$

Now, when $\Omega = \mathbb{R}^d$, by Corollary 4.9, we have that

$$\|m_{\sigma_t}(x/\alpha_t) - \text{proj}_\Omega(x/\alpha_t)\| = O(\sigma_t) = O(\beta_t).$$

In this case, $\text{proj}_\Omega(x) = x$. This implies that for t close to 1, we have that

$$\left\| \frac{x - \alpha_t m_t(x)}{\beta_t} \right\| \leq O\left(\frac{1 - \alpha_t}{\beta_t}\right) + O(1).$$

The right hand side is bounded since $\lim_{t \rightarrow 1} \frac{1 - \alpha_t}{\beta_t} = \lim_{t \rightarrow 1} \frac{-\dot{\alpha}_t}{\dot{\beta}_t} = \frac{-\dot{\alpha}_1}{\dot{\beta}_1}$ exists. Therefore, the vector field $u_t(x)$ is uniformly bounded for all $t \in [0, 1)$.

If $\Omega \neq \mathbb{R}^d$ and $x \notin \Omega \cup \Sigma_\Omega$, then $\text{proj}_\Omega(x) \neq x$. By Corollary 4.4, we have that $m_t(x) \rightarrow \text{proj}_\Omega(x)$ as $t \rightarrow 1$. This implies that $\|x - \alpha_t m_t(x)\| \rightarrow \|x - \text{proj}_\Omega(x)\| > 0$. Then, as the denominator $\beta_t \rightarrow 0$, we have that $\lim_{t \rightarrow 1} \|u_t(x)\| = \infty$. \square

Proof of Theorem 3.5. We consider the change of variable $\lambda = -\log(\sigma)$. We let $z_\lambda := x_\sigma(\lambda)$ for all $\lambda \in [\lambda_1 := \lambda(\sigma_1), \lambda_2 := \lambda(\sigma_2)]$. Then, $(z_\lambda)_{\lambda \in [\lambda_1, \lambda_2]}$ satisfies the nice ODE as in Equation (10). By assumption we have that z_{λ_1} is outside the convex set K . For any $\lambda \in [\lambda_1, \lambda_2]$, by Corollary A.12 we have that

$$\frac{d}{d\lambda} d_K^2(z_\lambda) = -2 \langle z_\lambda - \text{proj}_K(z_\lambda), z_\lambda - m_\lambda(z_\lambda) \rangle \quad (19)$$

$$\begin{aligned} &= -2 (\langle z_\lambda - \text{proj}_K(z_\lambda), z_\lambda - \text{proj}_K(z_\lambda) \rangle + \langle z_\lambda - \text{proj}_K(z_\lambda), \text{proj}_K(z_\lambda) - m_\lambda(z_\lambda) \rangle) \\ &\leq -2 (\langle z_\lambda - \text{proj}_K(z_\lambda), z_\lambda - \text{proj}_K(z_\lambda) \rangle) \\ &= -2 d_C^2(z_\lambda). \end{aligned} \quad (20)$$

Here the inequality follows from the fact that the medial axis of the convex hull is empty and hence Item 2 of Corollary A.6 applies which guarantees that $\langle z_\lambda - \text{proj}_K(z_\lambda), \text{proj}_K(z_\lambda) - m_\lambda(z_\lambda) \rangle \geq 0$ since z_λ is outside C and $m_\lambda(z_\lambda)$ is within C . Multiplying with the exponential integrator $e^{a\lambda}$, we have that

$$\frac{d}{d\lambda} (e^{2\lambda} d_K^2(z_\lambda)) \leq 0$$

Then we have that

$$d_C^2(z_\lambda) \leq e^{-2(\lambda-\lambda_1)} d_C^2(z_{\lambda_1})$$

This implies that $d_K(z_\lambda) \leq e^{-(\lambda-\lambda_1)} d_K(z_{\lambda_1})$ and hence $d_K(x_\sigma) \leq \frac{\sigma}{\sigma_1} d_K(x_{\sigma_1})$. \square

Proof of Theorem 3.6. We utilize the parameter λ as in the proof of Theorem 3.5.

Item 1. Suppose otherwise that z_{λ_1} lies in K but its later trajectory leaves K . Note that the function $d_K^2(z_\lambda)$ is a differentiable function of λ and there must exist time λ_b, λ_o such that $d_K^2(z_{\lambda_b}) = 0$ and $d_K^2(z_{\lambda_o}) > 0$. Then in particular, there is a time λ_i between λ_b and λ_o such that the derivative

$$\frac{d d_K^2(z_{\lambda_i})}{d\lambda} > 0.$$

As already shown in Equation (19) that $\frac{d}{d\lambda} d_K^2(z_\lambda) = -2 \langle z_\lambda - \text{proj}_K(z_\lambda), z_\lambda - m_\lambda(z_\lambda) \rangle$. So, if $d_K^2(z_{\lambda_i}) = 0$, one would have that $\frac{d d_K^2(z_{\lambda_i})}{d\lambda} = 0$. This would violate the assumption that $\frac{d d_K^2(z_{\lambda_i})}{d\lambda} > 0$ and hence we must have that $d_K^2(z_{\lambda_i}) > 0$. Then, by Equation (20), we have that in this case, $\frac{d d_K^2(z_{\lambda_i})}{d\lambda} \leq -2 d_K^2(z_{\lambda_i}) \leq 0$. This leads to a contradiction and hence the trajectory z_λ (resp. x_σ) must stay inside K for all $\lambda \in [\lambda_1, \lambda_2]$ (resp. all $\sigma \in (\sigma_2, \sigma_1]$).

Item 2. Suppose otherwise that z_{λ_1} lies in K but its later trajectory leaves K . Note that the function $d_K^2(z_\lambda)$ is a differentiable function of λ and there must exist times λ_b, λ_o such that

- $z_{\lambda_b} \in \partial K$ and
- for any $\lambda \in (\lambda_b, \lambda_o]$, $d_K^2(z_\lambda) > 0$.

Similarly as above, there is a time λ_i between λ_b and λ_o such that the derivative

$$\frac{d d_K^2(z_{\lambda_i})}{d\lambda} > 0.$$

Then, by Equation (20), we have that in this case, $\frac{d d_K^2(z_{\lambda_i})}{d\lambda} \leq -2d_K^2(z_{\lambda_i}) \leq 0$. Here we used the fact that z_{λ_i} is outside K and $m_{\lambda_i}(z_{\lambda_i})$ is within K . This leads to a contradiction and hence the trajectory z_λ (resp. x_σ) must stay inside K for all $\lambda \in [\lambda_1, \lambda_2]$ (resp. all $\sigma \in (\sigma_2, \sigma_1]$). \square

B.3 Proofs in Section 4

Proof of Proposition 4.1. Let $R_1 = \|x - \mathbb{E}(p)\|$. Consider the function $g_\sigma(y) = \exp\left(-\frac{\|x-y\|^2}{2\sigma^2}\right)$. By the fact that $\|x - \mathbb{E}(p)\| \leq \text{diam}(\Omega)$ for any $x \in \Omega$, we have that:

$$\exp\left(-\frac{(R_1 + \text{diam}(\Omega))^2}{2\sigma^2}\right) \leq g_\sigma(y) \leq \exp\left(-\frac{(R_1 - \text{diam}(\Omega))^2}{2\sigma^2}\right)$$

for all $y \in \Omega$. Then for any Borel measurable set $A \subseteq \Omega$, we can bound the ratio of the posterior and prior measures as:

$$\begin{aligned} \frac{p(A|x_\sigma = x)}{p(A)} &= \frac{\int_A g_\sigma(y)p(dy)}{p(A) \int_\Omega g_\sigma(y)p(dy)} \\ &\leq \frac{\exp\left(-\frac{(R_1 - \text{diam}(\Omega))^2}{2\sigma^2}\right) \int_A p(dy)}{p(A) \exp\left(-\frac{(R_1 + \text{diam}(\Omega))^2}{2\sigma^2}\right) \int_\Omega p(dy)} \\ &= \underbrace{\exp\left(\frac{(R_1 + \text{diam}(\Omega))^2}{2\sigma^2} - \frac{(R_1 - \text{diam}(\Omega))^2}{2\sigma^2}\right)}_a. \end{aligned}$$

Similarly, we can bound the ratio from below:

$$\begin{aligned} \frac{p(A|x_\sigma = x)}{p(A)} &\geq \frac{\exp\left(-\frac{(R_1 + \text{diam}(\Omega))^2}{2\sigma^2}\right) \int_A p(dy)}{p(A) \exp\left(-\frac{(R_1 - \text{diam}(\Omega))^2}{2\sigma^2}\right) \int_\Omega p(dy)} \\ &= \exp\left(\frac{(R_1 - \text{diam}(\Omega))^2}{2\sigma^2} - \frac{(R_1 + \text{diam}(\Omega))^2}{2\sigma^2}\right) \\ &= 1/a \end{aligned}$$

Since $a > 1$, we have $|1/a - 1| \leq a - 1$. Therefore, we have:

$$\left| \frac{p(A|x_\sigma = x)}{p(A)} - 1 \right| \leq a - 1$$

In particular, there is $|p(A|x_\sigma = x) - p(A)| \leq a - 1$ for all $A \subseteq \Omega$ which by definition bounds the total variation distance between $p(\cdot|x_\sigma = x)$ and p by $a - 1$. Then the Wasserstein distance $d_{W,1}(p(\cdot|x_\sigma = x), p)$ can be bounded by $(a - 1)\text{diam}(\Omega)$, see e.g [Vil03, Proposition 7.10]. \square

Proof of Theorem 4.2. We let $\Phi_x := d_{\Sigma_\Omega}(x)/2 > 0$ and $\Delta_x := d_\Omega(x) \geq 0$. We let $x_\Omega := \text{proj}_\Omega(x)$. According to Lemma A.7, for any $\epsilon > 0$, if we define the radius

$$r_{x,\epsilon} := \sqrt{\Delta_x^2 + \epsilon^2 \left(1 - \frac{\Delta_x}{\Delta_x + \Phi_x}\right)}$$

then we have the following inclusion

$$B_{r_{x,\epsilon}}(x) \cap \Omega \subseteq B_\epsilon(x_\Omega) \cap \Omega.$$

For the other direction, we have that

$$B_{r_{x,\epsilon}^*}(x_\Omega) \cap \Omega \subseteq B_{r_{x,\epsilon}}(x) \cap \Omega$$

where

$$r_{x,\epsilon}^* := r_{x,\epsilon} - \Delta_x = \frac{\Phi_x}{(\Phi_x + \Delta_x)(r_{x,\epsilon} + \Delta_x)} \epsilon^2.$$

Here $r_{x,\epsilon}^*$ satisfies that as $d_\Omega(x) \rightarrow 0$, $r_{x,\epsilon}^* \rightarrow \epsilon$. So $B_{r_{x,\epsilon}^*}(x_\Omega)$ can be thought of as an approximation of $B_\epsilon(x_\Omega)$.

Then, we estimate the two terms below separately:

$$\begin{aligned} d_{W,2}(p(\cdot|x_\sigma = x), \delta_{x_\Omega})^2 &= \int_\Omega \|x_0 - x_\Omega\|^2 \frac{\exp\left(-\frac{\|x-x_0\|^2}{2\sigma^2}\right)}{\int_\Omega \exp\left(-\frac{\|x-x'_0\|^2}{2\sigma^2}\right) p(dx'_0)} p(dx_0) \\ &= \underbrace{\int_{B_{r_{x,\epsilon}}(x) \cap \Omega} \|x_0 - x_\Omega\|^2 \frac{\exp\left(-\frac{\|x-x_0\|^2}{2\sigma^2}\right)}{\int_\Omega \exp\left(-\frac{\|x-x'_0\|^2}{2\sigma^2}\right) p(dx'_0)} p(dx_0)}_{I_1} \\ &\quad + \underbrace{\int_{B_{r_{x,\epsilon}}(x)^c \cap \Omega} \|x_0 - x_\Omega\|^2 \frac{\exp\left(-\frac{\|x-x_0\|^2}{2\sigma^2}\right)}{\int_\Omega \exp\left(-\frac{\|x-x'_0\|^2}{2\sigma^2}\right) p(dx'_0)} p(dx_0)}_{I_2} \end{aligned}$$

For I_1 , we have the following estimate:

$$I_1 \leq \int_{B_\epsilon(x_\Omega) \cap \Omega} \|x_0 - x_\Omega\|^2 \frac{\exp\left(-\frac{\|x-x_0\|^2}{2\sigma^2}\right)}{\int_\Omega \exp\left(-\frac{\|x-x'_0\|^2}{2\sigma^2}\right) p(dx'_0)} p(dx_0) \leq \epsilon^2$$

For the second term I_2 , we have the following estimate:

$$\begin{aligned}
I_2 &\leq \int_{B_{r_{x,\epsilon}}^c(y) \cap \Omega} (2\|x_0\|^2 + 2\|x_\Omega\|^2) \frac{\exp\left(-\frac{\|x-x_0\|^2}{2\sigma^2}\right)}{\int_{\Omega} \exp\left(-\frac{\|x-x'_0\|^2}{2\sigma^2}\right) p(dx'_0)} p(dx_0) \\
&= \int_{B_{r_{x,\epsilon}}^c(y) \cap \Omega} \frac{2\|x_0\|^2 + 2\|x_\Omega\|^2}{\int_{\Omega} \exp\left(\frac{\|x-x_0\|^2}{2\sigma^2} - \frac{\|x-x'_0\|^2}{2\sigma^2}\right) p(dx'_0)} p(dx_0) \\
&\leq \int_{B_{r_{x,\epsilon}}^c(y) \cap \Omega} \frac{2\|x_0\|^2 + 2\|x_\Omega\|^2}{\int_{B_{r_{x,\epsilon/\sqrt{2}}}(y) \cap \Omega} \exp\left(\frac{\|x-x_0\|^2}{2\sigma^2} - \frac{\|x-x'_0\|^2}{2\sigma^2}\right) p(dx'_0)} p(dx_0) \\
&\leq \int_{B_{r_{x,\epsilon}}^c(y) \cap \Omega} \frac{2\|x_0\|^2 + 2\|x_\Omega\|^2}{\int_{B_{r_{x,\epsilon/\sqrt{2}}}(y) \cap \Omega} \exp\left(\frac{\epsilon^2}{4\sigma^2} \left(1 - \frac{\Delta_x}{\Delta_x + \Phi_x}\right)\right) p(dx'_0)} p(dx_0) \\
&= \exp\left(-\frac{\epsilon^2}{4\sigma^2} \left(1 - \frac{\Delta_x}{\Delta_x + \Phi_x}\right)\right) \frac{2\|x_\Omega\|^2 + 2M_2(p)}{p\left(B_{r_{x,\epsilon/\sqrt{2}}}(y) \cap \Omega\right)} \\
&\leq \exp\left(-\frac{\epsilon^2}{4\sigma^2} \left(1 - \frac{\Delta_x}{\Delta_x + \Phi_x}\right)\right) \frac{2\|x_\Omega\|^2 + 2M_2(p)}{p\left(B_{r_{x,\epsilon/\sqrt{2}}}^*(x_\Omega)\right)}
\end{aligned}$$

Since Ω is the support of p , we have that $p\left(B_{r_{x,\epsilon/\sqrt{2}}}^*(x_\Omega)\right) > 0$. Hence, for any $\epsilon > 0$, we have

$$I_1 + I_2 \leq \epsilon^2 + \frac{2\|x_\Omega\|^2 + 2M_2(p)}{p\left(B_{r_{x,\epsilon/\sqrt{2}}}^*(x_\Omega)\right)} \exp\left(-\frac{\epsilon^2}{4\sigma^2} \left(1 - \frac{\Delta_x}{\Delta_x + \Phi_x}\right)\right)$$

By letting $\sigma \rightarrow 0$, we have that $I_1 + I_2 \leq \epsilon$. Therefore, we have that

$$\lim_{\sigma \rightarrow 0} d_{W,2}(p(\cdot|x_\sigma = x), \delta_{x_\Omega}) = 0.$$

□

Proof of Corollary 4.3. This is a direct consequence of the following property of the Wasserstein distance where the case $s = 1$ was proved in [RTG98] and the other cases follow from the fact that $d_{W,s}$ is increasing with respect to s [Vil09].

Lemma B.1. *For any probability measures μ, ν on \mathbb{R}^d and any $1 \leq p \leq \infty$, we have that $d_{W,p}(\mu, \nu) \geq \|\mathbb{E}(\mu) - \mathbb{E}(\nu)\|$.*

□

Proof of Corollary 4.4. In the proof of Theorem 4.2, we end up with

$$d_{W,2}(p(\cdot|x_\sigma = x), \delta_{x_\Omega})^2 \leq \epsilon^2 + \exp\left(-\frac{\epsilon^2}{4\sigma^2} \left(1 - \frac{\Delta_x}{\Delta_x + \Phi_x}\right)\right) \frac{2\|x_\Omega\|^2 + 2M_2(p)}{p\left(B_{r_{x,\epsilon/\sqrt{2}}}^*(x_\Omega)\right)}$$

for any arbitrarily chosen small ϵ .

By Lemma A.9, there exists a small $\xi > 0$ and a constant $C_\xi > 0$ such that for any $\|z - x\| < \xi$, one has $\|z_\Omega - x_\Omega\| < C_\xi \|z - x\|$. As both Δ_x and Φ_x are continuous in a local neighborhood of x , there exists a small $\xi_1 > 0$ such that for any z with $\|z - x\| < \xi_1$, one has

- $r_{z,\epsilon/\sqrt{2}}^* > \frac{1}{2}r_{x,\epsilon/\sqrt{2}}^*$;
- $1 - \frac{\Delta_x}{\Delta_x + \Phi_x} > \frac{1}{2} \left(1 - \frac{\Delta_z}{\Delta_z + \delta_z}\right)$;
- $\|z_\Omega\| \leq 2\|x_\Omega\|$.

Now, take $\Xi := \min \left\{ \xi, \xi_1, \frac{1}{2C_\xi} r_{z,\epsilon/\sqrt{2}}^* \right\}$. Then, it is easy to check that for any z such that $\|z - x\| < \Xi$, one has

$$B_{\frac{1}{4}r_{x,\epsilon/\sqrt{2}}^*}^*(x_\Omega) \subset B_{r_{z,\epsilon/\sqrt{2}}^*}^*(z_\Omega).$$

This implies that for any z such that $\|z - x\| < \Xi$, one has

$$\|m_\sigma(z) - z_\Omega\|^2 \leq d_{W,2}(p(\cdot|x_\sigma = z), \delta_{z_\Omega})^2 \leq \epsilon^2 + \exp\left(-\frac{\epsilon^2}{8\sigma^2} \left(1 - \frac{\Delta_x}{\Delta_x + \Phi_x}\right)\right) \frac{4\|x_\Omega\|^2 + 2M_2(p)}{p\left(B_{r_{x,\frac{1}{4}\epsilon/\sqrt{2}}^*}^*(x_\Omega)\right)}.$$

Hence, when σ is small enough (dependent on ϵ), we have that $\|m_\sigma(z) - z_\Omega\| \leq 2\epsilon$ for any z such that $\|z - x\| < \Xi$.

Now, we have that

$$\|m_t(x) - x_\Omega\| \leq \|m_{\sigma_t}(x/\alpha_t) - \text{proj}_\Omega(x/\alpha_t)\| + \|\text{proj}_\Omega(x/\alpha_t) - \text{proj}_\Omega(x)\|.$$

As $\alpha_t \rightarrow 1$, there exists t_0 such that when $t > t_0$, one has that $z = x/\alpha_t \in B_\Xi(x)$ and $\|\text{proj}_\Omega(x/\alpha_t) - \text{proj}_\Omega(x)\| \leq \epsilon$. By the analysis above, we can enlarge t so that σ_t is small enough so that $\|m_{\sigma_t}(z) - z_\Omega\| \leq 2\epsilon$. Therefore, for any $t > t_0$, we have that $\|m_t(x) - x_\Omega\| \leq 3\epsilon$. Since ϵ is arbitrary, we have that $\lim_{t \rightarrow 1} m_t(x) = x_\Omega$. \square

Proof of Theorem 4.5. Recall from the proof of Theorem 4.2 that for any $\epsilon > 0$, we have that

$$I_1 + I_2 \leq \epsilon^2 + \frac{2\|x_\Omega\|^2 + 2M_2(p)}{p\left(B_{r_{x,\epsilon/\sqrt{2}}^*}^*(x_\Omega)\right)} \exp\left(-\frac{\epsilon^2}{4\sigma^2} \left(1 - \frac{\Delta_x}{\Delta_x + \Phi_x}\right)\right).$$

Then, we have that $2\Phi_x \geq \tau_\Omega - \Delta_x$. So

$$\begin{aligned} r_{x,\epsilon}^* &= \frac{\Phi_x}{(\Phi_x + \Delta_x)(r_{x,\epsilon} + \Delta_x)} \epsilon^2 \\ &\geq \frac{\tau_\Omega - \Delta_x}{2\tau_\Omega} \cdot \frac{\epsilon^2}{\Delta_x + \sqrt{\Delta_y^2 + \epsilon^2}} \\ &\geq \frac{1}{4} \cdot \min\left\{ \frac{\epsilon}{(\sqrt{2} + 1)\Delta_x}, \frac{1}{\sqrt{2} + 1} \right\} \epsilon \\ &\geq \frac{\epsilon}{10} \min\left\{ \frac{\epsilon}{\tau_\Omega}, 1 \right\}. \end{aligned}$$

On the other hand, we have that

$$\begin{aligned} r_{x,\epsilon}^* &\leq \frac{\Phi_x}{(\Phi_x + \Delta_x)\epsilon\sqrt{\frac{\Phi_x}{\Delta_x + \Phi_x}}} \epsilon^2 \\ &= \epsilon\sqrt{\frac{\Phi_x}{\Delta_x + \Phi_x}} \leq \epsilon. \end{aligned}$$

Therefore, if one let $\epsilon = \sigma^\zeta$, when $\sigma < c^{1/\zeta}$ we have that $r_{x,\epsilon}^* < c$ and then

$$\begin{aligned} p\left(B_{r_{x,\epsilon/\sqrt{2}}^*}(x_\Omega)\right) &\geq C_\Omega \cdot \left(\frac{\epsilon}{10} \min\left\{\frac{\epsilon}{\tau_\Omega}, 1\right\}\right)^k \\ &= \frac{C_\Omega \sigma^{k\zeta}}{10^k} \min\left\{\frac{\sigma^{k\zeta}}{\tau_\Omega^k}, 1\right\}. \end{aligned}$$

Notice that $1 - \frac{\Delta_x}{\Delta_x + \Phi_x} \geq \frac{1}{2}$, we have that eventually

$$\begin{aligned} I_1 + I_2 &\leq \sigma^{2\zeta} + \frac{2M_2(\rho) + 2\|x_\Omega\|^2}{\frac{C_\Omega \sigma^{k\zeta}}{10^k} \min\left\{\frac{\sigma^{k\zeta}}{\tau_\Omega^k}, 1\right\}} \exp\left(-\frac{1}{8\sigma^{2(1-\zeta)}}\right) \\ &= \sigma^{2\zeta} + \frac{10^k(2M_2(\rho) + 2\|x_\Omega\|^2) \max\{\tau_\Omega^k, \sigma^{k\zeta}\}}{C_\Omega \sigma^{2k\zeta}} \exp\left(-\frac{1}{8}\sigma^{2(\zeta-1)}\right) \end{aligned}$$

The rightmost inequality in the theorem follows from the fact that the right most summand in the above equation has an exponential decay which is way faster than any polynomial decay. \square

Proof of Proposition 4.6. The case when $t = 0$ is trivial. When $t \in (0, 1]$, the statement follows from the following two results and from the fact that $p_t = (A_t^{-1})_{\#} q_{\sigma_t}$ where $A_t(x) = \alpha_t x$.

Lemma B.2 ([MMWW23, Lemma B.11]). *Let $\Psi : \mathbb{R}^d \rightarrow \mathbb{R}^d$ be a measurable map. Then, for any probability measures μ, ν with finite 2-moment, we have that $d_{W,2}(\mu, \nu) = d_{W,2}(\Psi_{\#}\mu, \Psi_{\#}\nu)$*

Lemma B.3 ([Vil03, Proposition 7.17]). *Let μ, ν be two probability measures on \mathbb{R}^d . We let $G_\sigma = \mathcal{N}(0, \sigma^2 I)$ and $\mu_\sigma := \mu * G_\sigma$ as well as $\nu_\sigma := \nu * G_\sigma$. Then, for any $\sigma > 0$, one has that*

$$d_{W,2}(\mu_\sigma, \nu_\sigma) \leq d_{W,2}(\mu, \nu).$$

\square

Proof of Theorem 4.10. When $\Delta_\Omega(x) = 0$, $\text{NN}_\Omega(x) = \Omega$ and $p(\cdot|x_\sigma = x) = p$ and then the Wasserstein distance becomes 0 which proves the statement.

Now, we will focus on the case when $\Delta_\Omega(x) > 0$. The posterior measure $p(\cdot|x_\sigma = x)$ is given by

$$p(\cdot|x_\sigma = x) = \sum_{i=1}^N \frac{a_i \exp\left(-\frac{1}{2\sigma^2}\|x_i - x\|^2\right)}{\sum_{j=1}^N a_j \exp\left(-\frac{1}{2\sigma^2}\|x_j - x\|^2\right)} \delta_{x_i}$$

For the ease of notation, we use $B_\sigma := \sum_{j=1}^N a_j \exp\left(-\frac{1}{2\sigma^2}\|x_j - x\|^2\right)$ to denote the normalization constant in $p(\cdot|x_\sigma = x)$, $B_{\sigma, x_i} := a_i \exp\left(-\frac{1}{2\sigma^2}\|x_i - x\|^2\right)$ to denote the i -th term in B_σ . We use $A = p(\text{NN}_\Omega(x))$ to denote the normalization constant in $\hat{p}_{\text{NN}(x)}$.

Observe that for any $x_i, x_j \in \text{NN}_\Omega(x)$, one has

$$p(x_i|x_\sigma = x)/p(x_j|x_\sigma = x) = \hat{p}_{\text{NN}(x)}(x_i)/\hat{p}_{\text{NN}(x)}(x_j).$$

This motivates the following construction of a coupling γ between $p(\cdot|x_\sigma = x)$ and $p_{\text{NN}(y)}$:

$$\gamma = \sum_{x_j \in \text{NN}_\Omega(x)} \frac{B_{\sigma, x_j}}{B_\sigma} \cdot \sum_{x_i \in \text{NN}_\Omega(x)} \frac{a_i}{A} \delta_{(x_i, x_i)} + \sum_{x_i \in \text{NN}_\Omega(x), x_j \in \Omega \setminus \text{NN}_\Omega(x)} \frac{B_{\lambda, x_j}}{B_\sigma} \frac{a_i}{A} \delta_{(x_i, x_j)}.$$

Then, we bound the Wasserstein distance between $p(\cdot|x_\sigma = x)$ and $\widehat{p}_{\text{NN}(x)}$ as follows:

$$\begin{aligned}
d_{\text{W},2}(p(\cdot|x_\sigma = x), \widehat{p}_{\text{NN}(x)})^2 &\leq \int \|x - y\|^2 \gamma(dx, dy), \\
&= \sum_{x_i \in \text{NN}_\Omega(x), x_j \in \Omega \setminus \text{NN}_\Omega(x)} \frac{B_{\lambda, x_j}}{B_\sigma} \frac{a_i}{A} \|x_i - x_j\|^2, \\
&\leq \sum_{x_i \in \text{NN}_\Omega(x), x_j \in \Omega \setminus \text{NN}_\Omega(x)} \frac{B_{\lambda, x_j}}{B_\sigma} \frac{a_i}{A} \text{diam}(\Omega)^2, \\
&= \text{diam}(\Omega)^2 \sum_{x_i \in \text{NN}_\Omega(x), x_j \in \Omega \setminus \text{NN}_\Omega(x)} \frac{a_j \exp\left(-\frac{1}{2\sigma^2} \|x_j - x\|^2\right)}{\sum_{j=1}^N a_j \exp\left(-\frac{1}{2\sigma^2} \|x_j - x\|^2\right)} \frac{a_i}{A}, \\
&\leq \text{diam}(\Omega)^2 \sum_{x_i \in \text{NN}_\Omega(x), x_j \in \Omega \setminus \text{NN}_\Omega(x)} \frac{a_j \exp\left(-\frac{1}{2} e^{2\lambda} d_\Omega^2(x, 2)\right)}{A \exp\left(-\frac{1}{2} e^{2\lambda} d_\Omega^2(x, 1)\right)} \frac{a_i}{A}, \\
&= \text{diam}(\Omega)^2 \frac{1 - A \exp\left(-\frac{1}{2} e^{2\lambda} d_\Omega^2(x, 2)\right)}{A \exp\left(-\frac{1}{2} e^{2\lambda} d_\Omega^2(x, 1)\right)}, \\
&= \text{diam}(\Omega)^2 \frac{1 - A}{A} \exp\left(-\frac{1}{2} e^{2\lambda} (d_\Omega^2(x, 2) - d_\Omega^2(x, 1))\right), \\
&\leq \text{diam}(\Omega)^2 \frac{1 - A}{A} \exp\left(-\frac{1}{2} e^{2\lambda} \Delta_\Omega(x)\right).
\end{aligned}$$

By taking the square roots on both sides, we conclude the proof. \square

Proof of Corollary 4.11. The result follows from Theorem 4.10 and the stability of the mean operation under the Wasserstein distance Lemma B.1. \square

B.3.1 Proof of Theorem 4.8

Part 1 We still let $\Delta_x := d_M(x) < \frac{1}{2} \tau_M$. Then, we let $q_\sigma^x := p(\cdot|x_\sigma = x)$ and hence,

$$dq_\sigma^x(x_1) := \frac{\exp\left(-\frac{\|x-x_1\|^2}{2\sigma^2}\right) \rho(x_1) d\text{vol}_M(x_1)}{\int_M \exp\left(-\frac{\|x-x'_1\|^2}{2\sigma^2}\right) \rho(x'_1) d\text{vol}_M(x'_1)}, \quad \text{for } x_1 \in M.$$

As $\sigma \rightarrow 0$, q_σ^x is concentrated around $x_M = \text{proj}_M(x)$. We let $r > 0$ be small enough and upper bounded by the injective radius r_M of M . Then, we have that

$$\begin{aligned}
d_{\text{W},2}(q_\sigma^x, \delta_{x_M})^2 &= \int_M \|x_1 - x_M\|^2 dq_\sigma^x(x_1) \\
&= \underbrace{\int_{B_r(x_M)} \|x_1 - x_M\|^2 dq_\sigma^x(x_1)}_{I_1} + \underbrace{\int_{M \setminus B_r(x_M)} \|x_1 - x_M\|^2 dq_\sigma^x(x_1)}_{I_2}
\end{aligned}$$

We first consider the term I_2 .

$$I_2 \leq \int_{M \setminus B_r(x_M)} (2\|x_1\|^2 + 2\|x_M\|^2) dq_\sigma^x(x_1).$$

As we have shown already in the proof of Theorem 4.2, we have that $B_{r_{x,r}}(x) \cap M \subset B_r(x_M) \cap M$. So, we have that

$$I_2 \leq \int_{M \setminus B_{r_{y,r}}(y)} (2\|x_1\|^2 + 2\|x_M\|^2) dq_\sigma^x(x_1) \quad (21)$$

$$\leq \exp\left(-\frac{r^2}{4\sigma^2} \left(1 - \frac{\Delta_x}{\Delta_x + \Phi_x}\right)\right) \frac{2M_2(p) + 2\|x_M\|^2}{p\left(B_{r_{x,r/\sqrt{2}}}^*(x_M)\right)} = O\left(\exp\left(-\frac{r^2}{8\sigma^2}\right)\right). \quad (22)$$

Now, we consider the term I_1 . Choose normal coordinates u centered at x_M defined on $B = B_r(x_M)$. In these coordinates, $x_1 = \exp_{x_M}(u)$ and we let $g(u)$ denote the metric tensor. Because B is small, we have expansions:

$$\rho(u)\sqrt{\det(g(u))} = \rho(0) + R_1(u), \quad |R_1(u)| \leq C_1\|u\|, \quad (23)$$

Define

$$f_\sigma(u) := \exp\left(-\frac{\|x - \exp_{x_M}(u)\|^2}{2\sigma^2}\right) \rho(u)\sqrt{\det(g(u))}.$$

Then, we have that

$$dq_\sigma^x(u) = \frac{f_\sigma(u)du}{\int_B f_\sigma(u')du' + \int_{M \setminus B} \exp\left(-\frac{\|x-x_1'\|^2}{2\sigma^2}\right) \rho(x_1')d\text{vol}_M(x_1')}.$$

Using the same technique as the one used for controlling I_2 in the proof of Theorem 4.2, we have that

$$\frac{\int_{M \setminus B} \exp\left(-\frac{\|x-x_1'\|^2}{2\sigma^2}\right) \rho(x_1')d\text{vol}_M(x_1')}{\int_B \exp\left(-\frac{\|x-x_1'\|^2}{2\sigma^2}\right) \rho(x_1')d\text{vol}_M(x_1')} = O\left(\exp\left(-\frac{r^2}{8\sigma^2}\right)\right) \quad (24)$$

So,

$$\int_B \|x_1 - x_M\|^2 dq_\sigma^x(x_1) = \frac{\int_B \|\exp_{x_M}(u) - x_M\|^2 f_\sigma(u)du}{\int_B f_\sigma(u')du'} \left(1 + O\left(\exp\left(-\frac{r^2}{8\sigma^2}\right)\right)\right).$$

Now, we derive a Taylor expansion of the squared distance from y to $\exp_{x_M}(u)$ around $u = 0$:

Lemma B.4. *Let $v := x - x_M$ and let \mathbf{II} denote the second fundamental form of M at x_M . Then, we have that*

$$\|x - \exp_{x_M} u\|^2 = \|v\|^2 + \|u\|^2 - \langle v, \mathbf{II}(u, u) \rangle + R_2(u) = \|v\|^2 + u^T(I - \mathbf{II}_v)u + R_2(u)$$

where $\mathbf{II}_v := (\langle v, \mathbf{II}_{ij} \rangle)_{i,j=1,\dots,k}$ and $|R_2(u)| \leq C_2\|u\|^3$ for some constant $C_2 = C_2(\mathbf{II}, \nabla \mathbf{II}) > 0$.

Proof of Lemma B.4. We first note that

$$\|x - \exp_{x_M} u\|^2 = \|x - x_M\|^2 + \|x_M - \exp_{x_M}(u)\|^2 + 2\langle x - x_M, x_M - \exp_{x_M}(u) \rangle.$$

Now, consider the Taylor expansion of $\exp_{x_M} u$ around $u = 0$ (see [MMASC14]):

$$\exp_{x_M} u = x_M + u + \frac{1}{2} \mathbf{\Pi}(u, u) + O(\|u\|^3)$$

where $O(\|u\|^3) \leq C_M(\mathbf{\Pi}, \nabla \mathbf{\Pi})\|u\|^3$ for some constant $C_M(\mathbf{\Pi}, \nabla \mathbf{\Pi}) > 0$.

Therefore, we have that

$$\begin{aligned} \|x - \exp_{x_M} u\|^2 &= \|v\|^2 + \|u\|^2 + \langle u, \mathbf{\Pi}(u, u) \rangle - 2\langle v, u \rangle - \langle v, \mathbf{\Pi}(u, u) \rangle + O(\|u\|^3) \\ &= \|v\|^2 + \|u\|^2 - \langle v, \mathbf{\Pi}(u, u) \rangle + O(\|u\|^3) \end{aligned}$$

where we used the fact that $\langle v, u \rangle = 0$ and $\langle u, \mathbf{\Pi}(u, u) \rangle = 0$. □

Since $\|v\| < \tau_M/2$, by [BHHS22, Theorem 2.1] we have that

$$\|\mathbf{\Pi}_v\| \leq \|v\| \cdot \max_{i,j} \|\mathbf{\Pi}_{ij}\| < \frac{1}{2} \tau_M \cdot 1/\tau_M = \frac{1}{2}.$$

So the matrix $I - \mathbf{\Pi}_v$ is positive definite and hence invertible. Therefore, we have that

$$\begin{aligned} &\int_B \|\exp_{x_M}(u) - x_M\|^2 f_\sigma(u) du \\ &= \exp\left(-\frac{\|v\|^2}{2\sigma^2}\right) \int_B u^T (I - \mathbf{\Pi}_v) u \exp\left(-\frac{u^T (I - \mathbf{\Pi}_v) u + R_2(u)}{2\sigma^2}\right) (\rho(0) + R_1(u)) du. \end{aligned}$$

and

$$\int_B f_\sigma(u) du = \exp\left(-\frac{\|v\|^2}{2\sigma^2}\right) \int_B \exp\left(-\frac{u^T (I - \mathbf{\Pi}_v) u + R_2(u)}{2\sigma^2}\right) (\rho(0) + R_1(u)) du.$$

We let $\lambda_{\min} > 0$ be the smallest eigenvalues of $I - \mathbf{\Pi}_v$. Note that $\lambda_{\min} \geq 1 - \|\mathbf{\Pi}_v\| \geq \frac{1}{2}$. So, we can choose r small enough at the beginning so that there exists some constant $C_3 > 0$ for all $u \in B$, we have that

$$u^T (I - \mathbf{\Pi}_v) u - R_2(u) \geq \lambda_{\min} \|u\|^2 - C_2 \|u\|^3 > C_3 \|u\|^2.$$

Consider the transformation $u = \sigma z$. Then, we let $M := (C_2 \sigma)^{-\frac{1}{3}}$ which goes to ∞ as $\sigma \rightarrow 0$. Then, we have that

$$\begin{aligned} &\int_B u^T (I - \mathbf{\Pi}_v) u \exp\left(-\frac{u^T (I - \mathbf{\Pi}_v) u + R_2(u)}{2\sigma^2}\right) (\rho(0) + R_1(u)) du \\ &= \sigma^{m+2} \int_{B/\sigma} z^T (I - \mathbf{\Pi}_v) z \exp\left(-\frac{z^T (I - \mathbf{\Pi}_v) z}{2} - \frac{R_2(\sigma z)}{2\sigma^2}\right) (\rho(0) + R_1(\sigma z)) dz \\ &= \sigma^{m+2} \underbrace{\int_{B_M} z^T (I - \mathbf{\Pi}_v) z \exp\left(-\frac{z^T (I - \mathbf{\Pi}_v) z}{2} - \frac{R_2(\sigma z)}{2\sigma^2}\right) (\rho(0) + R_1(\sigma z)) dz}_{J_1} \\ &\quad + \sigma^{m+2} \underbrace{\int_{B/\sigma \setminus B_M} z^T (I - \mathbf{\Pi}_v) z \exp\left(-\frac{z^T (I - \mathbf{\Pi}_v) z}{2} - \frac{R_2(\sigma z)}{2\sigma^2}\right) (\rho(0) + R_1(\sigma z)) dz}_{J_2} \end{aligned}$$

Now, for J_1 , since for any $z \in B_M$, $\frac{|R_2(\sigma z)|}{2\sigma^2} \leq \frac{C_2\sigma M^3}{2\sigma^2} = \frac{1}{2}$, we have that $\exp\left(-\frac{R_2(\sigma z)}{2\sigma^2}\right) = 1 + O(\sigma\|z\|^3)$. Therefore,
for any $y \in$ we have that

$$\begin{aligned} J_1 &= \int_{B_M} z^T(I - \mathbf{\Pi}_v)z \exp\left(-\frac{z^T(I - \mathbf{\Pi}_v)z}{2}\right) (1 + O(\sigma\|z\|^3))(\rho(0) + O(\|\sigma z\|))dz \\ &= \rho(0) \int_{B_M} z^T(I - \mathbf{\Pi}_v)z \exp\left(-\frac{z^T(I - \mathbf{\Pi}_v)z}{2}\right) dz + O(\sigma) \\ &= \rho(0) \int_{\mathbb{R}^m} z^T(I - \mathbf{\Pi}_v)z \exp\left(-\frac{z^T(I - \mathbf{\Pi}_v)z}{2}\right) dz + O(\sigma) \end{aligned}$$

where in the last part we used the fact that the the decay rate of such an integral as M goes to infinity (σ goes to 0) is exponential.

For J_2 , we similarly have that

$$\begin{aligned} |J_2| &\leq \int_{B/\sigma \setminus B_M} z^T(I - \mathbf{\Pi}_v)z \exp(-C_3\|z\|^2) (\rho(0) + O(\|\sigma z\|))dz \\ &= O(\sigma). \end{aligned}$$

Therefore,

$$\begin{aligned} &\int_B u^T(I - \mathbf{\Pi}_v)u \exp\left(-\frac{u^T(I - \mathbf{\Pi}_v)u + R_2(u)}{2\sigma^2}\right) (\rho(0) + R_1(u))du \\ &= \sigma^{m+2}\rho(0) \int_{\mathbb{R}^m} z^T(I - \mathbf{\Pi}_v)z \exp\left(-\frac{z^T(I - \mathbf{\Pi}_v)z}{2}\right) dz + O(\sigma^{m+3}). \end{aligned}$$

Similarly, we have that

$$\int_B \exp\left(-\frac{u^T(I - \mathbf{\Pi}_v)u + R_2(u)}{2\sigma^2}\right) (\rho(0) + R_1(u))du = \sigma^m \rho(0) \int_{\mathbb{R}^m} \exp\left(-\frac{z^T(I - \mathbf{\Pi}_v)z}{2}\right) dz + O(\sigma^{m+1}).$$

Therefore, we have that

$$\begin{aligned} \int_B \|x_1 - x_M\|^2 dq_\sigma^x(x_1) &= \frac{\int_B \|\exp_{x_M}(u) - x_M\|^2 f_\sigma(u) du}{\int_B f_\sigma(u') du'} \left(1 + O\left(\exp\left(-\frac{r^2}{8\sigma^2}\right)\right)\right) \\ &= \frac{\sigma^2 \int_{\mathbb{R}^m} z^T(I - \mathbf{\Pi}_v)z \exp\left(-\frac{z^T(I - \mathbf{\Pi}_v)z}{2}\right) dz + O(\sigma^3)}{\int_{\mathbb{R}^m} \exp\left(-\frac{z^T(I - \mathbf{\Pi}_v)z}{2}\right) dz + O(\sigma)} \left(1 + O\left(\exp\left(-\frac{r^2}{8\sigma^2}\right)\right)\right) \\ &= \sigma^2 \left(\frac{\int_{\mathbb{R}^m} z^T(I - \mathbf{\Pi}_v)z \exp\left(-\frac{z^T(I - \mathbf{\Pi}_v)z}{2}\right) dz}{\int_{\mathbb{R}^m} \exp\left(-\frac{z^T(I - \mathbf{\Pi}_v)z}{2}\right) dz} + O(\sigma)\right) \left(1 + O\left(\exp\left(-\frac{r^2}{8\sigma^2}\right)\right)\right) \\ &= m\sigma^2 + O(\sigma^3) \end{aligned}$$

where in the last equality we used the fact that $\mathbb{E}x^T A x = \text{tr}(A\Sigma)$ for a Gaussian random variable $x \sim \mathcal{N}(0, \Sigma)$.

Therefore, we have that

$$d_{W,2}(q_\sigma^x, \delta_{x_M}) = \sqrt{m}\sigma + O(\sigma^2).$$

B.4 Proofs in Section 5

Proof of Theorem 5.1. We prove that the vector field $u : [0, 1) \times \mathbb{R}^d \rightarrow \mathbb{R}^d$ is locally Lipschitz for any fixed t and that the integral $\int_0^1 \int_{\mathbb{R}^d} \|u_t(x)\| p_t(dx) dt < \infty$. Then, by the mass conservation formula (see for example [Vil09]), we conclude the proof.

To prove the local Lipschitz property, by Proposition 3.1, it suffices to show that the covariance matrix $\Sigma_t(x)$ of the posterior distribution $p(\cdot|x_t = x)$ is locally (w.r.t. x) uniformly bounded (w.r.t. t). We establish the following lemma for this purpose.

Lemma B.5. *Let p be a probability measure on \mathbb{R}^d with a finite 2-moment $\mathbf{M}_2(p)$. For any $x \in \mathbb{R}^d$, consider the posterior distribution:*

$$p(dz|x_t = x) = \frac{\exp\left(-\frac{\|x-\alpha_t z\|^2}{2\beta_t^2}\right) p(dz)}{\int_{\Omega} \exp\left(-\frac{\|x-\alpha_t z\|^2}{2\beta_t^2}\right) p(dz)}.$$

We let $N_t(x) := \int \exp\left(-\frac{\|x-\alpha_t z\|^2}{2\beta_t^2}\right) p(dz)$. Then, the covariance matrix $\Sigma_t(x)$ of $p(\cdot|x_t = x)$ satisfies:

$$\Sigma_t(x) \preceq \left(2\|m_t(x)\|^2 + \frac{2\mathbf{M}_2(p)}{N_t(x)}\right) I.$$

Proof of Lemma B.5. Fix a unit vector v . Then, we have that

$$v^\top \Sigma_t(x) v = \int \langle z - m_t(x), v \rangle^2 \frac{\exp\left(-\frac{\|x-\alpha_t z\|^2}{2\beta_t^2}\right) p(dz)}{\int \exp\left(-\frac{\|x-\alpha_t z'\|^2}{2\beta_t^2}\right) p(dz')}$$

For $z \in \mathbb{R}^d$, we have that

$$\langle z - m_t(x), v \rangle^2 \leq \|z - m_t(x)\|^2 \leq 2\|z\|^2 + 2\|m_t(x)\|^2.$$

Therefore, one has that

$$\begin{aligned} v^\top \Sigma_t(x) v &\leq 2\|m_t(x)\|^2 + 2 \int \|z\|^2 \frac{\exp\left(-\frac{\|x-\alpha_t z\|^2}{2\beta_t^2}\right) p(dz)}{\int \exp\left(-\frac{\|x-\alpha_t z'\|^2}{2\beta_t^2}\right) p(dz')} \\ &= 2\|m_t(x)\|^2 + \frac{2 \int \|z\|^2 p(dz)}{\int \exp\left(-\frac{\|x-\alpha_t z'\|^2}{2\beta_t^2}\right) p(dz')} \\ &= 2\|m_t(x)\|^2 + \frac{2\mathbf{M}_2(p)}{N_t(x)} \end{aligned}$$

Since v is arbitrary, this concludes the proof. \square

By dominated convergence theorem, it is straightforward to check that $N : [0, 1) \times \mathbb{R}^d \rightarrow \mathbb{R}$ is continuous. Hence, for any $x \in \mathbb{R}^d$ and any local compact neighborhood of x , N is uniformly bounded below by some positive constant. Furthermore, as $m_t(x)$ is differentiable (cf. Proposition 3.1), we have that $m_t(x)$ is locally uniformly bounded as well. These together with Proposition 3.1 and Equation (6) imply that the vector field $u : [0, 1) \times \mathbb{R}^d \rightarrow \mathbb{R}^d$ is locally Lipschitz for any $t \in [0, 1)$. This concludes the proof of the well-posedness of the flow map.

Now we verify the integrality of u_t .

$$\begin{aligned}
& \int_0^1 \int \|u_t(x)\| p_t(dx) dt \\
& \leq \int_0^1 \int \int \|u_t(x|x_1)\| p_t(dx|x_1) p(dx_1) dt \\
& = \int_0^1 \int \int \left\| \frac{\dot{\beta}_t}{\beta_t} x + \frac{\dot{\alpha}_t \beta_t - \alpha_t \dot{\beta}_t}{\beta_t} x_1 \right\| \frac{1}{(2\pi\beta_t^2)^{d/2}} \exp\left(-\frac{\|x - \alpha_t x_1\|^2}{2\beta_t^2}\right) dx p(dx_1) dt \\
& \leq \int_0^1 \int \int \left(\left\| \frac{\dot{\beta}_t}{\beta_t} x - \frac{\alpha_t \dot{\beta}_t}{\beta_t} x_1 \right\| + \|\dot{\alpha}_t x_1\| \right) \frac{1}{(2\pi\beta_t^2)^{d/2}} \exp\left(-\frac{\|x - \alpha_t x_1\|^2}{2\beta_t^2}\right) dx p(dx_1) dt
\end{aligned}$$

We split the integral by the two terms according to the summation $\|\frac{\dot{\beta}_t}{\beta_t} x - \frac{\alpha_t \dot{\beta}_t}{\beta_t} x_1\| + \|\dot{\alpha}_t x_1\|$. For the first term, we use $\tilde{x} = x - \alpha_t x_1$ and the fact about the expected norm of a Gaussian random variable with variance σ^2 is $\sigma \sqrt{\frac{\pi}{2} \frac{\Gamma((n+1)/2)}{\Gamma(n/2)}}$.

$$\begin{aligned}
& \int_0^1 \int \int \left| \frac{\dot{\beta}_t}{\beta_t} \right| \|x - \alpha_t x_1\| \frac{1}{(2\pi\beta_t^2)^{d/2}} \exp\left(-\frac{\|x - \alpha_t x_1\|^2}{2\beta_t^2}\right) dx p(dx_1) dt \\
& = \int_0^1 \int \left| \frac{\dot{\beta}_t}{\beta_t} \right| \beta_t \sqrt{\frac{\pi}{2}} \frac{\Gamma((d+1)/2)}{\Gamma(d/2)} p(dx_1) dt \\
& = \sqrt{\frac{\pi}{2}} \frac{\Gamma((d+1)/2)}{\Gamma(d/2)} \int_0^1 -\dot{\beta}_t dt \\
& = \sqrt{\frac{\pi}{2}} \frac{\Gamma((d+1)/2)}{\Gamma(d/2)},
\end{aligned}$$

where we use the assumption that β_t is a non-increasing function of t and hence $\dot{\beta}_t \leq 0$.

For the second term, we have that

$$\begin{aligned}
& \int_0^1 \int \int \|\dot{\alpha}_t x_1\| \frac{1}{(2\pi\beta_t^2)^{d/2}} \exp\left(-\frac{\|x - \alpha_t x_1\|^2}{2\beta_t^2}\right) dx p(dx_1) dt \\
& \leq \int_0^1 \int \dot{\alpha}_t \|x_1\| p(dx_1) dt \\
& \leq \int \|x_1\| p(dx_1) < \infty.
\end{aligned}$$

The last step follows from the fact that p has finite second moment and hence finite first moment. We also use the assumption that α_t is a non-decreasing function of t and hence $\dot{\alpha}_t \geq 0$. \square

Proof of Proposition 5.6. For any independent random variables $X \sim p$ and any $Z \sim N(0, \sigma^2 I)$, we have that $X + Z \sim q_\sigma = p * N(0, \sigma^2 I)$. Hence,

$$d_{W,2}(q_\sigma, p)^2 \leq \mathbb{E} [\|X + Z - X\|^2] = \mathbb{E} [\|Z\|^2] = O(\sigma^2).$$

The result follows. \square

Proof of Theorem 5.7.

$$\begin{aligned}
\tilde{m}_t(y) &= \int \frac{\exp\left(-\frac{\|y-\alpha_t y_1\|^2}{2\beta_t^2}\right) y_1}{\int \exp\left(-\frac{\|y-\alpha_t y'_1\|^2}{2\beta_t^2}\right) \tilde{p}(dy'_1)} \tilde{p}(dy_1) \\
&= \int \frac{\exp\left(-\frac{\|\mathbf{O}x+\alpha_t b-\alpha_t(\mathbf{O}x_1+b)\|^2}{2\beta_t^2}\right) (\mathbf{O}x_1+b)}{\int \exp\left(-\frac{\|\mathbf{O}x+\alpha_t b-\alpha_t(\mathbf{O}x'_1+\alpha_t b)\|^2}{2\beta_t^2}\right) p(dx'_1)} p(dx_1) \\
&= \int \frac{\exp\left(-\frac{\|x-\alpha_t x_1\|^2}{2\beta_t^2}\right) (\mathbf{O}x_1+b)}{\int \exp\left(-\frac{\|x-\alpha_t x'_1\|^2}{2\beta_t^2}\right) p(dx'_1)} p(dx_1) \\
&= \mathbf{O}m_t(x) + b.
\end{aligned} \tag{25}$$

where in the second equality we used the change of variable $y_1 = \mathbf{O}x_1 + b$ and the fact that $|\det(\mathbf{O})| = 1$.

Then, we have that

$$\begin{aligned}
\tilde{u}_t(y) &= \tilde{u}_t(\mathbf{O}x + \alpha_t b) = (\log \beta_t)' (\mathbf{O}x + \alpha_t b) + \beta_t \left(\frac{\alpha_t}{\beta_t}\right)' \tilde{m}_t(\mathbf{O}x + \alpha_t b) \\
&= \mathbf{O} \left((\log \beta_t)' x + \beta_t \left(\frac{\alpha_t}{\beta_t}\right)' m_t(x) \right) + \dot{\alpha}_t b \\
&= \mathbf{O}u_t(x) + \dot{\alpha}_t b.
\end{aligned}$$

Now, let x_t be an integral path w.r.t. u_t . Consider the path $y_t = \mathbf{O}x_t + \alpha_t b$. Then,

$$\frac{dy_t}{dt} = \mathbf{O} \frac{dx_t}{dt} + \dot{\alpha}_t b = \mathbf{O}u_t(x_t) + \dot{\alpha}_t b = \tilde{u}_t(y_t).$$

Therefore, $\tilde{\Psi}_t(y) = \mathbf{O}\Psi_t(x) + \alpha_t b$. □

Proof of Theorem 5.8. Consider $y = s_t x$. The transformed denoiser $\tilde{m}_t(y)$ w.r.t. $\bar{\alpha}_t$ and $\bar{\beta}_t$ is given by

$$\begin{aligned}
\tilde{m}_t(y) &= \int \frac{\exp\left(-\frac{\|y-\bar{\alpha}_t y_1\|^2}{2\bar{\beta}_t^2}\right) y_1}{\int \exp\left(-\frac{\|y-\bar{\alpha}_t y'_1\|^2}{2\bar{\beta}_t^2}\right) p(dy'_1)} p(dy_1) \\
&= \int \frac{\exp\left(-\frac{\|s_t x-\alpha_t s_t x_1\|^2}{2s_t^2 \beta_t^2}\right) s_t x_1}{\int \exp\left(-\frac{\|s_t x-\alpha_t s_t x'_1\|^2}{2s_t^2 \beta_t^2}\right) p(dx'_1)} p(dx_1) \\
&= \int \frac{\exp\left(-\frac{\|x-\alpha_t x_1\|^2}{2\beta_t^2}\right) kx_1}{\int \exp\left(-\frac{\|x-\alpha_t x'_1\|^2}{2\beta_t^2}\right) p(dx'_1)} p(dx_1) = km_t(x)
\end{aligned} \tag{26}$$

Let x_t denote an ODE path for $dx_t/dt = u_t(x_t)$. Then we consider the path $y_t = s_t x_t$. We need to check that $dy_t/dt = \tilde{u}_t(y_t)$.

$$\begin{aligned}
\frac{dy_t}{dt} &= s'_t x_t + s_t \frac{dx_t}{dt} = s'_t x_t + s_t ((\log \beta_t)' x_t + \beta_t (\alpha_t / \beta_t)' m_t(x_t)) \\
&= (s'_t / s_t + (\log \beta_t)') s_t x_t + \beta_t (\alpha_t / \beta_t)' s_t m_t(x_t) \\
&= (\log \bar{\beta}_t)' y_t + s_t \beta_t \left(\frac{\alpha_t}{k \beta_t} \right)' k m_t(x_t) \\
&= (\log \bar{\beta}_t)' y_t + \bar{\beta}_t \left(\frac{\bar{\alpha}_t}{\bar{\beta}_t} \right)' \bar{m}_t(y_t) = \bar{u}_t(y_t)
\end{aligned}$$

This finishes the proof. \square

B.4.1 Proof of Theorem 5.3

We utilize the change of variable $\lambda(t) = \log \frac{\alpha_t}{\beta_t}$ for $t \in (0, 1)$. We also let $t(\lambda)$ denote the inverse function of $\lambda(t)$.

Next, we consider $z_\lambda := \frac{x_{t(\lambda)}}{\alpha_{t(\lambda)}}$. Then, we have that z_λ satisfies ODE Equation (10): $dz_\lambda/d\lambda = m_\lambda(z_\lambda) - z_\lambda$. Recall the transformation A_t sending x to x/α_t . Then, we define $q_\lambda := (A_{t(\lambda)})_\# p_{t(\lambda)} = p * \mathcal{N}(0, e^{-2\lambda(t)} I)$.

By Theorem 4.5, we have the following convergence rate for $m_\lambda(z_\lambda)$:

Claim 1. For any radius $R > \frac{1}{2}\tau_\Omega$, $0 < \zeta < 1$ and all $z \in B_R(0)$ such that $d_\Omega(z) < \frac{1}{2}\tau_\Omega$, there exists $\lambda_R > -\infty$ such that for any $\lambda > \lambda_R$

$$\|m_\lambda(z) - \text{proj}_\Omega(z)\| \leq C_{\zeta, \tau, R} \cdot e^{-\zeta\lambda},$$

where $C_{\zeta, \tau, R}$ is a constant depending only on ζ and τ and R .

Proof of Claim 1. We let $z_\Omega := \text{proj}_\Omega(z)$. Note that $\|z_\Omega\| \leq \|z\| + d_\Omega(z) \leq 2R$. Since p satisfies Assumption 1, we have that $p(B_r(z_\Omega)) \geq C_{2R} r^k$ for small $0 < r < c_{2R}$. Now, we let $\lambda_R := -\log(c_{2R})/\zeta$. By Theorem 4.5, we conclude the proof. \square

Next we establish a concentration result for q_λ when λ is large.

Claim 2. For any small $\delta > 0$, there are $R_\delta, \lambda_\delta > 0$ large enough such that for any $\lambda \geq \lambda_\delta$ and $R > R_\delta$, we have that

$$q_\lambda(B_R(0) \cap B_\delta(\Omega)) > 1 - \delta.$$

Proof of Claim 2. Consider the random variable $X = Y + e^{-\lambda}Z$ where $Y \sim p$ and $Z \sim p_0 = \mathcal{N}(0, I)$ are independent but from the same probability space (Ω, \mathbb{P}) . Then, X has q_λ as its law. We have that $d_\Omega(x) \leq \|Y + e^{-\lambda}Z - Y\| = e^{-\lambda}\|Z\|$. For any $R > \delta$, we have that

$$\begin{aligned}
\mathbb{P}(\|X + e^{-\lambda}Z\| \leq 2R, e^{-\lambda}\|Z\| \leq \delta) &\geq \mathbb{P}(\|X\| \leq R, e^{-\lambda}\|Z\| \leq \delta) \\
&= \mathbb{P}(\|X\| \leq R) \mathbb{P}(\|Z\| \leq e^\lambda \delta)
\end{aligned}$$

Since Z follows the standard Gaussian, for any δ , there exists $\lambda_\delta > 0$ such that for all $\lambda \geq \lambda_\delta$, we have that

$$\mathbb{P}(\|Z\| \leq e^\lambda \delta) \geq \mathbb{P}(\|Z\| \leq e^{\lambda_\delta} \delta) > 1 - \frac{\delta}{2}.$$

Now, since p has finite 2-moment and hence finite 1-moment, there exists $R_\delta > 0$ such that $\mathbb{P}(\|X\| \leq \frac{R_\delta}{2}) > 1 - \frac{\delta}{2}$.

Therefore, for all $\lambda \geq \lambda_\delta$, we have that

$$\begin{aligned} q_\lambda(B_{R_\delta}(0) \cap B_\delta(\Omega)) &\geq \mathbb{P}(\|X + e^{-\lambda}Z\| \leq R_\delta, e^{-\lambda}\|Z\| \leq \delta) \\ &\geq (1 - \frac{\delta}{2})(1 - \frac{\delta}{2}) > 1 - \delta. \end{aligned}$$

□

The following Claim establishes an absorbing property for points in $z_{\lambda_\delta} \in B_{R_\delta}(0) \cap B_\delta(\Omega)$.

Claim 3. Consider $\delta > 0$ small such that $\delta < \frac{\tau_\Omega}{4}$. Fix any $R_\delta > 0$ such that $R_\delta > 2\delta$. Then, there exists $\lambda_\delta > \lambda_{2R_\delta}$ satisfying the following property: the trajectory $(z_\lambda)_{\lambda \in [\lambda_\delta, \infty)}$ starting at any initial point $z_{\lambda_\delta} \in B_{R_\delta}(0) \cap B_\delta(\Omega)$ of the ODE in Equation (10) satisfies that for any $\lambda \geq \lambda_\delta$:

- $\|z_\lambda\| \leq 2R_\delta$;
- $d_\Omega(z_\lambda) \leq 2\delta < \tau_\Omega/2$.

Proof of Claim 3. We first let $C := C_{\zeta, \tau, R}$ where $R := 2R_\delta$ and $C_{\zeta, \tau, R}$ is defined in Claim 1. Now we define (one can see how the definition is motivated from the following proof)

$$\lambda_\delta := -\frac{1}{\zeta} \cdot \min \left\{ \log \left(\frac{\delta\zeta}{2C} \right), 2 \log \left(\frac{\zeta}{8} \sqrt{\frac{(2-\zeta)\delta}{C}} \right), \log \left(\frac{\delta(2-\zeta)}{4C} \right) \right\}.$$

By continuity of the ODE path, there exists a maximal interval $I = [\lambda_\delta, \Lambda_\delta]$ satisfying the above two conditions. Now, we show that Λ_δ must be infinity by showing that otherwise the solution z_{Λ_δ} will not equate the two conditions and hence the trajectory will be able to extend without violating the conditions to $\Lambda_\delta + \epsilon$ for some small $\epsilon > 0$. In this way, we can extend the interval I to $[\lambda_\delta, \Lambda_\delta + \epsilon]$ which contradicts the maximality of I .

Now, assume that $\Lambda_\delta < \infty$. Then, by Corollary A.12, we have that for any $\lambda \in I$,

$$\begin{aligned} \frac{d(d_\Omega^2(z_\lambda))}{d\lambda} &= -2\langle z_\lambda - \text{proj}_\Omega(z_\lambda), z_\lambda - m_\lambda(z_\lambda) \rangle \\ &= -2(\langle z_\lambda - \text{proj}_\Omega(z_\lambda), z_\lambda - \text{proj}_\Omega(z_\lambda) \rangle + \langle z_\lambda - \text{proj}_\Omega(z_\lambda), \text{proj}_\Omega(z_\lambda) - m_\lambda(z_\lambda) \rangle) \\ &\leq -2d_\Omega^2(z_\lambda) + 2d_\Omega(z_\lambda)\|m_\lambda(z_\lambda) - \text{proj}_\Omega(z_\lambda)\|. \end{aligned}$$

Multiplying the exponential integrator $e^{2\lambda}$, we have that

$$\frac{d(e^{2\lambda}d_\Omega^2(z_\lambda))}{d\lambda} \leq 2e^{2\lambda}d_\Omega(z_\lambda)\|m_\lambda(z_\lambda) - \text{proj}_\Omega(z_\lambda)\|.$$

By our assumption on z_λ and Claim 1, we have that $d_\Omega(z_\lambda) \leq 2\delta$ and for any $\lambda > \lambda_{2R_\delta}$, $\|m_\lambda(z_\lambda) - \text{proj}_\Omega(z_\lambda)\| \leq C \cdot e^{-\zeta\lambda}$. Then, we have the differential inequality below:

$$\frac{d(e^{2\lambda}d_\Omega^2(z_\lambda))}{d\lambda} \leq 4\delta C e^{(2-\zeta)\lambda}.$$

Integrating both sides from λ_δ to any $s \leq \Lambda_\delta$, we have that

$$\begin{aligned} e^{2s}d_\Omega^2(z_s) - e^{2\lambda_\delta}d_\Omega^2(z_{\lambda_\delta}) &\leq 4\delta C \int_{\lambda_\delta}^s e^{(2-\zeta)\lambda} d\lambda \\ &\leq \frac{4\delta C}{2-\zeta} \left(e^{(2-\zeta)s} - e^{(2-\zeta)\lambda_\delta} \right). \end{aligned}$$

This implies that

$$d_{\Omega}^2(z_s) \leq e^{-2(s-\lambda_{\delta})} d_{\Omega}^2(z_{\lambda_{\delta}}) + \underbrace{\frac{4\delta C}{2-\zeta} \left(e^{-\zeta s} - e^{(2-\zeta)\lambda_{\delta}-2s} \right)}_{\leq \frac{4\delta C}{2-\zeta} e^{-\zeta s} \leq \delta^2}, \quad (27)$$

where the inequality under the brace bracket follows from the observation $e^{(2-\zeta)\lambda_{\delta}-2s} = e^{-\zeta s + (\lambda_{\delta}-s)(2-\zeta)} < e^{-\zeta s}$ and the definition of λ_{δ} . Hence, $d_{\Omega}^2(z_s) \leq d_{\Omega}^2(z_{\lambda_{\delta}}) + \delta^2$ for any $s \in [\lambda_{\delta}, \Lambda_{\delta}]$. So $d_{\Omega}(z_s) \leq \sqrt{2}\delta < 2\delta$.

Now we examine $\|z_{\lambda}\|$ along the integral path. We have that

$$\begin{aligned} \|z_s - z_{\lambda_{\delta}}\| &\leq \int_{\lambda_{\delta}}^s \|m_{\lambda}(z_{\lambda}) - z_{\lambda}\| d\lambda \\ &\leq \int_{\lambda_{\delta}}^s \|m_{\lambda}(z_{\lambda}) - \text{proj}_{\Omega}(z_{\lambda})\| + \|\text{proj}_{\Omega}(z_{\lambda}) - z_{\lambda}\| d\lambda \\ &\leq \int_{\lambda_{\delta}}^s C e^{-\zeta\lambda} + d_{\Omega}(z_{\lambda}) d\lambda. \end{aligned}$$

Now, for the integral of $d_{\Omega}(z_{\lambda})$, we have that

$$\begin{aligned} \int_{\lambda_{\delta}}^s d_{\Omega}(z_{\lambda}) d\lambda &\leq \int_{\lambda_{\delta}}^s \sqrt{e^{-2(\lambda-\lambda_{\delta})} d_{\Omega}^2(z_{\lambda_{\delta}}) + \frac{4\delta C}{2-\zeta} (e^{-\zeta\lambda} - e^{(2-\zeta)\lambda_{\delta}-2\lambda})} d\lambda \\ &\leq \int_{\lambda_{\delta}}^s \sqrt{e^{-2(\lambda-\lambda_{\delta})} d_{\Omega}^2(z_{\lambda_{\delta}}) + \frac{4\delta C}{2-\zeta} e^{-\zeta\lambda}} d\lambda \\ &\leq \int_{\lambda_{\delta}}^s \sqrt{e^{-2(\lambda-\lambda_{\delta})} d_{\Omega}^2(z_{\lambda_{\delta}}) + \frac{4\delta C}{2-\zeta}} e^{-\zeta\lambda/2} d\lambda \\ &\leq \delta(1 - e^{-s+\lambda_{\delta}}) + \sqrt{\frac{4\delta C}{2-\zeta}} \cdot \frac{2}{\zeta} \left(e^{-\zeta\lambda_{\delta}/2} - e^{-\zeta s/2} \right). \end{aligned}$$

Therefore,

$$\|z_s - z_{\lambda_{\delta}}\| \leq \underbrace{\frac{C}{\zeta} (-e^{-\zeta s} + e^{-\zeta\lambda_{\delta}})}_{\leq \frac{C}{\zeta} e^{-\zeta\lambda_{\delta}} \leq \delta/2} + \delta(1 - e^{-s+\lambda_{\delta}}) + \underbrace{\sqrt{\frac{4\delta C}{2-\zeta}} \cdot \frac{2}{\zeta} \left(e^{-\zeta\lambda_{\delta}/2} - e^{-\zeta s/2} \right)}_{\leq \sqrt{\frac{4\delta C}{2-\zeta}} \cdot \frac{2}{\zeta} e^{-\zeta\lambda_{\delta}/2} \leq \delta/2} \leq 2\delta$$

where we used the definition of λ_{δ} again to control all the exponential terms. This implies that $\|z_s\| \leq R_{\delta} + 2\delta < 2R_{\delta}$ for all $s \in [\lambda_{\delta}, \Lambda_{\delta}]$ (recall that we also assume that R_{δ} is larger than 2δ). This concludes the proof. \square

Now, we establish the desired convergence results for the scale of λ .

Claim 4. For any small $\delta > 0$, there exist large enough λ_{δ} , such that with probability at least $1 - \delta$, we have that $z_{\lambda_{\delta}} \sim q_{\lambda_{\delta}}$ satisfies the following properties:

1. z_{λ} converges along the ODE trajectory starting from $z_{\lambda_{\delta}}$ as $\lambda \rightarrow \infty$;

2. the convergence rate is given by $\|z_\lambda - z_{\lambda_\delta}\| = O(e^{-\frac{\zeta\lambda}{2}})$.

Proof of Claim 4. For any $\delta > 0$, by Claim 2 and Claim 3, there exist large enough λ_δ and R_δ , such that

- with probability at least $1 - \delta$, we have that $z_{\lambda_\delta} \sim q_{\lambda_\delta}$ lies in $B_{R_\delta}(0) \cap B_\delta(\Omega)$;
- the ODE trajectory $(z_\lambda)_{\lambda \in [\lambda_\delta, \infty)}$ starting at $z_{\lambda_\delta} \in B_{R_\delta}(0) \cap B_\delta(\Omega)$ satisfies that for all $\lambda \geq \lambda_\delta$, z_λ lies in $B_{2R_\delta}(0)$ and $d_\Omega(z_\lambda) \leq 2\delta$.

This implies that one can apply the convergence rate of denoiser in Claim 1 to the entire trajectory with $C := C_{\zeta, \tau, R}$ where $R := 2R_\delta$. Then, for any $\lambda_1 < \lambda_2$ in the interval $[\lambda_\delta, \infty)$, we have that

$$\begin{aligned} \|z_{\lambda_2} - z_{\lambda_1}\| &\leq \int_{\lambda_1}^{\lambda_2} \|m_\lambda(z_\lambda) - z_\lambda\| d\lambda \\ &\leq \int_{\lambda_1}^{\lambda_2} \|m_\lambda(z_\lambda) - \text{proj}_\Omega(z_\lambda)\| + \|\text{proj}_\Omega(z_\lambda) - z_\lambda\| d\lambda \\ &\leq \frac{C}{\zeta} (-e^{-\zeta\lambda_2} + e^{-\zeta\lambda_1}) + \delta e^{\lambda_\delta} (e^{-\lambda_1} - e^{-\lambda_2}) + \sqrt{\frac{4\delta C}{2-\zeta}} \cdot \frac{2}{\zeta} (e^{-\zeta\lambda_1/2} - e^{-\zeta\lambda_2/2}). \end{aligned}$$

This implies that the solution z_λ becomes a Cauchy sequence and hence converges to a limit z_∞ .

Now, we let λ_2 approach ∞ in the above inequality and replace λ_1 with λ to obtain the following convergence rate:

$$\|z_\infty - z_\lambda\| = O(e^{-\frac{\zeta\lambda}{2}}). \quad (28)$$

□

Now, we change the coordinate back to $t \in [0, 1)$ to obtain the following result. Since $\delta > 0$ is arbitrary so one can let δ approach 0 in the result below to conclude the proof of Theorem 5.3.

Claim 5. For any small $\delta > 0$, one can sample $x_0 \sim p_0$ with probability at least $1 - \delta$, such that the flow map $\Psi_t(x_0)$ converges to a limit $\Psi_1(x_0)$ as $t \rightarrow 1$.

Proof of Claim 5. Let λ_δ be the one given in Claim 4. Then, we let $t_\delta := t(\lambda_\delta)$. Consider the map $A_{t_\delta} : \mathbb{R}^d \rightarrow \mathbb{R}^d$ sending x to x/α_{t_δ} . Then, we have that

$$(A_{t_\delta})_\# p_{t_\delta} = q_{\lambda_\delta}. \quad (29)$$

Both maps A_{t_δ} and Ψ_{t_δ} (whose existence follows from Theorem 5.1) are continuous bijections. It is then easy to see that if an ODE trajectory of Equation (10) converges starting with some $z_{\lambda_\delta} \sim q_{\lambda_\delta}$ and has convergence rate $O(e^{-\frac{\zeta\lambda}{2}})$, then the corresponding trajectory of the ODE Equation (1) starting with $x_0 := (A_{t_\delta} \circ \Psi_{t_\delta})^{-1}(z_{\lambda_\delta})$ also converges to a limit as $t \rightarrow 1$ with the same convergence rate up to the change of variable $\lambda \rightarrow t$. Finally, by Equation (29) we also have that

$$p_0(x_0 \text{ with the desired properties}) = q_{\lambda_\delta}(z_{\lambda_\delta} \text{ with the desired properties}) > 1 - \delta,$$

which concludes the proof. □

Item 2 in the theorem is a direct consequence of item 1. As Ψ_1 is the pointwise limit of continuous maps Ψ_t (cf. Theorem 5.1), it is also measurable. We know that p_t weakly converges to $p_1 = p$ as $t \rightarrow 1$. Now, we just verify that $(\Psi_1)_\#p_0$ is also a weak limit of $p_t = (\Psi_t)_\#p_0$ to show that $(\Psi_1)_\#p_0 = p_1$.

For any continuous and bounded function f , we have that

$$\begin{aligned} \lim_{t \rightarrow 1} \int f(x)(\Psi_t)_\#p_0(dx) &= \lim_{t \rightarrow 1} \int f(\Psi_t(x))p_0(dx) \\ &= \int f(\Psi_1(x))p_0(dx) \end{aligned}$$

where we used the bounded convergence theorem in the last step. Therefore, we have that $(\Psi_1)_\#p_0 = p_1$ and hence Ψ_1 is the flow map associated with the ODE $dx_t/dt = u_t(x_t)$.

B.4.2 Proof of Theorem 5.4

Part 1. We first establish the following volume growth condition for the manifold M .

Lemma B.6. *For any $R > 0$, there exists a constant $C_R > 0$ so that for any radius $0 < r < r_M$ and any $x \in B_R(0)$, one has $p(B_r(x)) \geq C_R r^k$ for any $x \in M$.*

Proof. Notice that within the compact region $\overline{B}_{2R}(0) \cap M$, both the density ρ and its gradient $\nabla\rho$ is lower bounded. We also know that the curvature tensor is bounded due to the boundedness of second fundamental form. So at the normal coordinate chart around x , we have that

$$dp(u) = \rho(u)\sqrt{\det(g(u))}du = (\rho(0) + R(u))du,$$

where $|R(u)| \leq c_R\|u\|$ for some constant c_R depending only on the bounds of ρ within $B_{2R}(0)$ and the geometry of M (the bounds on second fundamental forms etc).

Now, since there exists $c_1, c_2 > 0$ depending only on the geometry of M (bounds on injective radius, second fundamental form etc) such that $c_1\|x - y\| \leq d_M(x, y) \leq c_2\|x - y\|$, we have that there exists $C_R > 0$ depending only on M so that for any $x \in M$ and $r < r_M$,

$$p(B_r(x)) \geq p(B_{r/c_2}^M(x)) \geq C_R r^k.$$

□

Then, we can replicate the proof of Theorem 5.3 with only small changes of the Claim 1 as follows and with using $\zeta = 1$:

Claim 6. Under the same assumptions as in Theorem 5.4, for any radius $R > 0$, all $z \in B_R(0)$ such that $d(z, M) < \frac{1}{2}\tau\Omega$, we have that

$$\|m_\lambda(z) - \text{proj}_M(z)\| \leq C_{\tau,R} \cdot e^{-\lambda},$$

where $C_{\tau,R}$ is a constant depending only on τ and R and the geometry of M .

Proof of Claim 6. This can be proved by carefully examining all bounds involved in the proof of Theorem 4.8.

- Equation (21): notice that now that y and x_M are bounded by $B_R(0)$, so $\|x_M\|$ in the numerator can be bounded by R . The big O is also bounded by R utilizing the volume growth condition of M (Lemma B.6).

- Equation (23): C_1 can be bounded by R and the bounds on the density and the second fundamental form up to the 1st order derivative.
- Equation (24): this one is bounded similarly as the one in Equation (21) by R .
- Lemma B.4: the bound C_2 is bounded by the bounds on the second fundamental form and its covariant derivatives.

□

Part 2. In the discrete case, we let $\Omega := \{x_1, \dots, x_N\}$. We can improve the convergence rate in Theorem 5.3 to be exponential by considering a direct consequence of Corollary 4.11:

Claim 7. For all $z \in \mathbb{R}^d$ such that $d_\Omega(z) < \frac{1}{4}\text{sep}_\Omega$, we have that

$$\|m_\lambda(z) - \text{proj}_\Omega(z)\| \leq C_2 \cdot \exp(-C_1 e^{\lambda^2}),$$

where C_1, C_2 only depends on $\text{sep}_\Omega := \min_{x_i \neq x_j \in \Omega} \|x_i - x_j\|$ is the minimal separation between the points in Ω .

Therefore, when λ_δ is large enough, we have that for any $\lambda_2 > \lambda_1 \geq \lambda_\delta$

$$\begin{aligned} \frac{d(e^{2\lambda} d_\Omega^2(z_\lambda))}{d\lambda} &\leq 2e^{2\lambda} d_\Omega(z_\lambda) \|m_\lambda(z_\lambda) - \text{proj}_\Omega(z_\lambda)\| \\ &\leq 2C_2 e^{2\lambda - C_1 e^{-\lambda^2}} d_\Omega(z_\lambda) \\ &\leq C_3 e^{-\lambda} d_\Omega(z_\lambda), \end{aligned}$$

where C_3 is a constant dependent on C_1, C_2 and the properties of the exponential function.

Now, following the rest of the estimations in the proof of Theorem 5.3, we can replace the rate $O(e^{-\frac{c\lambda}{2}})$ in Claim 4 with $O(e^{-\lambda})$ after the change above and conclude the proof.

B.5 Proofs in Section 6

Proof of Proposition 6.1. The proof is based on the following simple observation.

Lemma B.7. Let p_b be a distribution and let $p := p_b * \mathcal{N}(0, \delta^2 I)$. Let $(y_{\sigma_b})_{\sigma_b \in (0, \infty)}$ be an ODE trajectory of Equation (5) with data distribution p_b . We define $(x_\sigma := y_{\sigma_b = \sqrt{\sigma^2 + \delta^2}})_{\sigma \in (0, \infty)}$. Then, (x_σ) is an ODE trajectory of Equation (5) with data distribution p .

Proof of Lemma B.7. Let $q_{\sigma_b} := p_b * \mathcal{N}(0, \sigma_b^2 I)$ be the probability path with data distribution p_b . Then, we have that y_{σ_b} satisfies

$$\frac{d y_{\sigma_b}}{d \sigma_b} = -\sigma_b \nabla \log q_{\sigma_b}(y_{\sigma_b}),$$

With the change of variable $\sigma_b = \sqrt{\sigma^2 + \delta^2}$, we have that

$$\begin{aligned} \frac{d y_{\sigma_b}}{d \sigma} &= -\frac{d \sigma_b}{d \sigma} \sigma_b \nabla \log q_{\sigma_b}(y_{\sigma_b}), \\ &= -\frac{\sigma}{\sigma_b} \sigma_b \nabla \log q_{\sigma_b}(y_{\sigma_b}), \\ &= -\sigma \nabla \log q_{\sigma_b}(y_{\sigma_b}), \end{aligned}$$

One has that

$$\begin{aligned}
q_{\sigma_b}(y_{\sigma_b}) &= \frac{1}{(2\pi\sigma_b^2)^{d/2}} \int \exp\left(-\frac{\|y_{\sigma_b} - x\|^2}{2\sigma_b^2}\right) p_b(dx) \\
&= \frac{1}{(2\pi(\sigma^2 + \delta^2))^{d/2}} \int \exp\left(-\frac{\|x_\sigma - x\|^2}{2(\delta^2 + \sigma^2)}\right) p_b(dx) \\
&= q_\sigma(x_\sigma),
\end{aligned}$$

where $q_\sigma(x)$ denotes the density of $q_\sigma := p * \mathcal{N}(0, \sigma^2 I)$. Therefore, the trajectory $x_\sigma := y_{\sigma_b}$ satisfies

$$\frac{dx_\sigma}{d\sigma} = -\sigma \nabla \log q_\sigma(x_\sigma).$$

□

We will first consider the flow model ODE with data distribution p_b and we use the notation y_{σ_b} to denote the trajectory. We apply Proposition 4.1 to the ODE trajectory y_{σ_b} with data distribution p_b and with the fact that the function $f(s) = \frac{s}{\log(1+s)}$ is increasing for $s > 0$, we have that for any $\sigma_b > \sigma_{\text{init}}(\Omega, \zeta, R_0)$, and for all z with $\|z - \mathbb{E}(p_b)\| < R_0$, then

$$d_{W,1}(p_b(\cdot|y_{\sigma_b} = z), p_b) < \zeta \|z - \mathbb{E}(p_b)\|.$$

Then, by Lemma B.1, for any $z \in \partial B_{R_0}(\mathbb{E}(p_b))$, we have that

$$\|m_{\sigma_b}(z) - \mathbb{E}(p_b)\| = \|\mathbb{E}(p_b(\cdot|y_{\sigma_b} = z)) - \mathbb{E}(p_b)\| \leq W_1(p_b(\cdot|y_{\sigma_b} = z), p_b) < \zeta \|z - \mathbb{E}(p_b)\|.$$

Hence, the denoiser $m_{\sigma_b}(z)$ on the boundary of the ball $B_{R_0}(\mathbb{E}(p_b))$ will be inside the ball $B_{\zeta R_0}(\mathbb{E}(p_b))$ for all $\sigma_b > \sigma_{\text{init}}(\Omega, \zeta, R_0)$. Then, by applying Item 2 of Theorem 3.6 to the set $B_{R_0}(\mathbb{E}(p_b))$, we have that the trajectory $(y_{\sigma_b})_{\sigma_b \in (\sigma_{\text{init}}(\Omega, \zeta, R_0), \sigma_1]}$ will never leave the ball of radius R_0 centered at $\mathbb{E}(p_b)$.

We now analyze the ODE trajectory and utilize the $\lambda_b := -\log(\sigma_b)$ reparametrization to obtain the desired result. That is, we consider the trajectory $z_{\lambda_b} := y_{\sigma_b(\lambda_b)}$ that starts from x_0 at $\lambda_{b,1} = -\log(\sigma_1)$ and until $\lambda_{b,\text{init}} = -\log(\sigma_{\text{init}}(\Omega, \zeta, R_0))$. We have the following differential inequality:

$$\begin{aligned}
\frac{d}{d\lambda_b} \|z_{\lambda_b} - \mathbb{E}(p_b)\|^2 &= -2\langle z_{\lambda_b} - \mathbb{E}(p_b), z_{\lambda_b} - m_{\lambda_b}(z_{\lambda_b}) \rangle, \\
&= -2\|z_{\lambda_b} - \mathbb{E}(p_b)\|^2 + 2\langle z_{\lambda_b} - \mathbb{E}(p_b), z_{\lambda_b} - m_{\lambda_b}(z_{\lambda_b}) \rangle, \\
&\leq -2\|z_{\lambda_b} - \mathbb{E}(p_b)\|^2 + 2\|z_{\lambda_b} - \mathbb{E}(p_b)\| \|z_{\lambda_b} - m_{\lambda_b}(z_{\lambda_b})\|, \\
&< -2(1 - \zeta) \|z_{\lambda_b} - \mathbb{E}(p_b)\|^2.
\end{aligned}$$

Then multiply the integrating factor $e^{2(1-\zeta)\lambda_b}$:

$$\begin{aligned}
\frac{d}{d\lambda_b} \left(e^{2(1-\zeta)\lambda_b} \|z_{\lambda_b} - \mathbb{E}(p_b)\|^2 \right) &= e^{2(1-\zeta)\lambda_b} \frac{d}{d\lambda_b} \|z_{\lambda_b} - \mathbb{E}(p_b)\|^2 + 2(1 - \zeta) e^{2(1-\zeta)\lambda_b} \|z_{\lambda_b} - \mathbb{E}(p_b)\|^2, \\
&< 0.
\end{aligned}$$

Then for any λ_b in $(\lambda_{b0}, \lambda_{b,\text{init}}(\Omega, \zeta, R_0))$, we have

$$\|z_{\lambda_b} - \mathbb{E}(p_b)\|^2 < e^{-2(1-\zeta)(\lambda_b - \lambda_{b0})} R_0^2.$$

Using the reparametrization $\sigma_b = e^{-\lambda_b}$, we have that

$$\|y_{\sigma_b} - \mathbb{E}(p_b)\| < \frac{\sigma^{1-\zeta}}{\sigma_0^{1-\zeta}} R_0.$$

We now use the fact that $x_\sigma = y_{\sqrt{\sigma^2 + \delta^2}}$ to obtain the desired result. First note that $\mathbb{E}(p) = \mathbb{E}(p_b)$ due to p is obtained by convolving p_b with a Gaussian with zero mean. Then, whenever $\sigma > \sqrt{\sigma_{\text{init}}(\Omega, \zeta, R_0)^2 + \delta^2}$, we have that

$$\|x_\sigma - \mathbb{E}(p)\| < \frac{(\sigma^2 + \delta^2)^{(1-\zeta)/2}}{(\sigma_0^2 + \delta^2)^{(1-\zeta)/2}} R_0.$$

This concludes the proof. \square

Proof of Proposition 6.2. By Lemma B.7, we have that the trajectory x_σ of the flow matching ODE with data distribution $p = p_b * \mathcal{N}(0, \delta^2 I)$ starting from x_{σ_1} at time σ_1 can be obtained by the trajectory $y_{\sigma_b = \sqrt{\sigma^2 + \delta^2}}$ of the flow matching ODE with data distribution p_b starting from x_{σ_1} at time $\sqrt{\sigma_1^2 + \delta^2}$. Then by applying Theorem 3.5 to the ODE trajectory to y_{σ_b} , we have

$$d_{\text{conv}(\text{supp}(p_b))}(y_{\sigma_b}) \leq \frac{\sigma_b}{\sqrt{\sigma^2 + \delta^2}} d_{\text{conv}(\text{supp}(p_b))}(y_{\sigma_b = \sqrt{\sigma_1^2 + \delta^2}}),$$

We then complete the proof by change y_{σ_b} back to x_σ , and σ_b back to $\sqrt{\sigma_1^2 + \delta^2}$. \square

Proof of Proposition 6.3. For simplicity, we use $\eta_\sigma := p(\cdot | x_\sigma = x)$ to denote the posterior measure at x . We restrict η_σ on S to obtain the following probability measure

$$\eta_\sigma^S := \frac{1}{\eta_\sigma(S)} \eta_\sigma|_S.$$

It is easy to see that $\mathbb{E}(\eta_\sigma^S)$ lies in the convex hull of S . We can then bound the distance from the denoiser $m_\sigma(x)$ to the convex hull of S by the Wasserstein distance between η_σ and η_σ^S .

Similarly to the proof of Theorem 4.10, we construct the following coupling γ between η_σ and η_σ^S :

$$\gamma = \Delta_{\#}(\eta_\sigma|_S) + \eta_\sigma^S \otimes (\eta_\sigma|_{(\Omega \setminus S)}),$$

where $\Delta : \mathbb{R}^d \rightarrow \mathbb{R}^d \times \mathbb{R}^d$ is the diagonal map sending x to (x, x) .

We then have the following estimate:

$$\begin{aligned} d_{\text{W},2}^2(\eta_\sigma, \eta_\sigma^S) &\leq \iint \|y_1 - y_2\|^2 \frac{\eta_\sigma|_S}{\eta_\sigma(S)}(dy_1) \eta_\sigma|_{(\Omega \setminus S)}(dy_2), \\ &\leq \eta_\sigma((\Omega \setminus S)) (\text{diam}(\text{supp}(p)))^2 \\ &= (\text{diam}(\text{supp}(p)))^2 \frac{\int_{(\Omega \setminus S)} \exp(-\frac{1}{2\sigma^2} \|x - x_1\|^2) p(dx_1)}{\int_{S \cup (\Omega \setminus S)} \exp(-\frac{1}{2\sigma^2} \|x - x'_1\|^2) p(dx'_1)}, \\ &\leq (\text{diam}(\text{supp}(p)))^2 \frac{\int_{(\Omega \setminus S)} \exp(-\frac{1}{2\sigma^2} \|x - x_1\|^2) p(dx_1)}{\int_S \exp(-\frac{1}{2\sigma^2} \|x - x_1\|^2) p(dx_1)}, \end{aligned}$$

By the assumption that $d_{\text{conv}(S)}(x) \leq D/2 - \epsilon$, we have that for all $x_1 \in S$

$$\|x - x_1\| \leq D/2 - \epsilon + D = 3D/2 - \epsilon,$$

and for all $x_1 \in \Omega'$

$$\|x - x_1\| \geq 2D - (D/2 - \epsilon) = 3D/2 + \epsilon.$$

We then have that

$$\begin{aligned} d_{W,2}(\eta_\sigma, \eta_\sigma^S)^2 &\leq (\text{diam}(\text{supp}(p)))^2 \frac{\int_{(\Omega \setminus S)} \exp\left(-\frac{1}{2\sigma^2}(3D/2 + \epsilon)^2\right) p(dx_1)}{\int_S \exp\left(-\frac{1}{2\sigma^2}(3D/2 - \epsilon)^2\right) p(dx_1)}, \\ &= (\text{diam}(\text{supp}(p)))^2 \frac{1 - a_S}{a_S} \exp\left(-\frac{1}{2\sigma^2}((3D/2 + \epsilon)^2 - (3D/2 - \epsilon)^2)\right), \\ &\leq (\text{diam}(\text{supp}(p)))^2 \frac{1 - a_S}{a_S} \exp\left(-\frac{3D\epsilon}{\sigma^2}\right). \end{aligned}$$

Then by applying Lemma B.1 and the fact that $\mathbb{E}(\eta_\sigma^S) \in \text{conv}(S)$, we have that

$$d_{\text{conv}(S)}(m_\sigma(x)) \leq \text{diam}(\text{supp}(p)) \sqrt{\frac{1 - a_S}{a_S}} \exp\left(-\frac{3D\epsilon}{\sigma^2}\right).$$

□

The following result on the convergence of ODE under asymptotically vanishing perturbation will be used often in the proofs of this section.

Lemma B.8. *Let $(y_t \in \mathbb{R})_{t \in [t_1, \infty)}$ be a trajectory satisfying the following differential inequality*

$$\frac{dy_t}{dt} \leq -k y_t + \phi(t),$$

where $k > 0$ and $\phi : \mathbb{R} \rightarrow \mathbb{R}$ is such that $\lim_{t \rightarrow \infty} \phi(t) = 0$. Then, $\lim_{t \rightarrow \infty} y_t = 0$.

Proof of Lemma B.8. By multiplying the integrating factor e^{kt} , we have that

$$\frac{d e^{kt} y_t}{dt} = e^{kt} \frac{dy_t}{dt} + k e^{kt} y_t \leq \phi(t) e^{kt}.$$

Then for all $t_2 > t_1$, we have

$$\begin{aligned} e^{kt_2} y_{t_2} &\leq e^{kt_1} y_{t_1} + \int_{t_1}^{t_2} e^{kt} \phi(t) dt, \\ y_{t_2} &\leq e^{-k(t_2 - t_1)} y_{t_1} + \int_{t_1}^{t_2} e^{-k(t_2 - t)} \phi(t) dt. \end{aligned}$$

We will first show that y_t is bounded. As $\phi(t)$ decays to zero as t goes to infinity, so will be $|\phi(t)|$, and hence there exists some constant $C > 0$ such that $|\phi(t)| \leq C$ for all $t \geq t_1$. Then, we have that

$$\begin{aligned} |y_{t_2}| &\leq e^{-k(t_2 - t_1)} |y_{t_1}| + C \int_{t_1}^{t_2} e^{-k(t_2 - t)} dt, \\ &\leq e^{-k(t_2 - t_1)} |y_{t_1}| + \frac{C}{k} (1 - e^{-k(t_2 - t_1)}), \\ &\leq e^{-k(t_2 - t_1)} |y_{t_1}| + \frac{C}{k}. \end{aligned}$$

Hence, y_t is bounded for all $t \geq t_1$, and we denote by $C_y > 0$ any bound for y_t .

Next, we show that y_t converges to zero as t goes to infinity. For any $\epsilon > 0$, there is a sufficient large $t_\epsilon > t_1$ such that

1. $e^{-kt_\epsilon} C_y < \epsilon/2$.
2. $|\phi(t)| < \epsilon/2$ for all $t \geq t_\epsilon$.

Then for all $t_2 > 2t_\epsilon$, by integrating the inequality from t_ϵ to t_2 , we have that

$$\begin{aligned}
|y_{t_2}| &\leq e^{-k(t_2-t_\epsilon)} |y_{t_\epsilon}| + \int_{t_\epsilon}^{t_2} e^{-k(t_2-t)} \phi(t) dt, \\
&\leq e^{-k(t_\epsilon)} C_y + \epsilon/2 \int_{t_\epsilon}^{t_2} e^{-k(t_2-t)} dt, \\
&\leq \epsilon/2 + \epsilon/2(1 - e^{-k(t_2-t_\epsilon)}), \\
&\leq \epsilon.
\end{aligned}$$

This implies that y_t converges to zero as t goes to infinity. □

Proof of Proposition 6.4. Similarly as before, we consider the change of variable $\lambda = -\log \sigma$ and the corresponding trajectory $z_\lambda := x_{\sigma(\lambda)}$.

We consider the thickening $B_{D/2-\epsilon}(\text{conv}(S)) := \cup_{x \in \text{conv}(S)} B_{D/2-\epsilon}(x)$ of the convex hull of S with radius $D/2 - \epsilon$. Then, $B_{D/2-\epsilon}(\text{conv}(S))$ is convex itself.

Following a similar strategy of the proof of Proposition 6.7, we will first show the set $B_{D/2-\epsilon}(\text{conv}(S))$ is absorbing: there exist a parameter $\lambda_0(S, \epsilon)$ such that the denoiser $m_\lambda(y)$ is guaranteed to lie in the interior of $B_{D/2-\epsilon}(\text{conv}(S))$ for all $y \in \partial B_{D/2-\epsilon}(\text{conv}(S))$ for all $\lambda > \lambda_0(S, \epsilon)$.

Let $C_{S,\epsilon} = \frac{D/2-\epsilon}{\text{diam}(\text{supp}(p)) \sqrt{\frac{1-a_S}{a_S}}}$ and define the constant $\lambda_0(S, \epsilon)$ as

$$\lambda_0(S, \epsilon) := \begin{cases} \frac{1}{2} \log \left(-\frac{2}{3D\epsilon} \log(C_{S,\epsilon}) \right), & \text{if } C_{S,\epsilon} < 1, \\ -\infty, & \text{otherwise.} \end{cases}$$

Then by Proposition 6.3, we need to show

$$d_{\text{conv}(S)}(m_\lambda(y)) \leq \text{diam}(\text{supp}(p)) \sqrt{\frac{1-a_S}{a_S}} \exp\left(-\frac{3D\epsilon}{2} e^{2\lambda}\right) \leq D/2 - \epsilon.$$

That is, we then need to verify that when $\lambda > \lambda_0(S, \epsilon)$, the last inequality holds.

$$\begin{aligned}
\text{diam}(\text{supp}(p)) \sqrt{\frac{1-a_S}{a_S}} \exp\left(-\frac{3D\epsilon}{2} e^{2\lambda}\right) &\leq D/2 - \epsilon, \\
\exp\left(-\frac{3D\epsilon}{2} e^{2\lambda}\right) &\leq C_{S,\epsilon},
\end{aligned}$$

Then, when $C_{S,\epsilon} \geq 1$, the above inequality holds for all $\lambda > -\infty$ and when $C_{S,\epsilon} < 1$, the above inequality holds for all $\lambda > \lambda_0(S, \epsilon)$.

Then by an argument similar to the one in Proposition 6.7, whenever $\lambda_0 > \lambda_0(S, \epsilon)$, the trajectory $(z_\lambda)_{\lambda \in [\lambda_0, \infty)}$ starting from any y in $B_{D/2-\epsilon}(\text{conv}(S))$ will stay inside $B_{D/2-\epsilon}(\text{conv}(S))$ for all $\lambda > \lambda_0$.

Next, we show that the distance $d_{\text{conv}(S)}(z_\lambda)$ goes to zero as λ goes to infinity. By taking the derivative of $d_{\text{conv}(S)}^2(z_\lambda)$, and use the notation $v := \mathbb{E} \left(\frac{p(\cdot|z_\lambda)|_S}{p(\cdot|z_\lambda)(S)} \right)$, we have

$$\begin{aligned} \frac{d d_{\text{conv}(S)}^2(z_\lambda)}{d\lambda} &= -2 \langle z_\lambda - \text{proj}_{\text{conv}(S)}(z_\lambda), z_\lambda - m_\lambda(z_\lambda) \rangle, \\ &= -2 \langle z_\lambda - \text{proj}_{\text{conv}(S)}(z_\lambda), z_\lambda - \text{proj}_{\text{conv}(S)}(z_\lambda) \rangle, \\ &\quad + 2 \langle z_\lambda - \text{proj}_{\text{conv}(S)}(z_\lambda), \text{proj}_{\text{conv}(S)}(z_\lambda) - v \rangle \\ &\quad + 2 \langle z_\lambda - \text{proj}_{\text{conv}(S)}(z_\lambda), v - m_\lambda(z_\lambda) \rangle, \\ &\leq -2 d_{\text{conv}(S)}^2(z_\lambda) + 2 \|z_\lambda - v\| \|v - m_\lambda(z_\lambda)\|, \\ &\leq -2 d_{\text{conv}(S)}^2(z_\lambda) + 2(D/2 - \epsilon) \|v - m_\lambda(z_\lambda)\|. \end{aligned}$$

where in the second to last inequality we use the fact that $v \in \text{conv}(S)$ and hence

$$\langle z_\lambda - \text{proj}_{\text{conv}(S)}(z_\lambda), \text{proj}_{\text{conv}(S)}(z_\lambda) - v \rangle \leq 0.$$

Note that v is exactly the quantity used in the Proof of Proposition 6.3 where we have proved (in terms of λ)

$$\|v - m_\lambda(z_\lambda)\| \leq \text{diam}(\text{supp}(p)) \sqrt{\frac{1 - a_S}{a_S}} \exp\left(-\frac{3D\epsilon}{2} e^{2\lambda}\right).$$

Then by Lemma B.8, we have that $d_{\text{conv}(S)}(z_\lambda) \rightarrow 0$ as $\lambda \rightarrow \infty$ and hence $x_\sigma = z_{\lambda(\sigma)}$ converges to the convex hull of S as $\sigma \rightarrow 0$. \square

Proof of Proposition 6.6. Since each V_i^ϵ is a convex set and in fact, a closure of an open convex set, by item 2 of Theorem 3.6, it suffices to prove that for all $x \in \partial V_i^\epsilon$ and all $\sigma < \sigma_0(V_i^\epsilon)$, which is the boundary of V_i^ϵ , one has that $m_\sigma(x) \in \text{int} V_i^\epsilon$ which is the interior of V_i^ϵ .

First of all, we define

$$r_{i,\epsilon} := \frac{\text{sep}^2(x_i) - \epsilon^2}{2\text{sep}(x_i)}.$$

It is straightforward to check that $B_{r_{i,\epsilon}}(x_i) \subseteq V_i^\epsilon$. In fact, $r_{i,\epsilon} = \text{argmax}\{r > 0 : B_r(x_i) \subseteq V_i^\epsilon\}$.

Hence, by Corollary 4.11, for any $x \in \partial V_i^\epsilon$ we have that

$$\begin{aligned} \|m_\sigma(x) - x_i\| &\leq \text{diam}(\Omega) \sqrt{\frac{1 - a_i}{a_i}} \exp\left(-\frac{\Delta_\Omega(x)}{4\sigma^2}\right) \\ &\leq \text{diam}(\Omega) \sqrt{\frac{1 - a_i}{a_i}} \exp\left(-\frac{\epsilon^2}{4\sigma^2}\right) \end{aligned}$$

Therefore, we need to identify when the above inequality is less than $r_{i,\epsilon}$, that is,

$$\begin{aligned} \text{diam}(\Omega) \sqrt{\frac{1 - a_i}{a_i}} \exp\left(-\frac{\epsilon^2}{4\sigma^2}\right) &< r_{i,\epsilon}, \\ \exp\left(-\frac{\epsilon^2}{4\sigma^2}\right) &< \frac{r_{i,\epsilon}}{\text{diam}(\Omega) \sqrt{\frac{1 - a_i}{a_i}}}, \end{aligned}$$

Recall that $C_{i,\epsilon} = \frac{r_{i,\epsilon}}{\text{diam}(\Omega) \sqrt{\frac{a_i}{1 - a_i}}}$. Then, it is direct to check that when $C_{i,\epsilon} \leq 1$, the above inequality holds for all $0 \leq \sigma < \infty$ and when $C_{i,\epsilon} > 1$, the above inequality holds for all $\sigma < \sigma_0(V_i^\epsilon) = \frac{\epsilon}{2} (\log(C_{i,\epsilon}))^{-1/2}$. In summary, this implies that $m_\sigma(x) \in \text{int} B_{r_{i,\epsilon}}(x_i) \subset \text{int} V_i^\epsilon$ when $\sigma < \sigma_0(V_i^\epsilon)$. \square

Proofs of Proposition 6.7. We will first prove in the λ parameter and then the translation to the σ parameter is straightforward. We consider the trajectory $z_\lambda := x_{\sigma(\lambda)}$ for $\lambda \in [\lambda(\sigma_0), \lambda(0) = \infty)$. We first show that $d_\Omega(z_\lambda) \rightarrow 0$ as $\lambda \rightarrow \infty$.

Along the trajectory z_λ , by Corollary A.12 we have

$$\begin{aligned} \frac{d d_\Omega^2(z_\lambda)}{d\lambda} &= -2\langle z_\lambda - x_i, z_\lambda - m_\lambda(z_\lambda) \rangle, \\ &= -2\langle z_\lambda - x_i, z_\lambda - x_i \rangle + 2\langle z_\lambda - x_i, x_i - m_\lambda(z_\lambda) \rangle, \\ &\leq -2d_\Omega^2(z_\lambda) + 2d_\Omega(z_\lambda) \|x_i - m_\lambda(z_\lambda)\|, \end{aligned}$$

Applying Corollary 4.11 to points in V_i^ϵ , we have the following uniform bound for all $y \in V_i^\epsilon$,

$$\|m_\lambda(y) - x_i\| \leq \text{diam}(\Omega) \sqrt{\frac{1-a_i}{a_i}} \exp\left(-\frac{1}{4}e^{2\lambda}\epsilon^2\right).$$

By Proposition 6.6 we have that $z_\lambda \in V_i^\epsilon$. Therefore,

$$\frac{d d_\Omega(z_\lambda)}{d\lambda} \leq -2d_\Omega^2(z_\lambda) + \text{sep}(x_i) \text{diam}(\Omega) \sqrt{\frac{1-a_i}{a_i}} \exp\left(-\frac{1}{4}e^{2\lambda}\epsilon^2\right).$$

Then by Lemma B.8, we have that $d_\Omega(z_\lambda) \rightarrow 0$ as $\lambda \rightarrow \infty$. By the the fact that Ω is discrete and x_i is the nearest point to z_λ for all large λ , we must have $z_\lambda \rightarrow x_i$ as $\lambda \rightarrow \infty$. \square

Proof of Proposition 6.8. The proof idea follows the same line as the proofs of Proposition 6.6 and Proposition 6.7. Similarly as in the case of denoisers, we can also consider the change of variable $\lambda = -\log(\sigma)$ for handling m_σ^θ . We let $z_\lambda^\theta := x_{\sigma(\lambda)}^\theta$ and let $m_\lambda^\theta(x) := m_{\sigma(\lambda)}^\theta(x)$ for any $x \in \mathbb{R}^d$. Then, it is straightforward to check that

$$\frac{dz_\lambda^\theta}{d\lambda} = m_\lambda^\theta(z_\lambda^\theta) - z_\lambda^\theta \quad (30)$$

and converting everything back to σ is straightforward.

We first identify the parameter $\lambda_0(V_i^\epsilon, \phi)$ such that the denoiser $m_\lambda^\theta(x)$ is will always lie in the interior of V_i^ϵ for all $x \in \partial V_i^\epsilon$ and all $\lambda > \lambda_0(V_i^\epsilon, \phi)$.

By the triangle inequality, we have that

$$\begin{aligned} \|m_\lambda^\theta(y) - x_i\| &\leq \|m_\lambda^\theta(y) - m_\lambda^N(y)\| + \|m_\lambda^N(y) - x_i\|, \\ &\leq \phi(\lambda) + \text{diam}(\Omega) \sqrt{\frac{1-a_i}{a_i}} \exp\left(-\frac{1}{4}e^{2\lambda}\epsilon^2\right). \end{aligned}$$

Since $\phi(\lambda)$ goes to zero as λ goes to infinity, there exists a parameter $\lambda_0(V_i^\epsilon, \phi)$ such that for all $\lambda > \lambda_0(V_i^\epsilon, \phi)$, $\|m_\lambda^\theta(y) - x_i\| \leq \frac{\text{sep}^2(x_i) - \epsilon^2}{2\text{sep}(x_i)}$. Then, with the same argument as in the proof of Proposition 6.6, we can prove that the trajectory z_λ^θ will never leave V_i^ϵ for all $\lambda > \lambda_0(V_i^\epsilon, \phi)$.

Since the trajectory z_λ^θ never leaves V_i^ϵ for all $\lambda > \lambda_0(V_i^\epsilon, \phi)$, we can then apply the uniform decay of $\|m_\lambda^\theta(y) - x_i\|$ to the differential inequality of $d_\Omega^2(z_\lambda^\theta)$ as follows:

$$\begin{aligned} \frac{d d_\Omega^2(z_\lambda^\theta)}{d\lambda} &\leq -2d_\Omega^2(z_\lambda^\theta) + 2d_\Omega(z_\lambda^\theta) \|x_i - m_\lambda^\theta(z_\lambda^\theta)\|, \\ &\leq -2d_\Omega^2(z_\lambda^\theta) + 2d_\Omega(z_\lambda^\theta) \left(\phi(\lambda) + \text{diam}(\Omega) \sqrt{\frac{1-a_i}{a_i}} \exp\left(-\frac{1}{4}e^{2\lambda}\epsilon^2\right) \right). \end{aligned}$$

Now, we apply Lemma B.8 again as in the proof of Proposition 6.7, we have that $d_\Omega(z_\lambda^\theta)$ goes to zero as λ goes to infinity and hence z_λ^θ converges to x_i . \square